THE GEOLOGY AND GEOCHEMISTRY OF THE CAMBRIAN DEVIL RIVER VOLCANICS, ANATOKI RANGE, NORTHWEST NELSON

A Thesis submitted in partial fulfilment

of the requirements for the Degree

of

MASTER OF SCIENCE IN GEOLOGY

at the

University of Canterbury

by

DONALD ROSS MACLEAN

University Of Canterbury

1994

Abstract

Middle Cambrian Volcanics of the Takaka Terrane, the *Devil River Volcanics*, crop out in the Anatoki Range area of Northwest Nelson, New Zealand. Three units are recognised within the Devil River Volcanics. The oldest unit is the *Christmas Conglomerate Member*, which is overlain by two volcanic suites, the *Circular Bush suite* and the *Paradise suite*. All have greenschist facies metamorphic mineral assemblages. Overlying these is a post arc sedimentary sequence which progressively grades into *Tasman Formation-like* lithologies.

The Christmas Conglomerate Member is composed of polymict conglomerate containing chert, sandstone, siltstone, and volcanic clasts. Basaltic andesite clasts show geochemical affinities to low-K tholeiitic rocks.

The Circular Bush suite is at least 1200 metres in thickness, and contains volcanic derived debris flows, reworked tuffs and lapilli-tuffs, volcanic conglomerate and rare chert. Volcanic clasts are predominantly basaltic-andesitic to andesitic in composition, with subordinate basalt and rhyolite. Volcanic clasts have immobile element abundances similar to medium-K calc-alkaline series rocks.

The Paradise suite is composed of basaltic pillow lavas, massive flows and rare hyaloclastite pillow breccias, which have the geochemistry of high alumina basalts, but have a tholeiitic trend of iron enrichment. The suite ranges from 50 metres to in excess of 400 metres in thickness. The Paradise suite also has immobile element abundances similar to medium-K calc-alkaline rocks.

The Circular Bush and Paradise suites both show a subduction-related geochemical signature, however, it is not clear whether the arc was on a continental margin or in an intra-oceanic setting.

The succession is folded into a series of north-south striking, tight to isoclinal folds (F_1), which have been refolded by two subsequent phases of folding of unknown orientation (F_2 and F_3).

Basic alkaline dykes intrude the sequence, crosscutting F_1 fabrics. The dykes have a geochemistry broadly similar to continental flood basalts, and are inferred to have formed in an intraplate setting. Similar intrusives have been documented elsewhere throughout the Takaka Terrane.

with four separate maps in back pocket.

Acknowledgments

Many people have helped me in getting this thesis completed. Firstly I would like to thank my parents and family for their financial support and encouragement over the last five and a half years. Without them I would never have got this far.

My supervisors, Dr John Bradshaw and Dr Steve Weaver are thanked for their guidance and critical reviews of my various chapters. Thanks also Dr David Shelley who helped with microscope and universal stage work and Dr Roddy Muir who read a two of my chapters. Dr Roger Cooper is thanked for sharing some of his extensive knowledge on Northwest Nelson geology, and for the helicopter trip to Mount Benson. Carsten Munker helped me in starting to understand the geochemistry - danke.

I am indebted to the Mason Trust Fund for their generous grant which helped greatly with fieldwork related expenses.

The technical staff at the University of Canterbury are thanked for their work, in particular Rob Spiers, Kerry Swanson and Stephen Brown.

The staff of Westland Ilmenite are thanked for their help, especially for the generous provision of helicopter support during early 1993. Phil Savory, Ian Mathison and Gary Jones are thanked in particular.

Thanks to fellow research students Aaron, Tim, Todd, Richard Justice and Ginny for providing a great working environment. Richard Jongens, Hamish and little Bob are thanked for their help in the field (I forgive you Bob for making us sleep under an overhanging rock for the night). A big thanks to Coxy and Georg: without our stress-relieving sessions at various drinking establishments I would never have got through this. Cheers.

Finally, a special thank-you to Annette. I look forward to seeing more of you now that I have got this thing finished.

TABLE OF CONTENTS

LIST OF FIGURES

LIST OF TABLES

CHAPTER ONE: INTRODUCTION

1.1 Regional Geology

Lower Paleozoic rocks of Northwest Nelson form three distinctive north-south trending sedimentary belts, separated by two major faults of regional extent; the Anatoki Thrust and the Devil River Thrust (Figure 1.1). The Western Sedimentary Belt is part of the Buller Terrane, and consists of a thick sequence of quartz-rich turbidites, siltstones, and carbonaceous shales ranging in age from Lower Ordovician (possibly Upper Cambrian) to Upper Ordovician. The belt is believed to have been deposited as submarine fan and slope deposits on the margin of a continental region (Cooper, 1989).

The Central and Eastern Sedimentary Belts constitute part of the Takaka Terrane. The Central Belt is composed of a diverse array of lithologic units and lithofacies, characterised by volcanics, volcaniclastics, calcareous and siliceous sediments, conglomerates, and carbonate rocks. The succession ranges in age from Middle Cambrian to Upper Ordovician (Cooper, 1989). Proximity to a volcanic arc is evident for the Cambrian part of the succession, whereas the Ordovician is represented by thick basinal carbonate and quartz-rich flysch, indicative of a more stable crustal setting (Cooper, 1989). The terrane boundary, the Anatoki Thrust, bounds the western margin of the Central Belt (Figure 1.1). The Eastern Sedimentary Belt is composed of coarse grained quartz-rich clastics, overlain by a thick sequence of basinal carbonates, quartz-rich flysch, mudstones and sandstones. These range in age from Lower Ordovician to Lower Devonian (Cooper, 1989).

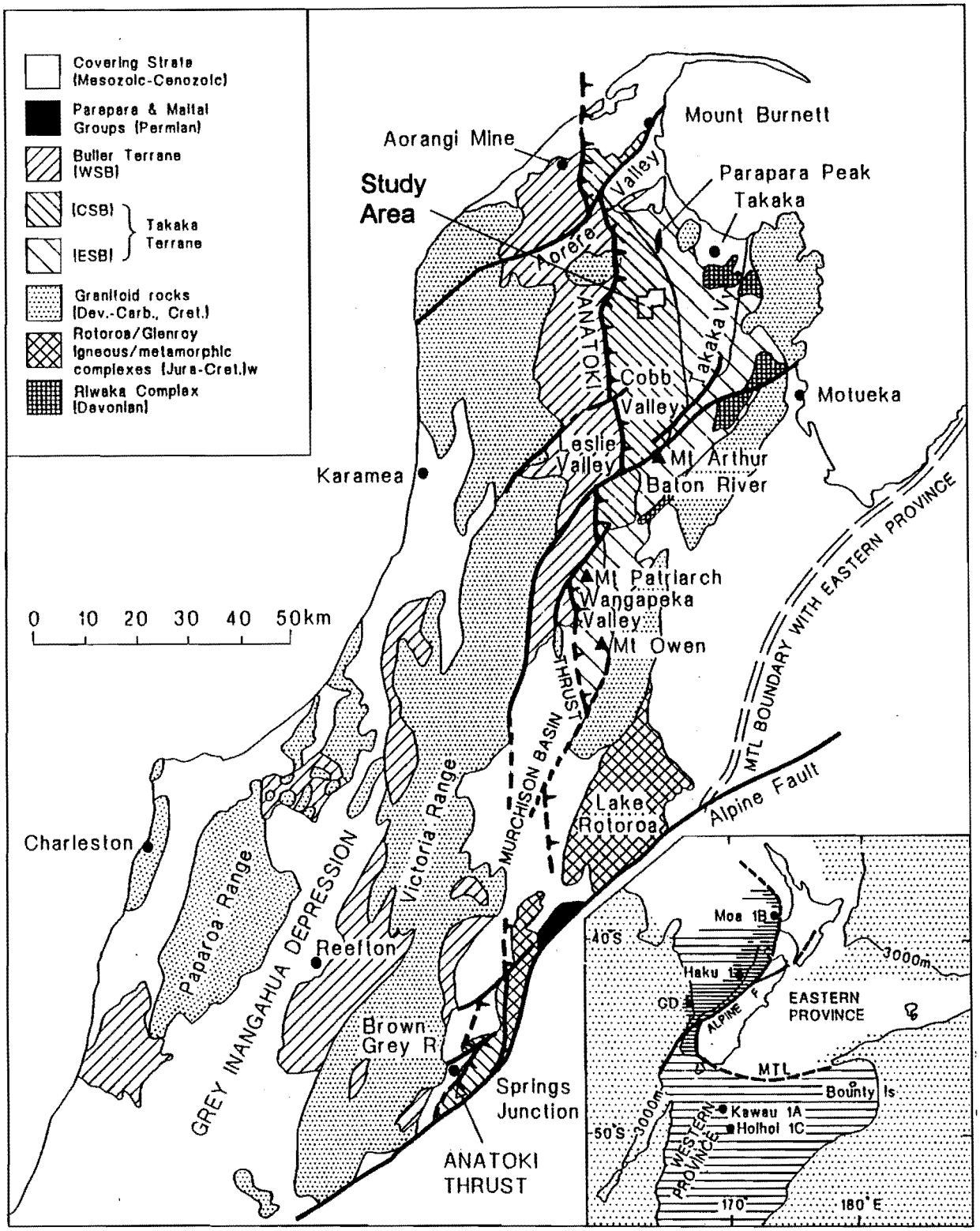

Figure 1.1: Generalised geology of West Nelson-North Westland, South Island, showing the distribution of the main rock belts and the position of the Anatoki Thrust. Inset: Known and inferred extent of Western Province rocks. (after Cooper and Tulloch, 1992)

1.2 Aim

Grindley (1961) proposed the name *Devil River Volcanics* for Cambrian volcanics within the Central Sedimentary Belt, and nominated a type section on the western margin of the Devil Range (Figure 1.2) (Grindley, 1971). This name was used in the subsequent New Zealand Geological Survey 1:63 360 geological map series; S3: Farewell-Kahurangi (Bishop, 1971), S8: Takaka, (Grindley, 1971), S13: Cobb (Grindley, 1971), and S19: Wangapeka (Coleman, 1981). However, no formal description of the Devil River Volcanics was ever published.

Recent work on Cambrian volcanics in the Cobb Valley area suggests that what was previously mapped by Grindley and co-workers as Devil River Volcanics, may contain more than one suite of volcanics. Therefore, it is the aim of this thesis is to describe the Devil River Volcanics in the vicinity of the type-section to allow better discrimination between volcanic units, and to improve correlation between volcanic suites throughout the Central Sedimentary Belt.

1.3 Study Area

Access to the type section on the Devil Range is difficult and proved impractical for detailed study and sampling. Mapping was concentrated in the Anatoki Range and Anatoki River area, a few kilometres to the north. A reconnaissance traverse of the type section of the Devil River volcanics was undertaken to ensure that there were no major changes in the volcanics along strike between the Devil Range and the Anatoki Range.

The study area covers approximately 15 km^2, and is located in the recently established Kahurangi National Park (previously Northwest Nelson Forest Park), centred on the Anatoki Range, Anatoki River area (Figure 1.3). The area is steep and rugged, with in excess of 1000 metres vertical relief. Cirques with small tarns are found on the Anatoki Range. The sides of the Anatoki Valley are dissected by numerous small creeks, many

with particularly large numbers of waterfalls. The Anatoki River contains numerous rapids and a number of steep sided gorges. The valley sides are vegetated by dense mixed Nothofagus-Podocarpus forest. Sub-alpine tussock and abundant spaniard are found above the bush-line.

Access is by a graded pack track (Anatoki Track), which was cut at the turn of the last century to service the Anatoki gold diggings. The track leads to a comfortable (but smoky) hut, the Anatoki Forks Hut, which has the luxury of a hot shower.

1.4 Fieldwork

Fieldwork was carried out over two summers, 1992-1993 and 1993-94, with approximately 8 weeks being spent in the field. Accommodation was at the Anatoki Hut or at a camp site at Circular Bush on the Anatoki Range. Helicopter support was kindly provided in 1992-93 by Westland Ilmenite, who were undertaking exploration work in the area.

Aerial photographs and 1:5000 scale map enlargements of NZMS 260 Sheet M26 (Cobb) were useful for delineating location in open terrain. In enclosed creeks and streams, hipchain and paced traverses were used for accurate location. Grid references are taken from NZMS 260 M26 (Cobb). Unweathered 1-3 kg rock samples were taken for geochemical analysis; their locations are given in Appendix 1.

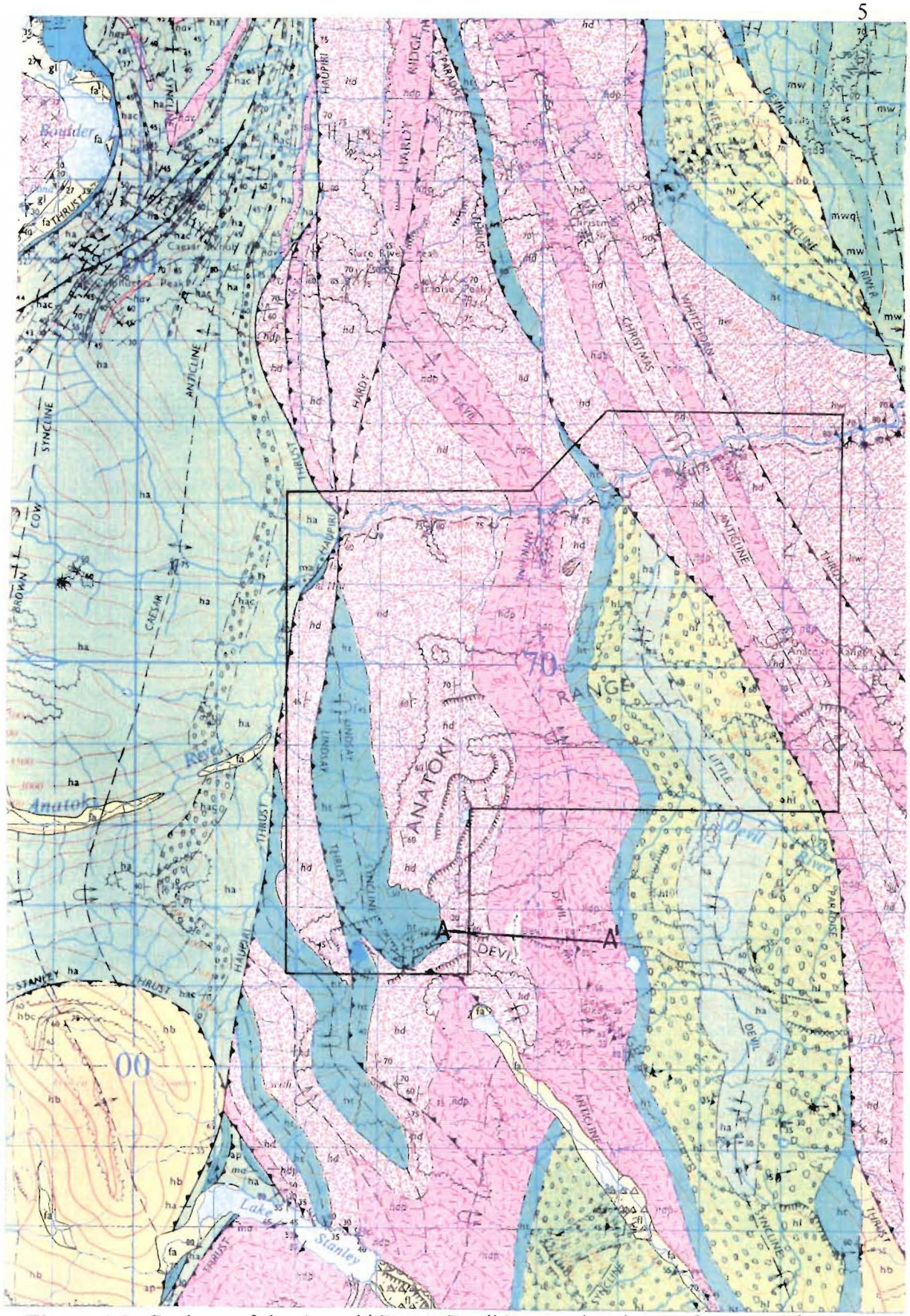

Figure 1.2: Geology of the Anatoki Range-Devil Range showing study area. The type-section of the Devil River Volcanics is shown by line A-A' (after Grindley, 1971). *Hd* = Devil River Volcanics, *Hdp* = porphyritic andesite sill within the Devil River Volcanics, *Ht* = Tasman Formation, *Hl* = Lockett Conglomerate, *Ha* = Anatoki Formation, *Hw* = Waingaro Schist Zone, *Mw* = Wangapeka Formation, *Ma* = Arthur Marble,

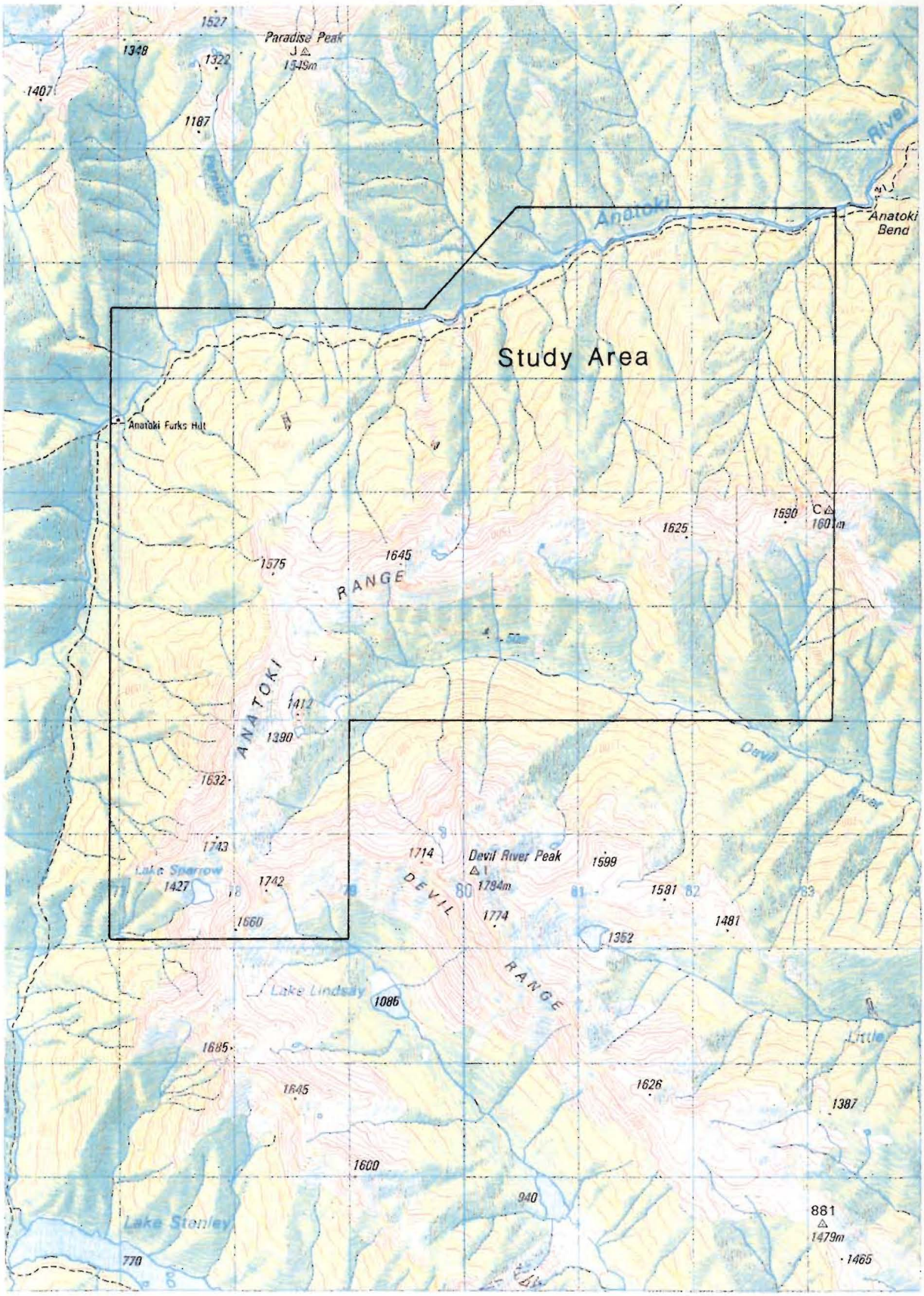

Figure 1.3: Topographic map showing location of study area (NZMS 260 Series: M26-Cobb). Scale 1:50 000.

CHAPTER TWO: REVIEW

2.1. Introduction

A number of models have been proposed to explain the Lower Palaeozoic geology of Northwest Nelson. The aim of this chapter is to provide a synthesis of these models and discuss their merits.

2.2. Early Models

Henderson (1923) divided the Palaeozoic of Northwest Nelson into four main groups of strata:

1. Haupiri Series (now Haupiri Group)
2. Baton River Series (now Ellis and Baton River Groups)
3. Aorere Series (now Aorere Group)
4. Mt Arthur Series (now Mt Arthur and Mt Patriarch Groups)

The Haupiri series was believed to be Upper Devonian in age, unconformably overlying the Baton River Series and Ordovician Aorere and Mt Arthur Series. Paleontological study of graptolites from the Aorere and Mt Arthur Series led Keble and Benson (1929) to conclude that, *"it is obvious that the rocks occurring east and west of the Haupiri Series belong to the same group of strata.....probably they owe to faulting or folding their position between belts of Ordovician strata differing little in age."*

Major revision of the stratigraphy was required when Benson (1950) discovered Cambrian trilobites in the Haupiri Series. This meant that although the Haupiri Series lay in a broadly synformal position, it was in fact older than the underlying Aorere and Mt Arthur Series, thus requiring a new structural interpretation.

2.3. Allochthonous Central Belt Model

Grindley (1961) proposed that the Central Belt consisted of a series of nappes thrust northwards over autochthonous basement (Western and Eastern Sedimentary Belts) (F1). The nappes were subsequently refolded about N-S axes (F2) to form a broadly synformal structure. The root zone of the nappes was inferred to be 100 km to the south (now occupied by the Rotoroa Igneous Complex). Five major nappes were recognised, each containing an overlapping portion of the stratigraphy (Figure 2.1) (Grindley, 1980, 1986). Grindley's model and regional stratigraphy (Figure 2.2) were adopted and used in the New Zealand Geological Survey 1:63,360 lithostratigraphic maps: S3 Farewell-Kahurangi, Bishop (1971); S8 Takaka, Grindley (1971); S13 Cobb, Grindley (1980); S19 Wangapeka, Coleman (1981). Table 2.1 outlines the major lines of evidence supporting Grindley's model, and the objections various authors have expressed.

Haupiri Nappe	Devil River Volcanics conformably overlying Balloon Formation (in tectonic contact with upthrust Cobb Igneous Complex
Waingaro Nappe	Devil River Volcanics unconformably overlain by Tasman Formation and Lockett Conglomerate. To the east, the Balloon Formation is overlain by Lockett Conglomerate
Anatoki Nappe	Anatoki Formation
Peel Nappe	Western Belt Peel Formation overlain conformably by Eastern Belt Wangapeka Formation
Mytton Nappe	Summit Limestone overlying Patriarch and Anatoki Formations

Figure 2.1: Grindley's five major nappes and the portions of the stratigraphy they contain (Oldest at top, youngest at bottom) (compiled from Grindley, 1980).

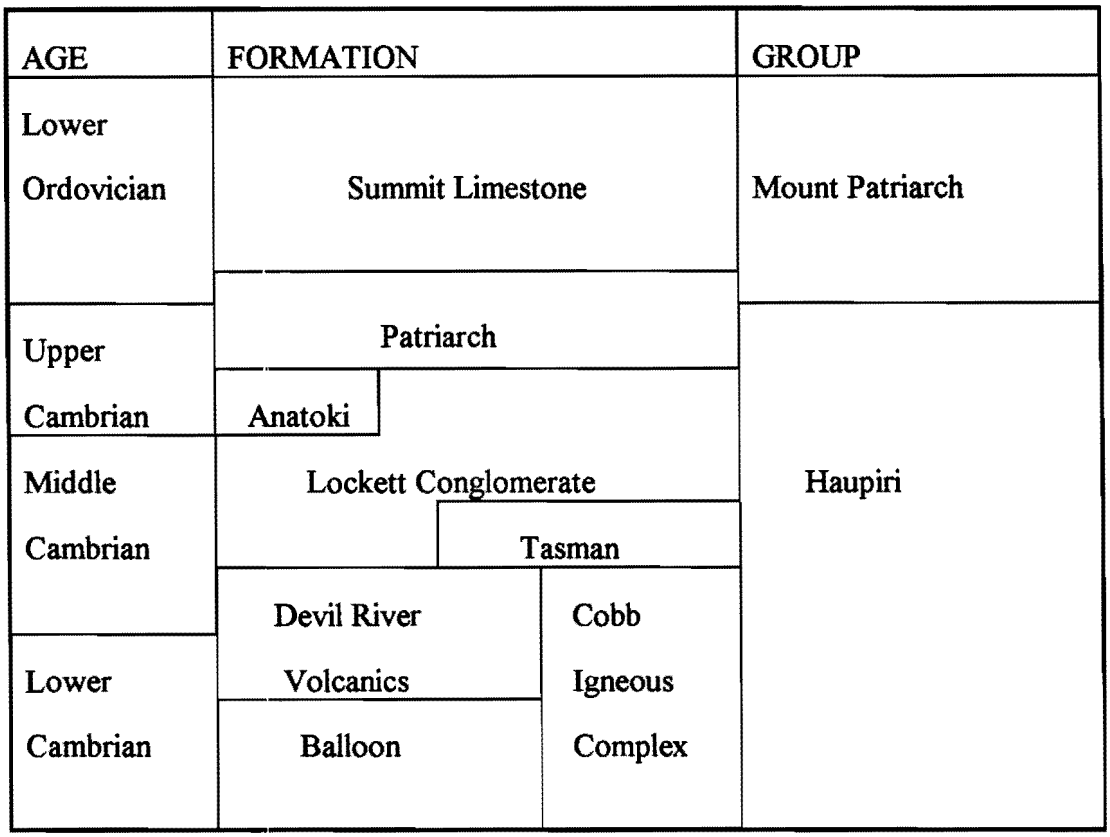

Figure 2.2: Central Belt stratigraphy of Grindley (1980).

2.4. Migrating Arc Models

A model of easterly migrating volcanic arcs in New Zealand was proposed by Shelley (1975). The Haupiri Group was inferred to be a non-orogenic andesitic arc, lying to the east of a sedimentary belt (i.e., Western Belt). A Pre-Tuhuan (Late Ordovician) orogeny was believed to have produced a paired metamorphic belt.

Crook and Feary (1982) explain the New Zealand Lower Palaeozoic in terms of Crook's (1980) model of forearc evolution. A west facing volcanic arc is postulated with a subduction complex (Balloon Formation, Waingaro Schist), overlain by an obducted ophiolite (Cobb Intrusives) and a forearc basinal sequence (Devil River Volcanics,

Evidence supporting the Allochthonous Central Belt Model: (Grindley, 1978, 1980)	• **Problems with the Allochthonous Central Belt Model:**
• Paleontological and sedimentological affinity of the Eastern and Western sedimentary belts (i.e. time and space correlates).	• Eastern and Central Belts have greater sedimentological and genetic affinity (single depositional regime) than the Eastern and Western Sedimentary Belts, which have significantly different geological histories (Cooper, 1979).
• Recognition of discrete nappes, each containing overlapping portions of the stratigraphy, stacks such that the youngest rocks are on the bottom, oldest on top.	• Grindley's model implies that the Central Belt must conveniently overlie a major facies boundary (Cooper, 1979)
• Inward dipping thrust faults on the margins of the Central Belt (mapped as closing northwards about the Central Belt).	• F2 structures mapped as being truncated by supposedly earlier F1 structures (Bradshaw, 1982)
• Tectonic windows into younger Cambrian, overthrust by older Cambrian (Waingaro, Stanley and Cobb Rivers) - indicate low angle thrusting.	• Nappes are mapped as being extensive in a N-S direction but thin rapidly in an E-W direction (e.g., Waingaro Nappe). This is not consistent with tectonic transport from the south (Bradshaw, 1982)
• Reclined recumbent folds in Western Belt rocks with similar vergences to those in Central Belt rocks - suggest northward overthrusting was accompanied by some folding within autochthonous basement.	• Massive tectonic transport from the south is not demonstrated (Bradshaw, 1982)
• Reclined north verging folds in Eastern Belt rocks that have been refolded by later N-S trending folds.	• Study of tectonites on the Anatoki and Devil River Thrusts suggest crustal shortening about E-W axes (rather than N-S) (Powell, 1985).
	• Western and Central Sedimentary Belts recognised in Fiordland, therefore the distance of tectonic transport must be much greater than previously thought (250 km +), making the model difficult to maintain (Ward, 1986). Grindley (1978) believed the source of the nappes to be somewhere in the region that is now occupied by the Rotoroa Igneous Complex (which may itself be allochthonous).
	• Validity of mapped folds depends on stratigraphy. Grindley's stratigraphy is based on gross lithological type. Recent detailed mapping indicates major revision of the stratigraphy is required, therefore some of the structural evidence for reclined recumbent folding may be invalid (Stewart, 1988, Cooper, 1989).

Table 2.1: Evidence for and against the Allochthonous Central Belt Model

Anatoki Formation). Volcanic activity is inferred to cease in the Lower Cambrian, and a post-arc sedimentary sequence of all Ordovician and younger Western, Central and Eastern belt lithologies follows.

Cooper (1989) notes that while both models may explain aspects of New Zealand's Lower Palaeozoic geology, they are unfortunately lacking in detail. Two main objections are raised to Shelley's model: (1) The grouping of the Western and Central Belts as lying adjacent to each other during the Cambrian (there is no Cambrian in the Western Belt), (2) The separation of the Eastern and Central belts in terms of their Cambrian - Ordovician successions (both have similar Late Cambrian-Ordovician successions). Crook and Feary's interpretation of the Central Belt as being a dismembered island arc is generally accepted, however their grouping of post-Cambrian Western, Central and Eastern Belt successions together as a post arc sedimentary sequence does not explain the major facies differences between the belts (Cooper, 1989).

2.5. Two Terrane Model

Cooper (1979) recognised that the Central and Eastern sedimentary belts share greater genetic and stratigraphic similarity than the Eastern and Western belts. The Central and Eastern belts have nearly identical post-Cambrian successions. On this basis Cooper (1984) and Bishop et al. (1985) divided the Palaeozoic of NW Nelson into two separate tectonostratigraphic terranes: the Golden Bay Terrane (Central and Eastern Belts) and Karamea Terrane (Western Belt). These names were later changed by Cooper (1989) to the Takaka Terrane (Golden Bay Terrane) and the Buller Terrane (Karamea Terrane). In the two-terrane model, the Central Belt is considered to be basement to the Eastern Belt, and has been thrust westwards over the Western Sedimentary Belt. Thus the terrane boundary, the Anatoki Thrust, is inferred to be east-dipping (Figure 2.4b), rather than originally horizontal, as is implied by Grindley's model (Cooper, 1989). The Central Belt and Eastern Belts are believed to have originally lain some distance from the Western

Belt, implying considerable strike slip movement before westward overthrusting took place (Cooper, 1989).

The Takaka Terrane is composed of a collage of tectonic slices - termed *fault-bounded slices* by Cooper (1986, 1989) and Cooper and Tulloch (1992) (Figure 2.4a) - each with its own different internal stratigraphy (Figure 2.3, 2.4). The Central belt is composed of at least 11 fault bounded slices, containing a diverse array of lithologic units and lithofacies, inferred to be the telescoped remnants of an once extensive volcanic arc (Figure 2.3, 2.5) (Cooper and Tulloch, 1992).

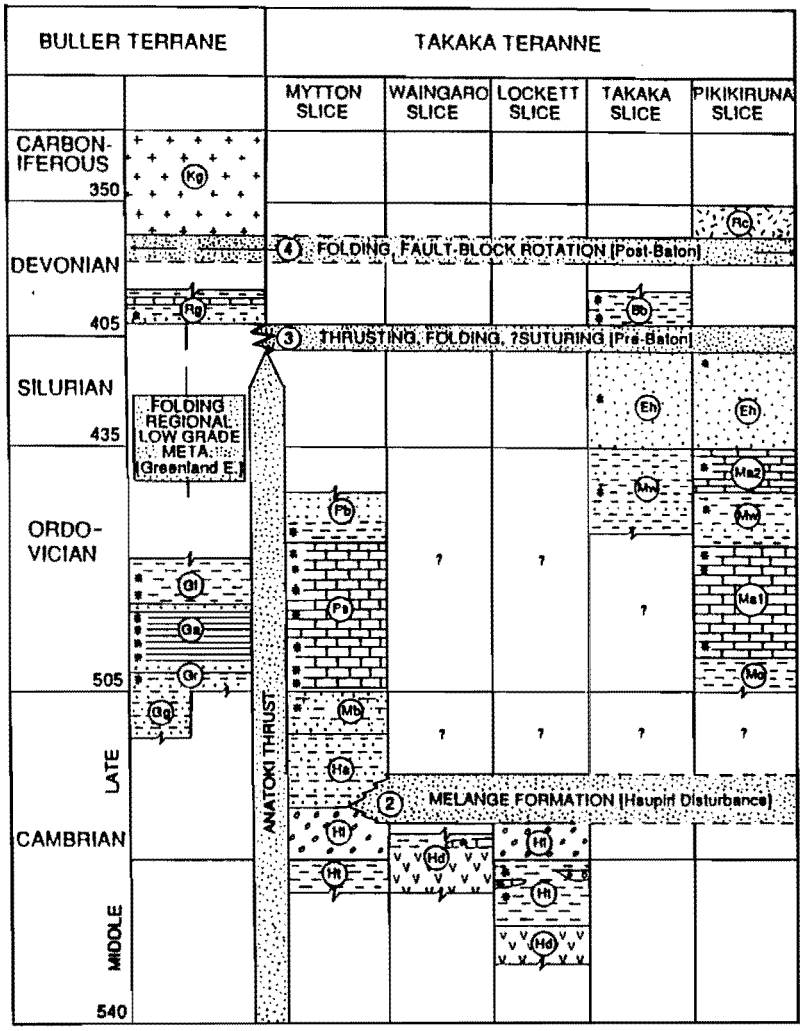

Figure 2.3: Terrane sequences of the northern part of Northwest Nelson, showing 5 of the 11 or more tectonic slices. The most likely time of suturing (basal Devonian) is indicated. *Hd* = Devil River Volcanics, *Ht* = Tasman Formation, *Hl* = Lockett Conglomerate, *Ha* = Anatoki Formation (after Cooper and Tulloch, 1992).

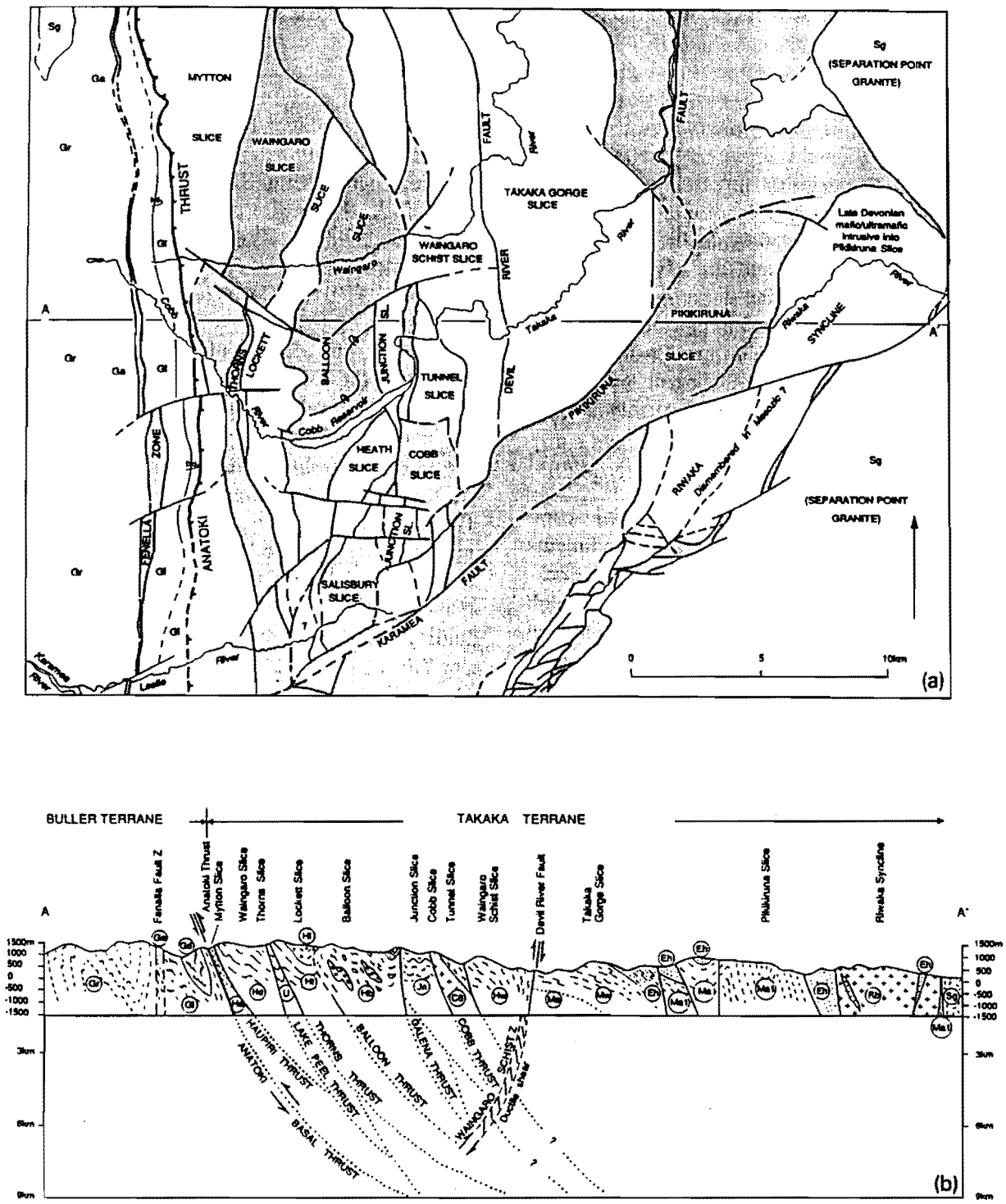

Figure 2.4: (a) Map of Fault Bounded Slices within the Takaka Terrane, central Northwest Nelson. (b) Cross-section A-A' showing a listric system of major faults. Symbol *Hd* represents 'Devil River Volcanics' (after Cooper and Tulloch, 1992).

Fault Bounded Slice	**Lithology**
Waingaro Schist Zone	Greenschist facies highly strained metavolcanic schist
Tunnel	Melange zone containing a variety of sedimentary and igneous rocks: *Northeast Melange*
Cobb	Altered ultramafics: *Cobb Igneous Complex*
Junction	Feldspathic sandstone and siltstone turbidites: *Junction Formation*
Salisbury	Tholeiitic basalts: *Mataki/Salisbury Volcanics*, overlain by polymict volcanic conglomerate: *Salisbury Conglomerate*
Heath	Siltstone, limestone and andesitic to dacitic volcanics: *Heath Volcanics*
Balloon	Melange zone of variably deformed turbidites and exotic blocks: *Balloon Melange*
Lockett	Siliceous chertwacke, siltstone, limestone and debris flow conglomerates: *Tasman Formation*, overlain by granule to cobble polymict conglomerate: *Lockett Conglomerate*
Thorns	Limestone with rare black sandstone and volcaniclastics: *Tasman Formation*
Waingaro	Basaltic to basaltic andesitic volcanics interbedded with turbidites: *Benson Volcanics*
Mytton	Limestone, sandstone, shales and rare granule conglomerates: *Summit Limestone* and *Baldy Formations*

Figure 2.5: Lithologic units of the Fault Bounded Slices of the Central Belt, Cobb Valley area (compiled from Cooper, 1993, Munker, 1993, Pound, 1993).

2.6. Previous Work on Cambrian Volcanics Within the Central Belt

The first worker to mention the volcanic rocks of the 'Haupiri Series' was Bell (1907). He describes tuffs, agglomerates, dykes, plugs and flows of *basic to semibasic affinity*, noting that they were extensively altered. Bell also noted that the volcanics appeared to form two northerly trending belts, one in the head-waters of Snow's River and another in the Slate River.

The name *Devil River Volcanics* was first proposed by Grindley (1961) for the Cambrian volcanics within the Haupiri Group, and was used in the subsequent New Zealand Geological Survey 1:63,360 lithostratigraphic map series (Takaka, Farewell-Kahurangi, Cobb, Wangapeka). The type locality for the volcanics was nominated on the western side of Devil River Peak (Figure 1.2) (Grindley, 1971). Grindley recognises two phases of volcanism within the volcanics:

1. A minor basal acidic phase consisting of pink weathering rhyolites and dacites forming tabular flows and crystal tuffs (Cobb, Waingaro and Baton Valleys).
2. Andesitic to basaltic lava flows, agglomerates, breccias, and interbedded green current bedded or finely laminated tuffaceous sediments (forming the bulk of the Devil River Volcanics).

A thick porphyritic andesite sill intruding the top of the volcanic pile is mapped on Mount Snowden and further to the north. Grindley (1978) suggests that the Devil River Volcanics are an island arc suite erupted onto oceanic or thinned sialic crust.

Devil River Volcanics in the Mount Benson area were studied by Coleman, 1971. He describes a thick (900m) sequence of volcaniclastic sediments and interbedded lava flows. Lavas were found to range from andesitic-basalt to andesite. Based on petrological evidence, Coleman inferred that the volcanics were a calc-alkaline suite related to island arc volcanism.

Reconnaissance geochemical work on Devil River Volcanics was undertaken by Powell (1986a). Ti-Zr and Cr-Y abundances suggested island arc affinities, consistent with the large proportion of fragmentary material in the volcanic succession. The presence of arc ankaramites was also noted. These are porphyritic high-Mg basalts that are high in Ni, Cr, and low in Zr and TiO2. Powell infers the presence of ankaramatic lavas to indicate intra-arc rifting or the subduction of a spreading ridge.

The two terrane model has been adopted in more recent papers and the Central Belt has been mapped in terms of Fault-bounded Slices (Cooper, 1986, 1989, Stewart, 1988, Pound 1993, Munker, 1993). Within this context it has become apparent that what was previously mapped as Devil River Volcanics by Grindley and co-workers, may contain more than one suite of volcanics. As no data on the Devil River Volcanics in the vicinity of the type section was available, workers have given different names to the various volcanics until links can be established.

Volcanics within the Balloon and Salisbury/Mataki fault bounded slices have been mapped and described by Stewart (1988). The Balloon slice contains hornblende andesite sills (Heath Volcanics). Major and trace element geochemistry suggests that the andesites are calc-alkaline and are of convergent margin origin (Stewart, 1988). Pound (1993) suggests that the Heath Volcanics represent a calc-alkaline continental arc. Tholeiitic basalts outcrop in the Mataki/Salisbury slice. A definitive tectonic setting was not established from the basalts geochemistry, however, based on sedimentological evidence Stewart (1988) inferred the basalts to be of seamount origin. In contrast, Pound (1993) postulates that the basalts are of back arc origin.

Munker (1993) has studied the Benson Volcanics within the Waingaro Fault Bounded slice. Three basaltic to basaltic-andesitic volcanic suites are recognised, interbedded in a non-volcanic trough turbidite sequence. The suites show an evolution from low-K island arc tholeiite through to more evolved calc-alkaline and high-K volcanics. Doleritic intrusions cut the sequence, showing compositions indicative of intraplate settings.

CHAPTER THREE: FIELD RELATIONSHIPS

3.1 Stratigraphy

Figure 3.1 shows the stratigraphy established from mapping. The mapped volcanics are considered to be part of the Devil River Volcanics because they are in close proximity to the type-section on the Devil Range (see Figure 1.2). A geological map of the Anatoki Range area is included in the map pocket at the back of this thesis. Figures 3.2 and 3.3 show measured representative sections and their inferred relationships. Two different suites of volcanic rock have been identified within the Devil River Volcanics, based on field and geochemical evidence. The *Circular Bush suite* is composed of volcanic derived submarine mass flows and intercalated tuffs, which contain basaltic-andesitic and andesitic volcanic material with subordinate basalt and rhyolite. The *Paradise suite* contains basaltic pillow lavas and rarer massive flows and pillow breccias. Underlying these two suites is the *Christmas Conglomerate Member*, which contains predominantly sedimentary-rock clasts (chert, siltstone, sandstone) but contains some basaltic-andesitic clasts, and is thus grouped with the Devil River Volcanics. Interbedded with and overlying the Devil River Volcanics are sandstones and siltstones with relatively little volcanic material, which are inferred to represent the background sedimentation . These grade upward into *Tasman Formation-like* lithologies (laminated siltstones, sandstones, chertwacke, thin debris flow conglomerate).

Grindley (1971) maps a thick unit of *"porphyritic andesite containing sheared xenoliths of andesite porphyrite"* as outcropping on the Anatoki Range. This, however, was not observed where mapped. Rocks fitting the description of the Anatoki Formation could not be found where they had been mapped on the Anatoki Range (see Figure 1.2).

Petrology of the sandstones, siltstones and tuffacous sandstones is discussed in this chapter where appropriate. Petrology of flows, intrusives, volcanic clasts and tuffs is discussed in the following chapter.

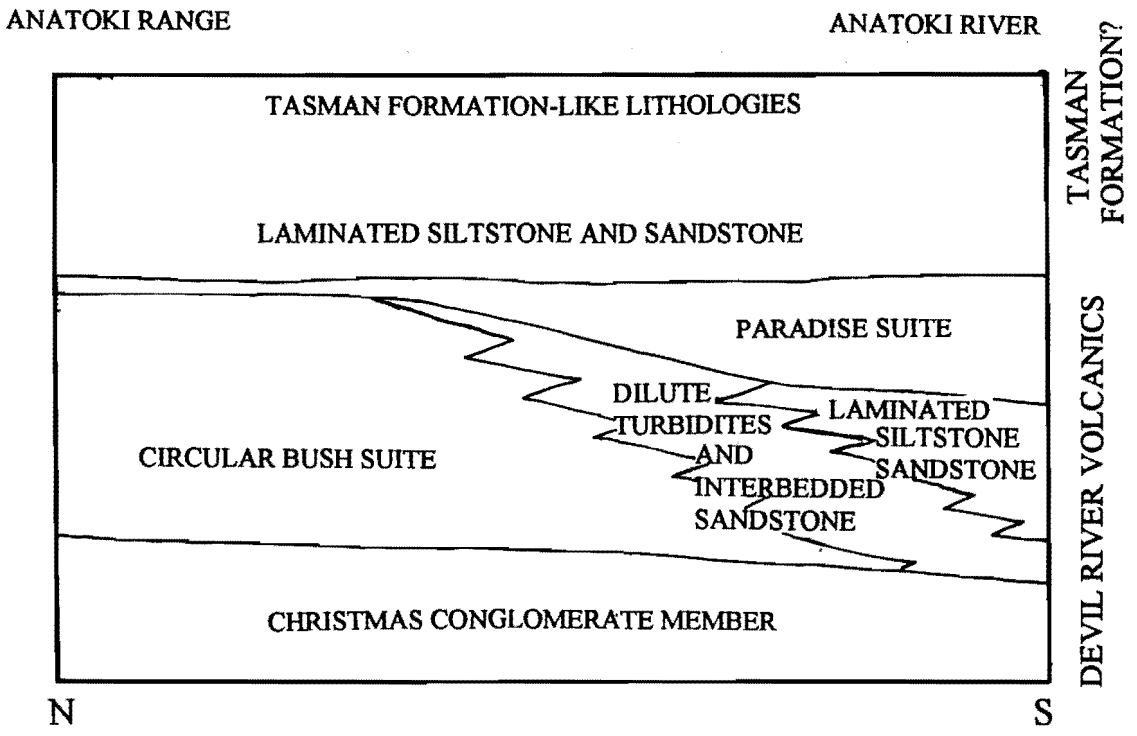

Figure 3.1: Inferred stratigraphic relationships within the Devil River Volcanics in the Anatoki Range, Anatoki River area.

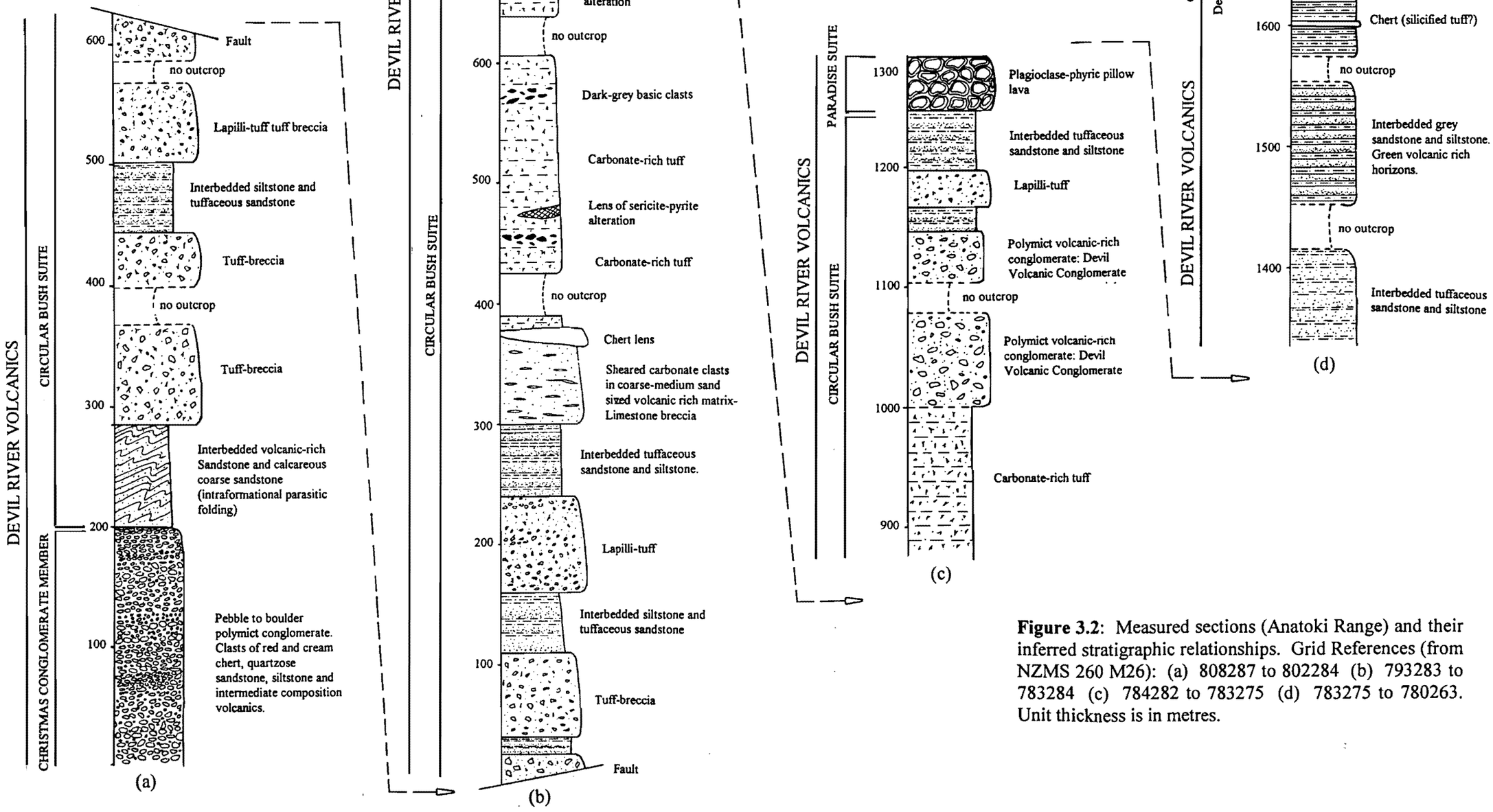

Figure 3.2: Measured sections (Anatoki Range) and their inferred stratigraphic relationships. Grid References (from NZMS 260 M26): (a) 808287 to 802284 (b) 793283 to 783284 (c) 784282 to 783275 (d) 783275 to 780263. Unit thickness is in metres.

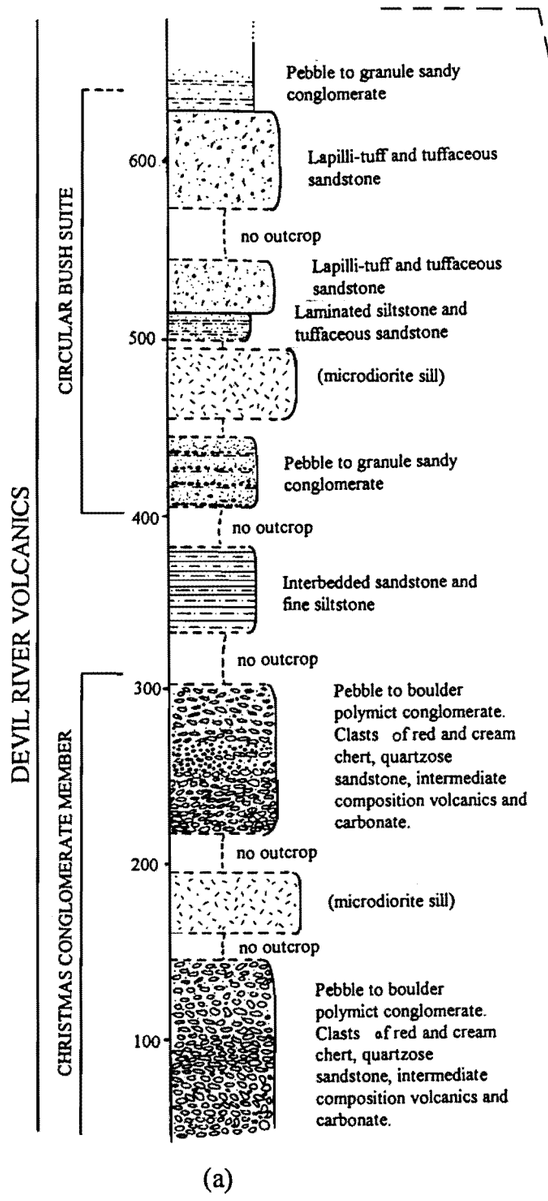

(a)

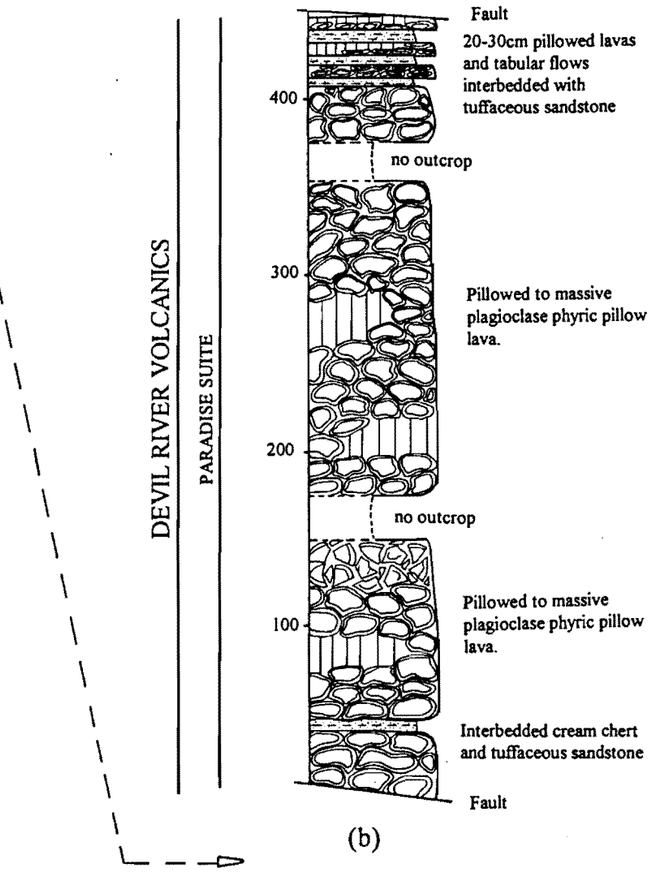

(b)

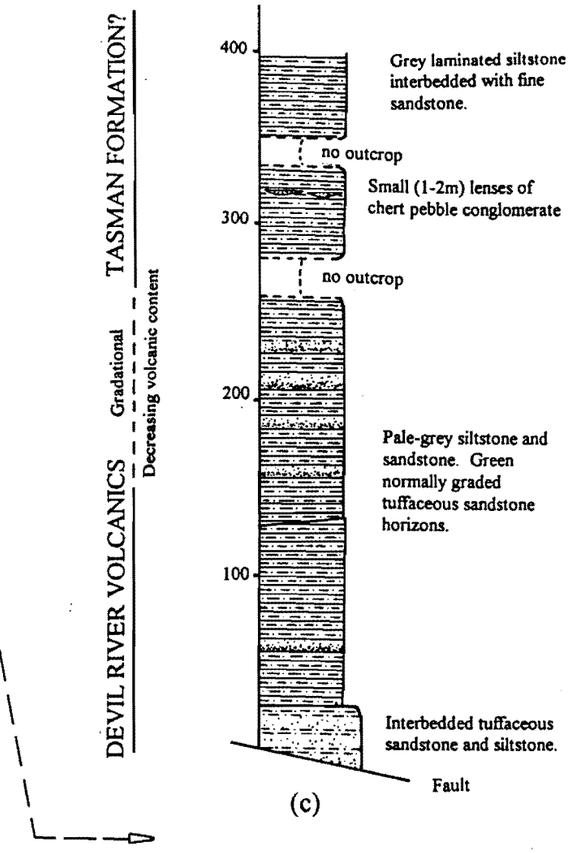

(c)

Figure 3.3: Measured sections (Anatoki River) and their inferred stratigraphic relationships. Grid References (from NZMS 260 M26): (a) 805308 to 797306 (b) 791305 to 785305 (c) 783304 to 782295. Unit thickness is in metres.

3.1.1 Christmas Conglomerate Member

The name *Christmas Conglomerate Member* is proposed for rocks on the Anatoki Range previously mapped by Grindley (1971) as Lockett Conglomerate (see Figure 1.2). True Lockett Conglomerate stratigraphically overlies the Tasman Formation and Devil River Volcanics (Grindley, 1971). However mapping suggests that the conglomerate lies at, or near, the base of the Devil River Volcanics (Figures 3.2a and 3.3a). The best exposure is along the Anatoki Range (NZMS 260 M26: 806286 to 812288) and in the Anatoki River near the confluence of a creek draining Mount Christmas (M26: 807309). No stratigraphic bottom was found, and its thickness must be at least 300 metres.

The Christmas Conglomerate consists of pebble to boulder sized, matrix supported, polymict conglomerate (Figure 3.4). Clasts range from subrounded to rounded, and are mostly composed of sedimentary material, with lesser amounts of volcanics. Red and cream coloured chert are prominent in outcrop. Clast populations were counted at three locations in the field (Figure 3.7). The matrix is poorly sorted, coarse to medium sandstone, which has a strongly developed tectonic fabric in many places.

Near the contact with the overlying Devil River Volcanics gravel filled channels and rare cross bedding were observed, indicating younging towards the volcanics. Graded beds, 40 cm to 2 metres thick, were seen at several locations (e.g., M26: 808287 and 806308) (Figure 3.5).

The conglomerate shows variable response to strain which is believed to be a function of: (1) clast size and (2) the relative percentage of matrix. Coarse, matrix supported horizons show little response to strain, but framework supported pebble conglomerate exhibits a well defined fabric and steeply plunging stretching lineation, parallel to the dip-direction of east dipping cleavage. The pebble sized clasts show variable response to strain (Figure 3.6). Most clasts have been rotated and flattened parallel to the fabric.

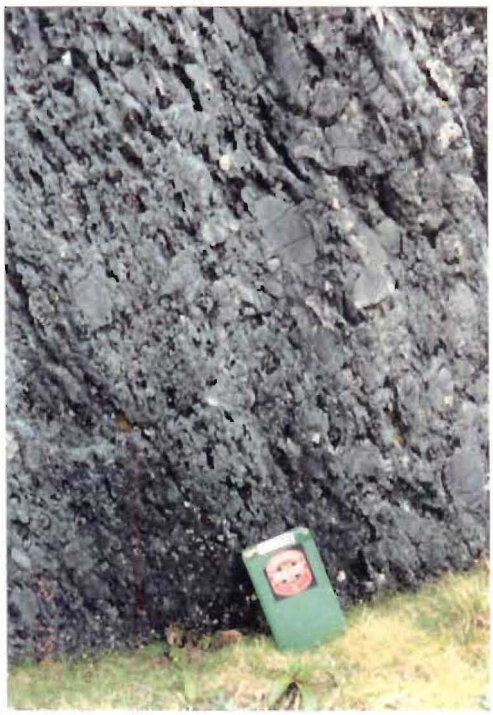

Figure 3.4: Typical outcrop of Christmas Conglomerate. Clasts are elongate parallel to an east dipping cleavage.

Figure 3.5: Crudely (normally?) graded beds within the Christmas Conglomerate.

Figure 3.6: Hand-specimen of Christmas Conglomerate. Clasts include red/cream chert, sandstone and volcanics. Clasts show rotation and extension parallel to S_1. The large sandstone clast at the left has reacted in a brittle fashion to stress. The fissures produced have been infilled by quartz.

However, a small number of clasts have deformed in a brittle manner, and are cut by regular space fractures perpendicular to the stretching direction. These fractures have been filled by precipitation of quartz during subsequent pressure solution.

LITHOLOGY	Grid Ref. 808287	Grid Ref. 807286	Grid Ref. 806307
Red and cream chert	34 %	42%	35 %
Grey-green and pale-grey sandstone	35 %	31 %	36 %
Fine-medium grained volcanic.	23 %	25 %	15-20%
Coarse grained volcanic	4 %	-	-
Carbonate material	4%	2%	5%

Figure 3.7: Clasts populations of the Christmas Conglomerate, Anatoki Range, Anatoki River (grid references from NZMS 260: M26).

3.1.2 Circular Bush Suite

(a) Epiclastic Tuff-breccias and Lapilli-tuff

Volcanic tuff-breccias make up much of the exposure along the Anatoki Range section of the Devil River Volcanics. Breccia sheets range in thickness from 20 to 150 metres (Figures 3.2a and 3.2b).

The breccias are generally matrix supported, consisting of cream coloured clasts set in a green crystal rich matrix (Figure 3.8). Clasts range from 1 to 40 cm in diameter (lapilli to block) and are angular to sub-rounded. Cream coloured andesitic clasts are the most prominent in outcrop, some exhibiting primary flow banding (Figure 3.9). Darker, more basic clasts are also present. The matrix is very similar in composition to the clasts, made up of coarse to medium sandstone sized ash with broken and intact crystals of plagioclase feldspar and chlorite (after pyroxene and amphibole). No size grading is evident among the clasts or in the matrix.

An interesting unit outcrops within the tuff breccias near Circular Bush (M26: 783284). It is a two metre thick lens of monomict clast supported breccia containing 4 to 40 cm sub angular clasts of rhyolite (Figure 3.10).

Intercalated with the epiclastic tuff breccias are medium to coarse lapilli tuffs and tuffaceous sandstones that have relatively few clasts, but are almost identical in composition to the matrix of the tuff breccias (Figure 3.11). These horizons range from 5 to 30 metres in thickness. A pressure solution cleavage (S_1) is apparent in many of these units. The tuffs and lapilli tuffs contain cuspate shaped vitric shards, which are produced by phreatomagmatic volcanic eruptions, and equidimensional angular shards

characteristic of hydroclastic processes (see section 4.1.2). This suggests an input of volcanic material from both subaerial and submarine sources.

The absence of sorting, lack of internal sedimentary structure, the ash rich nature, and the presence of large clasts in abundant matrix suggests that the tuff breccias have been emplaced as high density subaqueous debris flows. In such flows particle freedom is inhibited thus size grading is not developed or only poorly developed (Cas and Wright, 1987). Such types of deposits are common in submarine volcanic successions (Houghton and Landis, 1989, Busby-Spera, 1988, and Sigurdsson et al., 1980) . Very little rounding takes place in debris flows, so any rounding of clasts must have taken place prior to entrainment in debris flows, probably as a result of tumbling downslope.

The densely packed framework supported nature of the rhyolite breccia suggests that it is relatively close to its source. Thus this unit is inferred to be a thin channel deposit within the tuff-breccia and lapilli-tuff that has tapped a rhyolitic source, suggesting proximity a rhyolite flow or dome.

Figure 3.8: Angular - subangular andesite clasts in a crystal-rich matrix. Tuff-breccia, Anatoki Range.

Figure 3.9: Sub-angular clasts in tuff-breccia (note large flow-banded clast at bottom right).

Figure 3.10: Lens of rhyolite clast breccia.

Figure 3.11: Lapilli-tuff, tuff hand-specimen, showing a pressure solution cleavage parallel to S_1

Figure 3.12: Debris flow unit with elongate carbonate lenses (weathered out) which have been sheared parallel to S_1. The carbonate lenses were probably limestone clasts originally.

Figure 3.13: Normally graded bedding, asymmetric scour marks and poorly developed flame structures in turbidity current deposited reworked tuffaceous sandstone/siltstone. The sample is orientated as taken in the field (ie. overturned).

(b) Limestone Breccia

This unit crops out on the Anatoki Range - thickness varies from 40 to 100 metres (Figure 3.2b). It consists of lenticular carbonate lenses, generally 10 to 20 cm and rarely up to 2 m, in a matrix of coarse to medium volcanic sandstone. The shape and orientation of the carbonate lenses appears to be due to later shearing parallel to an S_1 cleavage (Figure 3.12). A thin section of a carbonate lens was examined, and was found to be very fine grained, containing almost entirely calcite/dolomite, with a small amount of quartz. The relative purity of the carbonate lenses suggests that they were originally limestone clasts, rather than concretionary features (concretions would contain abundant sandy sediment cemented by carbonate). The dispersion of large clasts throughout an abundant sandy matrix is consistent with a debris flow origin.

(c) Tuffaceous Sandstone and Siltstone

Tuffaceous sandstone and siltstone beds are found throughout the study area - thicknesses range from 5 to 40 metres. They are very distinctive in the field, typically weathering to red and green. They consist of 2 to 4 cm beds of coarse to fine, tuffaceous sandstone, interbedded with 1 to 3 cm beds of thinly laminated (.5 - 2mm) fine sandstone and siltstone (Figure 3.13). Normal graded bedding, asymmetric scours at the base of coarse sands, small ripples and poorly developed flame structures within this unit provide useful indicators of younging direction. Numerous small conjugate faults truncate bedding, offsetting beds on a centimetre scale.

Thin section examination shows the coarse layers contain variably altered plagioclase (sericitized, sausuratized and albitized), andesitic to basaltic rock fragments, epidote and subangular grains of chlorite (replacing ferromagnesian minerals - pyroxene?

amphibole?). The medium to fine sandstones contain sericite, albite, epidote and chlorite.

The tuffaceous sandstones/siltstones are interpreted to have been deposited by turbidity currents. The finely laminated layers are either the result of settling from suspension as the current slows (Bouma d-horizon) or background sedimentation.

(d) Carbonate-rich Tuffs

This unit outcrops near Circular Bush on the Anatoki Range and varies in thickness from 50 to 180 metres. It is composed of pale grey, medium to fine grained, tuffaceous sandstone, which typically weathers to an orange colour. In outcrop it has a flaggy appearance that is produced by the intersection of shallow east and west dipping cleavages. Shearing and alteration has, unfortunately, obliterated most of the original textures. Dark grey lenticular clasts, 2 to 25 cm in diameter, can be recognised at some localities, and thin (1-2cm) laminations can be observed at others. Small (<10m) highly sericitized lenses concordant with bedding containing finely disseminated pyrite (<5%) are also present.

Thin sections show that the rock is extremely altered. Totally sericitized and albitized plagioclase laths 1-2 mm long are set in a medium to fine grained matrix of sericite, albite, chlorite and ilmenite. The rock contains abundant secondary carbonate, mostly ankerite, which is probably the result of carbonate metasomatism. It appears to fill voids, so its deposition may have been controlled by an original sorting.

The obliteration of original textures and minerals by metasomatism and deformation makes interpretation of this rock type difficult. The relatively intact plagioclase laths suggest a pyroclastic origin. The sericite-pyrite lenses could be the product of

metamorphism, or more probably, they are small centres of submarine hydrothermal activity.

(e) Devil Volcanic Conglomerate

This unit outcrops in the headwaters of the Devil River and is 100 metres thick. It consists of grey, well indurated, polymict, matrix supported, massive, volcanic conglomerate.

Clasts vary from subangular to subrounded and range in size from 2 to 50 cm with an average size of 3-4 cm. Clasts are predominantly andesitic, with lesser amounts of pale grey siltstone and chert (silicified volcanic?). No size sorting was observed in the field. The matrix is grey-blue in colour, sandy and poorly sorted. It has a strong fabric in some places which appears to wrap and flow around some of the larger clasts. The fabric is probably as a result of shearing parallel to the S_1 cleavage (see section 3.2.7).

The Devil Volcanic Conglomerate is inferred to have been deposited as a submarine debris flow, composed primarily of volcanic material, but with other material from within the depositional basin (siltstone, chert). The rounding of clasts may reflect fluvial or shoreline processes.

(f) Cherts

A small number of thin chert lenses and sheets occur within the volcanic pile. Typically they are grey (weathering to pale orange) massive, and very well indurated. Ghosts of small angular crystal (2-4mm) are observed on fresh surfaces. True marine cherts are normally found interbedded with hemipelagic and pelagic sediments, in relatively quiescent environments. However the cherts encountered are interbedded with volcanic

derived debris flows, which would have been deposited very rapidly. Thus the mapped cherts must either be tectonically included or silicified pyroclastic airfall material. The later interpretation is preferred (see section 4.1.2).

3.1.3 Paradise Suite

The name *Paradise suite* is proposed for the thick sequence of pillow lavas outcropping in the Anatoki River downstream from the confluence of Paradise Creek (M26: 785305 to 794304). A total thickness of 900 metres is exposed at the core of a major anticline, suggesting a minimum true thickness of at least 400 metres. Pillow lava outcropping on the Anatoki Range is also included within the Paradise suite (783275), but is only 50 metres thick.

The Paradise suite consists of basaltic pillows (Figure 3.14, 3.15) and rarer massive tabular flows (Figure 3.3b). Both types of lava are vesicular and porphyritic, containing 1 to 8 mm plagioclase phenocrysts set in a fine grained, pale to dark green, vesicular ground mass (Figure 3.16). The pillows range in size from 10 cm to 2 metres. Interstices between pillows are often filled with cream coloured material containing epidote and zoisite (interpreted as altered glassy material), and more rarely, red coloured chert.

At the top of the lava pile in the Anatoki River small (20 to 30 cm) pillows and tabular flows are interbedded with thin, green to cream, coarse to medium, tuffaceous sandstones (Figure 3.3b). However, within the lava pile sediments are relatively rare.

Figure 3.14: Paradise suite pillow lava, Anatoki River. Note distinctive weathering pattern of concentric rings.

Figure 3.15: Paradise suite pillow lava, Anatoki River (pillow interstices are filled with red chert).

Figure 3.16: Hand-specimen of Paradise suite pillow lava. Large (1-8mm) glomeroporphyritic masses of plagioclase are set in a fine grained groundmass.

3.1.4 Sandstone and Siltstone

A thick sequence of predominantly non-volcanic sandstone and siltstone interfingers with and overlies the volcanics (Figures 3.2d, 3.3a, 3.3c, 3.17). The sandstones are grey green, fine to medium grained, moderately well sorted and form 2 to 20 cm thick beds. The sandstones contain quartz, albite, sericite, chlorite and pyrite. Rarely the sandstones show normal grading or small crossbeds. Interbedded with the sandstones are 2 to 10 cm thick beds of finely laminated (1-5mm) grey siltstone.

Some sandstone horizons are darker green in colour as a result of a higher volcanic derived component (Figure 3.2d, 3.3c) . Often these layers exhibit normal grading and are inferred either to be dilute turbidity current deposited volcanic material or pyroclastic airfall. The laminated sandstones and siltstones progressively grade into 'Tasman-like' lithologies (siliceous chertwacke, laminated siltstones, sandstones) (Figure 3.2d, 3.3c).

Lower in the sequence there are a series of gravelly turbidites (Figure 3.3a). These consist of 2 to 30cm thick beds of poorly sorted, subangular to subrounded, coarse sand to small pebble sized conglomerate (Figure 3.18). Commonly small channels (1 m wide by 10-20 cm thick) can be observed at the base of the conglomerate units. These horizons contain quartz, chlorite, albite, volcanic and sandstone rock fragments. Interbedded with these are medium to fine, thinly laminated sandstones.

The interbedded sandstones and laminated siltstones are believed to be the background sedimentation, deposited in a basin adjacent to the volcanic arc. The thin conglomeratic and coarse sandstone beds are probably distal turbidity currents which have sampled intrabasinal material (sandstone and volcanic detritus).

In a number of localities these rocks contain abundant disseminated pyrite (up to 10%). Normally these units show almost total obliteration of original sedimentary structure and

texture and have a pale green colour. The pyrite and accompanying alteration could be attributed to a number of factors; Sea-floor hydrothermal activity, alteration by metasomatic fluids during late diagenesis and metamorphism or metasomatism related to granite emplacement (Separation Point Granite?). It is unclear which is the major contributor.

3.1.5 Intrusive Rocks

(a) Sills

Sills of intermediate composition outcrop throughout the study area, occurring as 10 to 50 metre thick sheets, generally concordant with bedding. Unfortunately no contacts with surrounding rock were observed, however, the sheets are found at a number of stratigraphic positions (intruding Christmas Conglomerate Member, Circular Bush suite volcaniclastics) (Figure 3.3a), which is consistent with an intrusive origin, rather than effusive. The sills have a weakly developed tectonic fabric, which suggests that they pre-date cleavage development. Outcrops are typically iron stained. Fresh surfaces show a medium grained equigranular texture of plagioclase, a chloritic altered ferromagnesian mineral (hornblende?), and quartz. The relationship of the sills to the fragmental and effusive rocks within the Devil River Volcanics is unclear based on the field evidence, but will be discussed later in relation to geochemistry.

(b) Basic Dykes

A small number of thin basic dykes intrude the volcanic pile, cross-cutting F_1 fabrics, and are much younger than the volcanic rocks and first deformation (see section 3.2.8). The dykes vary in colour from pale to dark grey, are fine grained and range in thickness from

20 to 50cm (Figure 3.19). Chilled margins were observed on one dyke, with small grey speckles toward the centre of the dyke that are inferred to be sheared out vesicles.

3.1.6 Anatoki Formation

The Anatoki Formation is found to the west of the Haupiri Fault. It consists of a sequence of well-bedded, red, green and grey turbidites with lenses of granule to pebble conglomerate, greenschist and rare ultramafic lenses. The type section on the western margin of the Haupiri range, where Braithwaite (1968) has measured a section of 1300 metres without a top or base. It does not occur on the Anatoki Range as previously mapped by Grindley (1971) (Figure 1.2).

3.1.7 Waingaro Schist

The Waingaro Schist outcrops to the east of the mapped area, bounded by the Whitehorn Thrust. It consists of weakly foliated, greenschist facies, metamorphosed older Central Belt lithologies (predominantly metavolcanics - Devil River Volcanics ?) (Powell, 1984).

Figure 3.17: Interbedded medium to fine sandstone and laminated grey siltstone (Anatoki River).

Figure 3.18: Turbidity current deposited pebble to granule sandy conglomerate interbedded with fine to medium sandstone (Anatoki River).

Figure 3.19: Basic dyke intruding a microdiorite sill, Anatoki River.

3.2 Structure

The structure of the Anatoki Range and Anatoki River area at first appears to be relatively simple. However, detailed mapping shows reversals of face within often relatively uniformly dipping stratigraphy, indicative of large tight or isoclinal folds (see geological map, cross sections and block diagram in map pocket at the back). These folds have been given informal names for the purposes of mapping and description. Folds can be correlated from the Anatoki Range down to the Anatoki River. However, the succession on the Anatoki Range dips moderately to steeply east and fold axial planes dip east, whereas bedding and fold axial planes all dip steeply west in the Anatoki River. A number of north-south trending faults cut through the area, the largest being the Haupiri Fault. Younger E-W trending faults offset beds by tens of metres and show both dextral and sinistral sense of movement.

3.2.1 Devil Anticline and Devil Syncline

On the Anatoki Range the Devil Anticline is a tight to isoclinal, moderate to gently plunging, gently inclined fold. The axial plane strikes N to NNE, dips to the east, and the fold hinge plunges northward at 20°. Rocks on the eastern limb of the fold are the right way up, whereas the western limb is overturned. A thrust is inferred to occupy the hinge zone, probably forming contemporaneously with folding. The Devil Anticline appears to continue into the Anatoki River area. However, here it is not as tight, is steeply inclined, and the axial plane dips steeply to the west (instead of the east).

The Devil Syncline occurs to the east of the Devil Anticline and is a tight moderately inclined, gently plunging structure. Again the axial plane strikes N to NNE and the hinge plunges to the north at 15° to 20°. The fold has a moderately dipping upright limb and a steeply dipping overturned limb. Parasitic mesoscopic scale folds in tuffaceous

sandstones and siltstones delineate the major structure. The Devil Syncline also appears to continue into the Anatoki River and again the axial plane changes from east dipping to west dipping.

3.2.2 Lucifer Anticline

Relatively little is known about the Lucifer Anticline. It is inferred to fold the Christmas Conglomerate. However the massive nature of the conglomerate and lack of distinctive marker beds make delineation of this fold difficult. It appears to be very similar in style and attitude to the Devil Anticline and Syncline.

3.2.3 Lindsay Syncline

The Lindsay Syncline is very well exposed on southern face of Peak 1772 m, southeast of Lake Sparrow (Figure 3.20). Photographs of it have been shown in many publications on Northwest Nelson geology (Grindley, 1978, Cooper, 1979, Grindley, 1982). It folds laminated sandstones, siltstones and volcanic sandstones believed to be Tasman Formation, stratigraphically overlying the Devil River Volcanics. Grindley (1982, Figure 2 caption) describes the syncline as occurring on the western face of Devil River Peak. He describes it as *' a large recumbent fold.....Fold vergence is to the north and the axial plane dips east at 40°.....The fold and underlying Lindsay Thrust Plane were produced during the early (F_1) phase of the Tuhua Orogeny and tilted during later (F_2) phase.'* Unfortunately this caption appears to be in error. Devil River Peak clearly has no western face, the syncline actually outcrops on the southern face (which is shown in his photograph). Whilst the axial plane does dip to the east (40-50^0), it strikes NNW, and the fold hinge plunges gently northward (10-15°). The fold has a gently easterly dipping upright limb and a steeply dipping overturned limb, fold vergence is clearly not to the north but to the west.

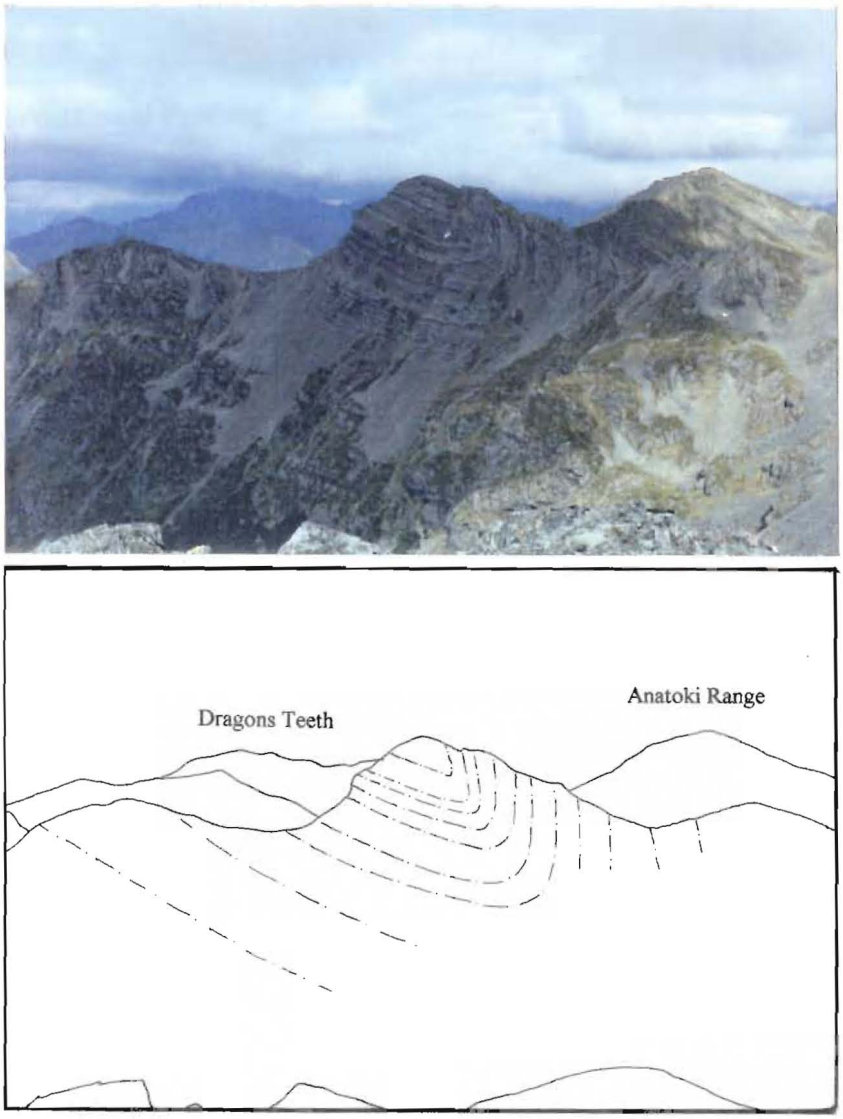

Figure 3.20: Lindsay syncline looking toward the northwest. The axial plane of the fold dips at 40-50° to the east an the fold hinge plunges towards the NNW at 10-20°. The syncline folds *Tasman Formation-like* lithologies.

Figure 3.21: Intraformational folding within interbedded volcanic sandstone and carbonate-rich coarse sandstone. Fold axial planes strike N and dip at 60-70° to the east. Folds "step-up" to a major anticline (Lucifer Anticline) to the east.

3.2.4 Intraformational Folding

Intraformational folding is well developed in the interbedded coarse grey volcanic sandstones and carbonate rich coarse sandstone on the Anatoki Range (Figure 3.21). These folds are parasitic and 'step up' to the major structures. Parasitic folding is better developed in these well bedded units. The massive volcanic breccias are not able to fold on this scale.

3.2.5 Haupiri Fault

The Haupiri Fault separates the Anatoki Formation from the Devil River Volcanics. It is best exposed in the Anatoki River near the Anatoki Forks Hut. The fault strikes roughly north-south and dips at 60° to 70° to the east. A strong fabric is produced in the rock near the fault, along with small metre scale folds. The fault probably accompanied the development of the large north-south striking tight to isoclinal folds, suggesting it was initially a reverse-fault or steeply dipping thrust.

A large lens of calc-mylonite is tectonically included in the fault zone near the Anatoki Forks Hut. It has a strong fabric sub-parallel to the dip of the fault. A prominent lineation dips moderately southeast. An orientated sample was taken of the calc-mylonite, and thin sections were cut parallel and perpendicular to the lineation. The rock is totally recrystallised to a fine/medium grained mosaic of calcite and rare quartz. Thin (1-4 mm) streaked out dolomitic layers may result from the transposition of bedding. Dolomitic porphyroclast-like structures exhibit ambiguous senses of shear. In the section cut parallel to the lineation, whilst many calcite grains are equidimensional due to recrystallisation, some grains exhibit a well developed elongation at 20-30° to the lithological layering. The lithologic layering and direction of grain elongation appear to

form a crude S-C fabric, with the lithologic layers representing the C-planes and the elongate grains lying in the S-planes.

Calcite c-axes and twin lamellae were measured using a universal stage. From these measurements, compression directions were determined using the method of Turner (1953). Figures 3.22 and 3.23 summarise these results. Calcite c-axes in the section parallel to the lineation appear to form two maxima, rather than one as is normally the case (Turner, 1953). The compression directions calculated for this section fall within a girdle at an angle of 15-20^{o} to the layering, and with the mean compression axis position at a high angle to the grain elongation (Figures 3.22, 3.23). This suggests a normal sense of movement. Any substantial deformation completely twins all calcite, which is then in an orientation unfavourable for further twinning. Due to this, visible twinning in complexly deformed and/or well crystallised material, such as the sample examined, usually represents a late minor strain unrelated to the principal deformation (Shelley, 1993). Thus it may be that the normal sense of shear recorded here for the Haupiri Fault represents only its last ductile movement phase. Universal stage methods were only applied to one sample, so further work is required to support these findings.

The results suggest that the last movement on the Haupiri Fault had a normal sense of shear. Harrison (1993) and Rennison (1992) record normal movement for the sub-parallel Anatoki Thrust, which occurs 8 km to the west of the Haupiri Fault. Rennison (1992) notes that normal movement appears to post-date emplacement of the Cretaceous Olympus Pluton. The later stage normal movement may have taken place at a similar time to that on the Anatoki Thrust.

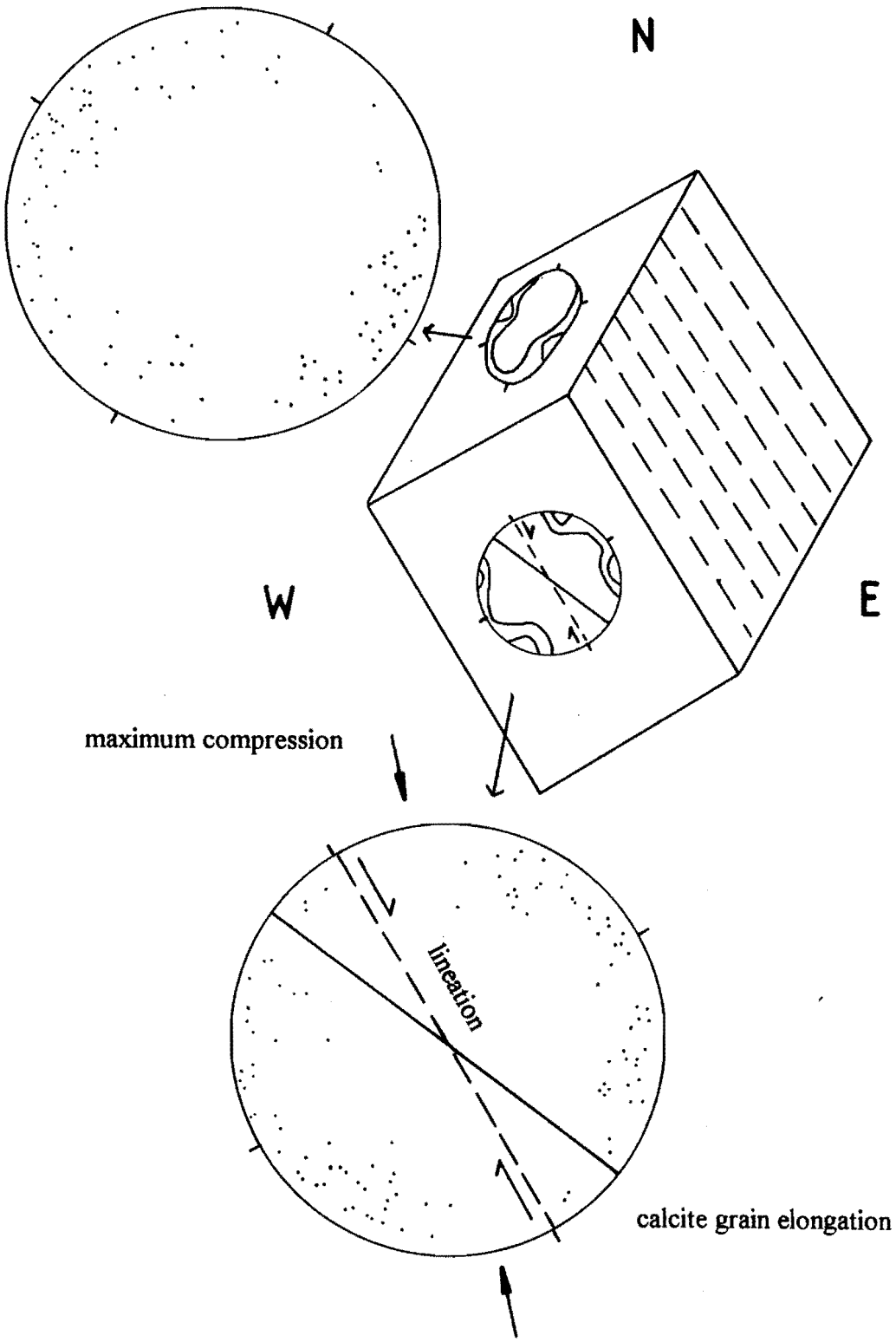

Figure 3.22: Stereographic plots of calcite c-axes in sections perpendicular and parallel to the lineation of a calc-mylonite from the Haupiri Fault. The Haupiri Fault dips sub-parallel to the orientated sample and strikes north-south (view looking from the south).

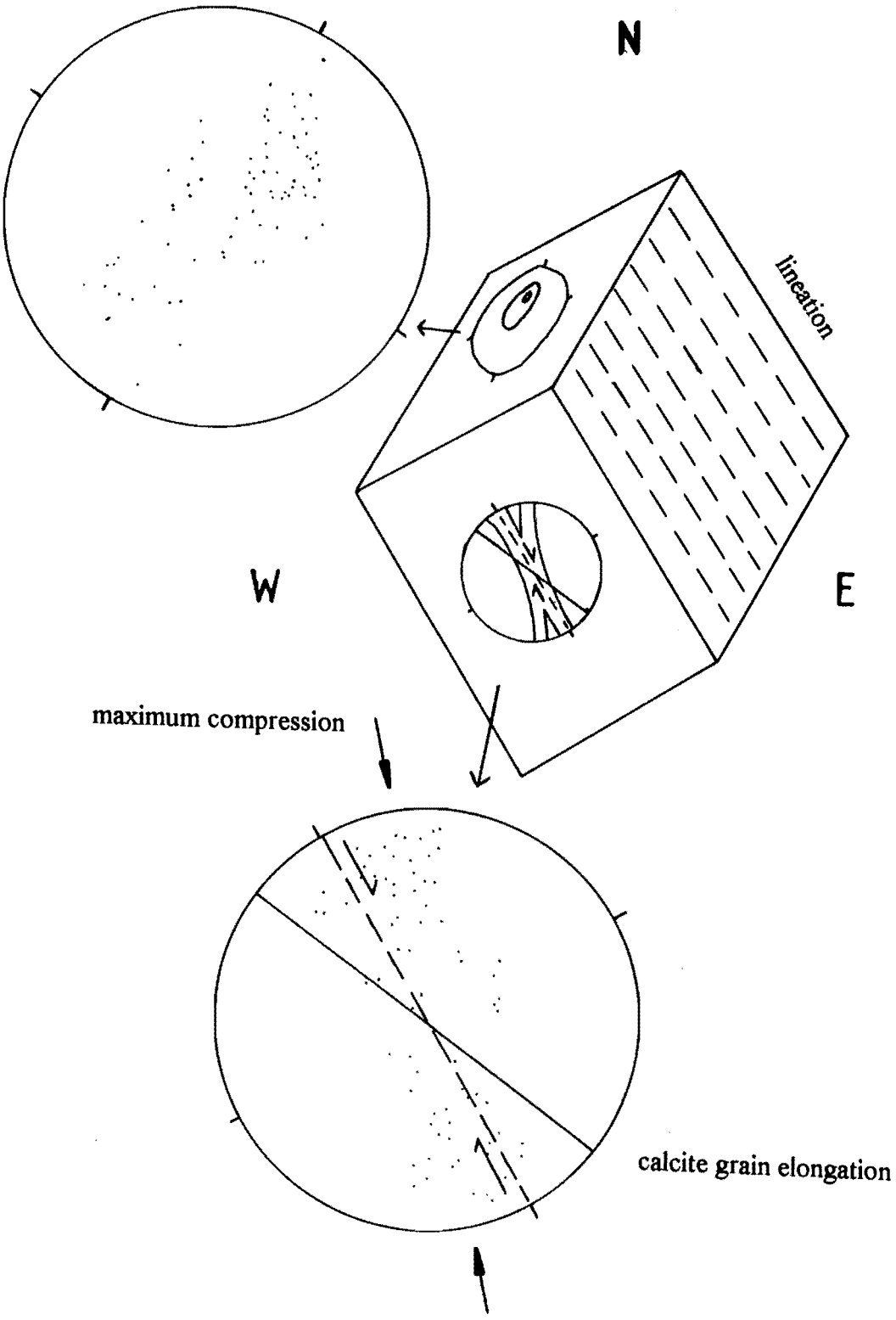

Figure 3.23: Stereographic plots of compression directions (determined using the method of Turner, 1953). Sections are parallel and perpendicular to the lineation. Haupiri Fault dips and strikes sub-parallel to the orientated sample.

3.2.6 East West Trending Faults

The area mapped is dissected by a number of roughly east-west trending dextral and sinistral faults. They are not obvious in the field, but are inferred by offsets in beds by tens of metres or more. The age of faulting is not well constrained. Similar faults in the Cobb Valley have been suggested to be of Late Tertiary to Quaternary age (Munker, 1993, Stewart, 1988).

3.2.7 Cleavage

Two intersecting cleavages occur throughout the mapped area. However, many of the rock types are not amenable to cleavage development, thus cleavage is often not well defined or not observed at all. On the Anatoki Range a NW to NNE striking, east dipping (30 to 80°) cleavage (S_1), is intersected by a NNW to NE striking, predominantly west dipping (40-85°) cleavage (S_2) (Figure 3.24a). The S_1 cleavage is best expressed as axial planer cleavage parallel to parasitic folds in finer grained and more well bedded units, particularly the interbedded volcanic sandstone and calcareous coarse sandstone (Figure 3.21). It is also seen in fine grained sandstones and siltstones. In the more massive units (volcanic derived debris flows) S_1 is sometimes seen as a spaced fracture cleavage (1-5 cm spacing) or as a weak pressure solution cleavage (Figure 3.11). S_2 is most commonly seen as thin (<2mm) quartz and carbonate veins or a 2-5 cm spaced fracture cleavage, normally perpendicular to S_1. Crenulation of S_1 by S_2 is observed at some localities.

In the Anatoki River area S_1 strikes NNW to ENE and dips 30 to 80° west. S_2 strikes NW to NNE, and tends to dip more steeply (60 to 85°) (Figure 3.24b). S_1 and S_2 show similar relationships and styles of cleavage in this area as on the Anatoki Range, but both cleavages appear to have been rotated. The change in dip of S_1 corresponds to the

change in dip of S_0 and fold axial planes. S_1 in the Anatoki River is not thought to correlate with S_2 on the Anatoki Range.

3.2.8 Structural Interpretation

The reversal of bedding and fold axial surfaces from predominantly east dipping (Anatoki Range) to predominantly west dipping (Anatoki River) creates a structural problem.

Bedding /S_1 cleavage intersection lineations were plotted in order to determine the orientation of folding. A tight group of points defining the axis of folding would be expected if there was only one phase of folding. However Figure 3.25a shows a strong concentration of lineations plunging to the north, but many lineations do not fit this trend, and are scattered about a great circle distribution. This could be attributed to one of two factors (1) the lineations have been refolded by a later phase (2) the S_1 cleavage is overprinted over already deformed rocks (ie. the rocks were folded before the superposition of the S_1 cleavage). The problem with the second solution is that there is no obvious cause for the cleavage development.

Poles to S_1 cleavage are shown in Figure 3.25b. These are very scattered, but appear to form a cone (small circle distribution), rather than a single concentration of points. This suggests post-F_1 refolding. The exact geometry of refolding can not be determined, as the stereographic pattern produced depends on the orientation of the lineation was before folding, which is unknown. The S_2 cleavage may be an axial planar cleavage which accompanied a second phase of folding (F_2), of unknown orientation. Both S_1 and S_2 maintain their angular relationship between the Anatoki River and the Anatoki Range, but change in dip and dip-direction, suggesting post S_2 rotation (ie. an F_3 phase of folding).

Thus it is probable that the rocks have undergone three phases of folding as follows:

F_1: Tight to isoclinal folding producing an axial planar cleavage (S_1). This may relate to westward overthrusting along north-south trending, east dipping thrust faults.

F_2: Refolding producing a second axial planar cleavage (S_2), probably with an axis of folding at a similar orientation to F_1. F_2 may have happened relatively soon after F_1.

F_3: A third phase of folding about an unknown axes which rotates S_1 and S_2 but does not change significantly the angle between the two cleavages. This refolding appears to be less ductile in style (there does not appear to be an associated cleavage), which would suggest it occurred at a higher structural level.

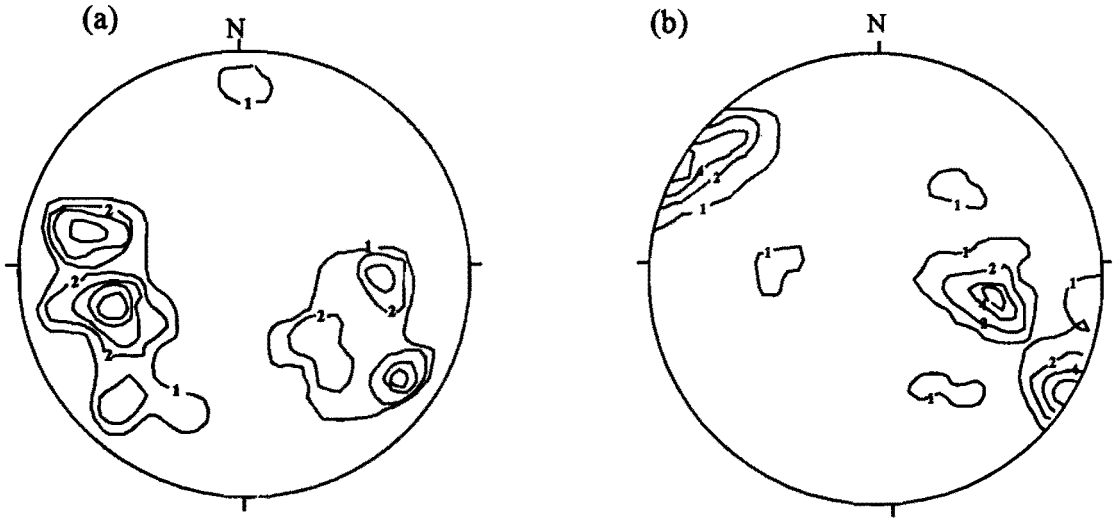

Figure 3.24: Schimdt net contoured stereographic projections of poles to cleavages (a) Anatoki Range area n=58 (b) Anatoki River area n=53

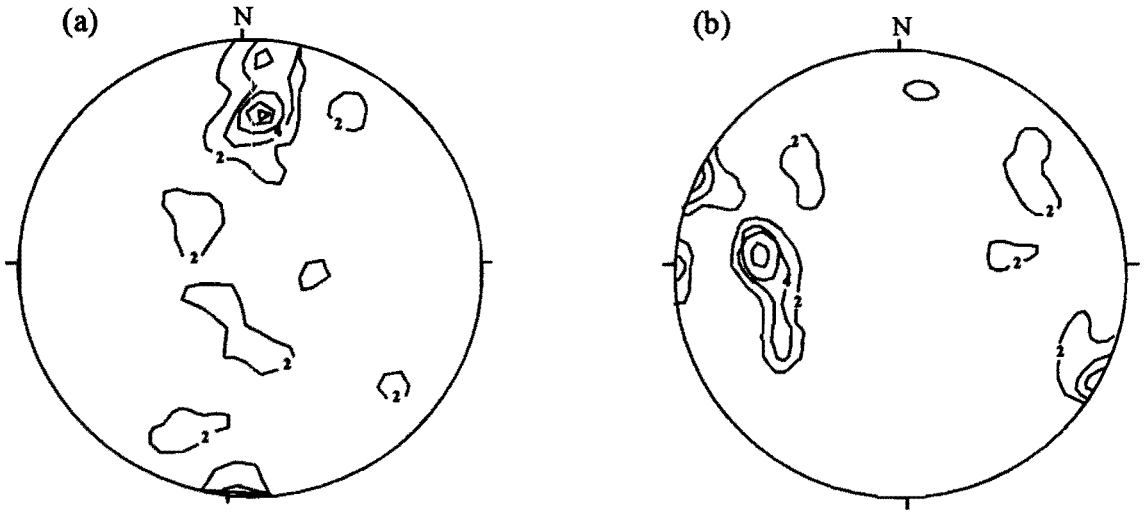

Figure 3.25: Schimdt net contoured stereographic projections of : (a) Bedding/S_1 cleavage intersection lineations, n=62 (b) Poles to S_1 cleavage, n=56. Contour values in percent.

CHAPTER FOUR: PETROLOGY OF THE VOLCANIC ROCKS

In this chapter the petrology of volcanic and volcaniclastic rocks is discussed. Selected thin section descriptions are presented in Appendix 2.

4.1 Circular Bush Suite

4.1.1 Volcanic Clasts

Andesitic clasts typically exhibit porphyritic textures. Plagioclase is saussuritized and sericitized, occurring as 2 to 5mm tabular to subrounded crystals. Relic zoning within the plagioclase is preserved as alternating saussuritized and sericitized layers (Figure 4.1). It seems that sericite tends to replace the more calcic plagioclase, whereas zoisite replaces the sodic plagioclase (Dr D. Shelley, pers. comm.). Euhedral crystals, 1-3 mm in diameter, totally replaced by chlorite are predominantly altered amphibole (hornblende?), although some have the crystal form of pyroxene. The groundmass is typically felsitic, often with albite enclosing tiny crystals of sericite and chlorite forming a poikilomosaic texture. Magnetite and ilmenite are finely disseminated throughout the groundmass. Amygdales are infilled by recrystallised quartz.

Basaltic-andesitic clasts are very altered, but some show a porphyritic texture. Sericitized (3-5 mm) plagioclase phenocrysts are set in an intergranular groundmass of saussuritized plagioclase microlites, chlorite and epidote. Vesicles are infilled by carbonate and quartz. One section contained fresh pale yellow pleochroic amphibole (Figure 4.2). The two basaltic clasts examined were quite altered, consisting of an intersertal texture of plagioclase in a groundmass of albite, epidote, zoisite and chlorite.

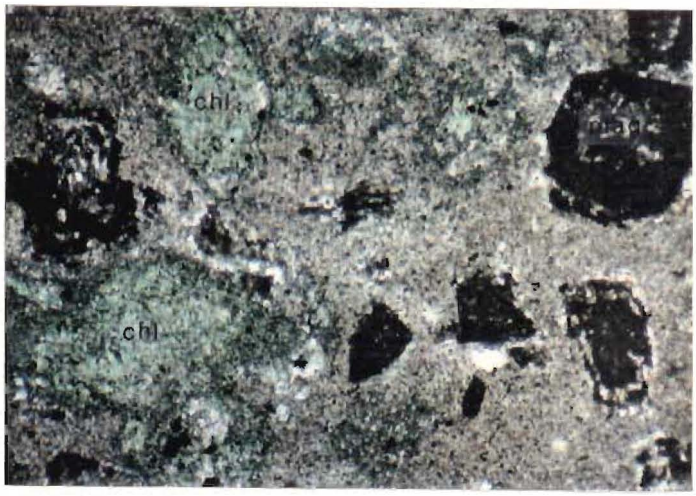

Figure 4.1: Andesite clast (DRM 74) showing a porphyritic texture. Plagioclase is saussuritized and sericitized, some preserving relic compositional zoning. Chlorite has replaced amphibole and clinopyroxene (field of view 4mm across).

Figure 4.2: Yellow pleochroic amphibole phenocryst in a basaltic-andesite clast (DRM 20) (field of view 3mm across).

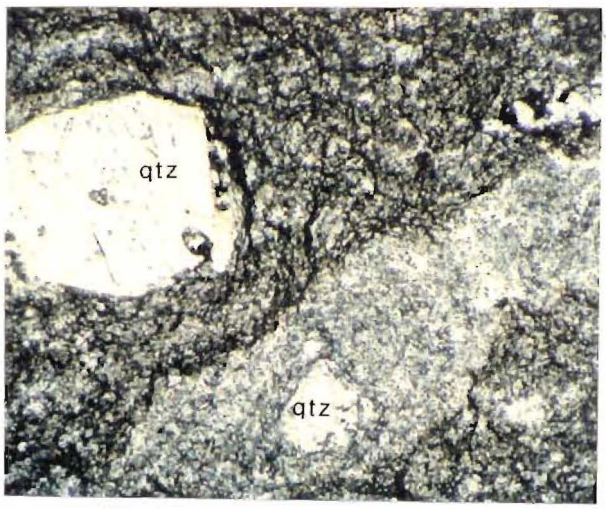

Figure 4.3: Rhyolite clast (DRM 71) with embayed quartz phenocryst, containing small rounded glassy inclusions, in a felsitic flow banded groundmass of quartz, albite, sericite and rare chlorite (field of view 3mm across).

Thin sections of three rhyolite clasts were examined. All are weakly porphyritic, containing phenocrysts of quartz, plagioclase, K-feldspar? and biotite set in a felsitic cryptocrystalline groundmass. Quartz phenocrysts are embayed (indicative of resorption) and often contain small rounded inclusions of fine grained quartz and albite (recrystallised fluid inclusions) (Figure 4.3). Plagioclase occurs as euhedral crystals, usually sericitized and overgrown by carbonate. Application of the Michel-Levy technique on preserved twins indicates that the plagioclase has been albitized (An 5 - 10%). K-feldspar may also be present. Biotite microphenocrysts are totally degraded to carbonate and a dark grey isotropic mineral, but still preserve biotite crystal form (Figure 4.4). Tiny (<.05mm) euhedral apatite crystals can be seen within some degraded biotite grains. The groundmass is composed of quartz, albite and sericite and minor chlorite, which often forms a poikilomosaic texture. DRM 71 shows primary flow banding, consisting of thin 1-2mm felsic layers interlaminated with slightly darker (more basic) layers (Figure 4.3).

4.1.2 Tuffs, Lapilli Tuffs

Reworked tuffs are interbedded with the epiclastic tuff-breccia and lapilli-tuffs (see sections). They are typically coarse to medium sand sized, composed of broken and intact crystals of variably sericitized and saussuritized plagioclase and chlorite (totally replacing amphibole and pyroxene). DRM 17 and DRM 41 both contain cuspate shards of tachylytic glass (Figure 4.5). Cuspate shards are produced by explosive magmatic or phreatomagmatic eruptions from (broken) pumiceous or scoriaceous material (Shelley, 1993). These types of shards are typically produced by subaerial volcanism, which implies a subaerial input of volcaniclastic material into these tuffs.

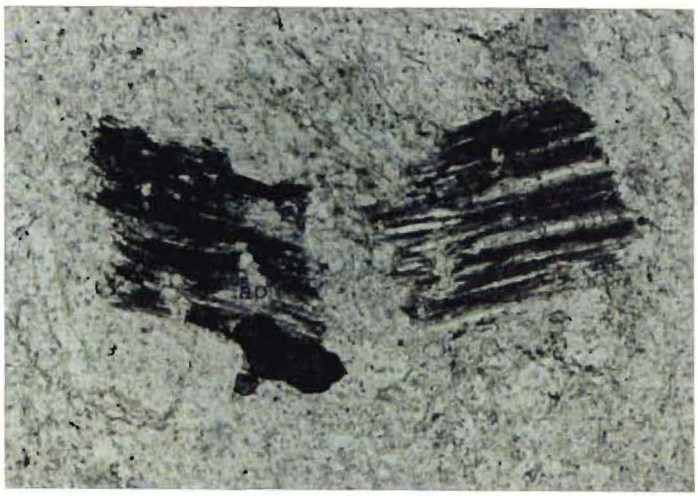

Figure 4.4: Biotite microphenocryst degraded to carbonate and a dark-grey isotropic mineral (rhyolite clast - DRM 72). Apatite occurs as small grains within the biotite (field of view 0.5 mm across).

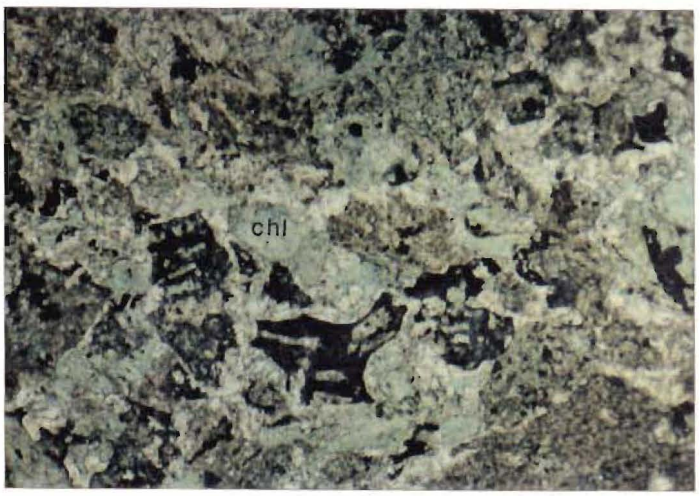

Figure 4.5: Cuspate vitric shards (produced by phreatomagmatic subaerial volcanism) in an altered reworked tuff (DRM 17). Chlorite has totally replaced ferromagnesian minerals (field of view 3 mm across).

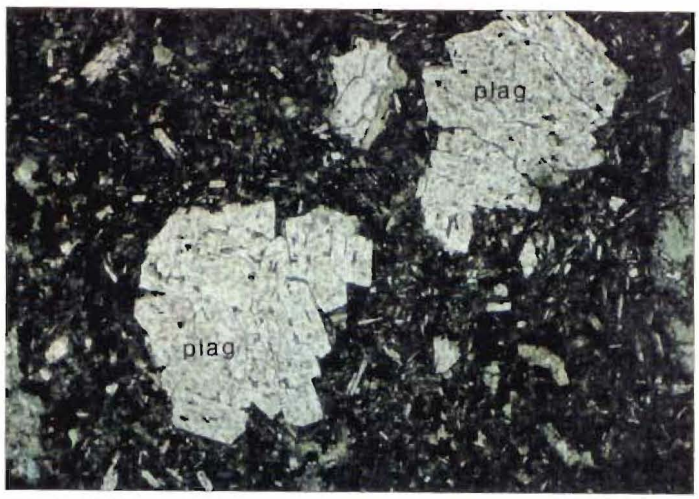

Figure 4.6: Paradise suite pillow lava (DRM 26). Glomeroporphyritic masses of plagioclase in a fine grained matrix of albite and chlorite. Plagioclase exhibits a sieve texture. Swallow tailed albite microlites in the groundmass indicate rapid quenching (field of view 4mm across).

DRM 3 and DRM 8 exhibit somewhat different textures. They contain broken and intact crystals of plagioclase and chlorite altered to hornblende and pyroxene. These show blocky, equidimensional form, indicative of quenching by water (hydroclastic fracturing). Thus the material in these deposits has most probably been formed by submarine explosive volcanism.

Samples from two chert lenses from within the volcanic pile were examined microscopically. One sample (DRM 137) contained 3-5 mm rounded clots of zoisite, quartz and epidote set in a fine grained felsitic matrix of quartz, albite and rare zoisite. Fine apatite needles are also present in the matrix. DRM 124 was made up of 3-6 mm angular grains (replaced by chlorite, zoisite and albite) in a recrystallised fine grained mosaic of quartz, albite and sericite. Small calcite crystals are also present. The chert lenses may represent silicified rhyolitic tuffs. The rounded clots in DRM 137 could be altered spherulites, whereas the angular features in DRM 124 may be altered feldspar crystals. They contain relatively low contents of SiO_2 for cherts (74-78 wt%) (see Geochemical Data Appendix), which would be consistent with the above (true marine cherts contain much higher SiO_2).

4.2 Paradise Suite

Seven thin sections of Paradise suite pillow lava were examined, each showing varying degrees of alteration.

Sample DRM 26 is the least altered pillow lava. It is composed of 2 to 5 mm glomeroporphyritic masses of weakly sericitized plagioclase set in a fine grained matrix (Figure 4.6). Determination of the feldspar composition using the Michel-Levy method shows that plagioclase has been albitized (An% ranges from 7% to 15%). Plagioclase exhibits a sieve texture consisting of finely dispersed clots of chlorite enclosed within it.

This was most probably originally volcanic glass. The groundmass consists of skeletal albite microlites immersed in a glassy mesostasis of chlorite +/- clinozoisite. Swallow tailed plagioclase albite microlites are common, indicative of rapid quenching. Small (<1mm) rounded vesicles are infilled with calcite rimmed by chlorite. Chlorite also replaces a number of small (<1mm) euhedral crystals that are likely to have been pyroxene.

Sample DRM 138 has undergone greater alteration than DRM 26 but still preserves many of the same textures. Plagioclase is sericitized, albitized and weakly saussuritized. The groundmass is overgrown by numerous small, yellow, high birefringence, grains of epidote. Vesicles, 1-5 mm in diameter, are infilled with quartz and chlorite.

The most altered pillow lava examined is DRM 92 (Figure 4.7). Plagioclase has been completely altered to a mixture of epidote + clinozoisite + zoisite (strongly saussuritized). The matrix has been almost completely recrystallised to sericite + chlorite + albite +/- zoisite. Small vesicles infilled with carbonate, rimmed by chlorite are distinguishable.

4.3 Intrusive Rocks

4.3.1 Microdiorite

Three sections of microdiorite were examined. They are relatively altered and show a fine grained intergranular to sub-ophitic texture. Albitized plagioclase is intergrown with chlorite (originally altered amphibole or pyroxene), albite and quartz. All samples contain leucoxene, which has formed as a breakdown product of ilmenite. Sample DRM 148 contains a small amount of unaltered hornblende (Figure 4.8).

Figure 4.7: Highly altered Paradise suite pillow lava (DRM 92). Highly saussuritized plagioclase phenocrysts are set in a groundmass altered to carbonate, sericite, zoisite and chlorite (field of view 4mm across).

Figure 4.8: Microdiorite (DRM 148) with green pleochroic hornblende in a matrix of albite, chlorite and quartz. Leucoxene has formed as a break-down product of ilmenite (field of view 1mm across).

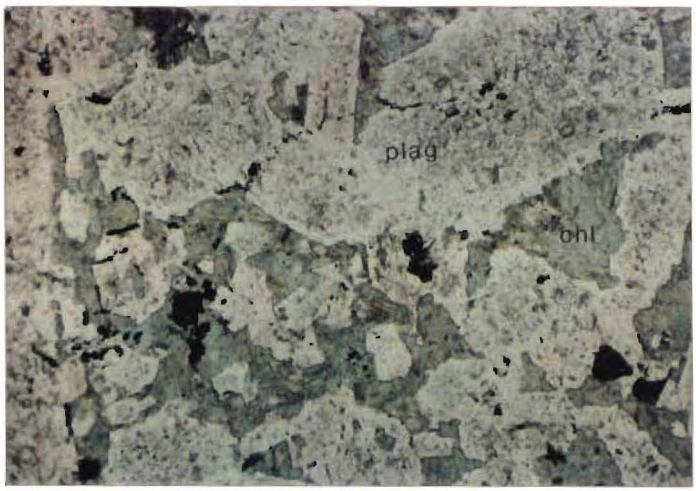

Figure 4.9: Basaltic andesite clast from the Christmas Conglomerate Member exhibiting an intersertal texture. Large (1-4mm) albitized and weakly sericitized plagioclase laths with interstices filled by chlorite and rare brown-green pleochroic hornblende (field of view 4mm across).

4.3.2 Basic Dykes

Two thin sections of basic dykes cutting the sequence were examined. They are fine grained, exhibiting an intergranular texture, consisting of albitized and sericitized plagioclase laths intergrown with skeletal ilmenite, fined grained chlorite, sericite and minor magnetite. Plagioclase laths often contain small (<.1mm) apatite needles as inclusions. Many plagioclase laths have high aspect ratios, indicative of rapid quenching, suggesting emplacement into cool rock. One sample examined (DRM 112) contains 1-3 mm euhedral patches of carbonate + chlorite. These are either infilled vesicles or the altered remains of a phenocryst phase (pyroxene?).

4.4 Miscellaneous

One basaltic-andesite clast from the Christmas Conglomerate was examined. It exhibits an intersertal texture of large plagioclase (2-6 mm) laths (sericitized and albitized), with chlorite and rare green - brown pleochroic amphibole infilling the interstices (Figure 4.9). Magnetite is disseminated throughout.

One sample from the Devil Range of basaltic volcanic breccia was examined. This contained albitized and saussuritized plagioclase and large clinopyroxene crystals (7-20 mm) pseudomorphed by chlorite in the clasts and matrix.

4.5 Metamorphism

Relatively little work has been done on metamorphism within the Central Belt rocks. Powell (1986b) recognises two discrete pre-Devonian metamorphic/tectonic events within the core of the Central Belt. The earliest phase (M1) consisted of incipient recrystallisation under prehnite-pumpellyite to lower greenschist facies conditions, producing a mineral assemblage of :

quartz + albite + clinozoisite + chlorite + titanite +/- actinolite +/- carbonate +/- pumpellyite +/- prehnite +/- hematite

A second metamorphic event (M2) accompanied the formation of penetrative lineation and foliation, synkinematic with folding. This is of lower to upper greenschist facies and locally up to amphibolite facies (Shelley, 1981). It produced a mineral assemblage of:

ankerite + quartz + albite + chlorite + chlorite + rutile + muscovite

A third event (M3) (Cretaceous?), which is most apparent north of the Cobb River, was accompanied by little deformation (units affected show well-preserved earlier textures). Powell (1986b) also notes that metamorphic grade appeared to increase northwards through the Takaka Terrane.

The rocks studied here typically show a greenschist facies metamorphic mineral assemblage of:

chlorite + albite + sericite + zoisite + epidote +/- quartz +/- carbonate +/- clinozoisite

The metamorphic history of the studied rocks is difficult to determine as, according to Powell (1986b), there are three separate events in which greenschist facies pressures and temperatures were attained .

Much of the greenschist facies assemblage within the Paradise Pillow Lavas could probably be attributed to the M1 event. The differing degrees of alteration seen within the pillow lavas was probably caused by fluxing of the lava pile by hydrothermal (metasomatic) fluids soon after deposition. Seawater and diagenetic fluids percolating through the pile would have tended to alter the more permeable pillows, whereas impermeable parts would have remained relatively untouched.

Many of the tuff-breccias, lapilli-tuffs and tuffs contain abundant pressure solution seams, generally parallel to S_1 cleavage. Much of the alteration could be attributed to solution transfer during the deformation that accompanied this event. This appears to correlate with Powell's M2 event.

The basic dykes also contain a greenschist facies mineral assemblage, however they cross cut S_1 fabrics. This implies they have been emplaced post-Devonian, and therefore they must have been metamorphosed during M3.

CHAPTER FIVE: GEOCHEMISTRY

5.1 Introduction

Two distinctly different suites of volcanic rocks have been recognised within the volcanic pile. The older Circular Bush suite contains basalt, basaltic-andesite, andesite and minor rhyolite. The overlying Paradise suite is dominated by pillow basalts. The two suites show different geochemical trends implying differing petrogenetic histories. Basic dykes cutting the volcanic succession have different geochemical affinities from the Circular Bush and Paradise suites.

5.2 Method

33 samples were analysed for major and trace element compositions using a Philips PW1400 XRF spectrometer (see Appendix Three). Au and Mo tubes were used for trace elements and major elements were analysed using a Sc tube. Rock was crushed into pea sized fragments in a hydraulic crusher, then milled to a powder using a tungsten carbide ring mill. Samples for major element analysis were prepared as fused disks following the method of Norrish and Hutton (1969). Trace element analyses were carried out on 50 mm pressed powder pellets bonded with 7% PVA solution.

5.3 Effects of Metamorphism and Alteration on Elemental Abundances

All rocks studied have undergone varying degrees of alteration as a result of low grade metamorphism, hydrothermal alteration and metasomatism. Plagioclase is invariably altered to mixtures of albite, sericite, zoisite, clinozoisite, epidote and calcite. Ferromagnesian minerals (clinopyroxene, orthopyroxene, amphibole) are altered to chlorite, and quartz and carbonate veins are common. Comments on the effects of the

above are clearly required before drawing petrogenetic or tectonic interpretations from the data.

Na, Ba, Sr, K, and Rb are mobile in aqueous fluids, and therefore their abundances will be severely affected by the style of alteration that the rocks have undergone. Interpretation must therefore be largely based on elements that are relatively immobile under such conditions. HFSE (Nb, Zr, Y) and REE elements concentrations are believed to be largely unaffected, as are TiO_2, Th, Ni, Cr, MgO and P_2O_5 (Crawford et al, 1992). Silica concentrations are probably within 1-3% of primary values except for cases of secondary silicification, which can usually be identified from field evidence.

5.4 Classification

The TAS (total alkalis vs silica) (Figure 5.1) diagram of Le Maitre (1989) provides a useful starting point for discussion. Circular Bush suite rocks plot in a spectrum from basalt through to rhyolite with a compositional gap between 62 and 73 wt% SiO_2. The majority of samples is in the basaltic andesite to andesite range. Sills intruding the volcanic pile plot in the basaltic andesite field. Paradise suite rocks plot predominantly in the trachybasalt field. Whether this is indicative of original compositions is unclear, as the pillow lavas may have gained Na during subsequent metasomatism, and therefore originally would have been basalts. The later stage basic dykes also plot as basalts.

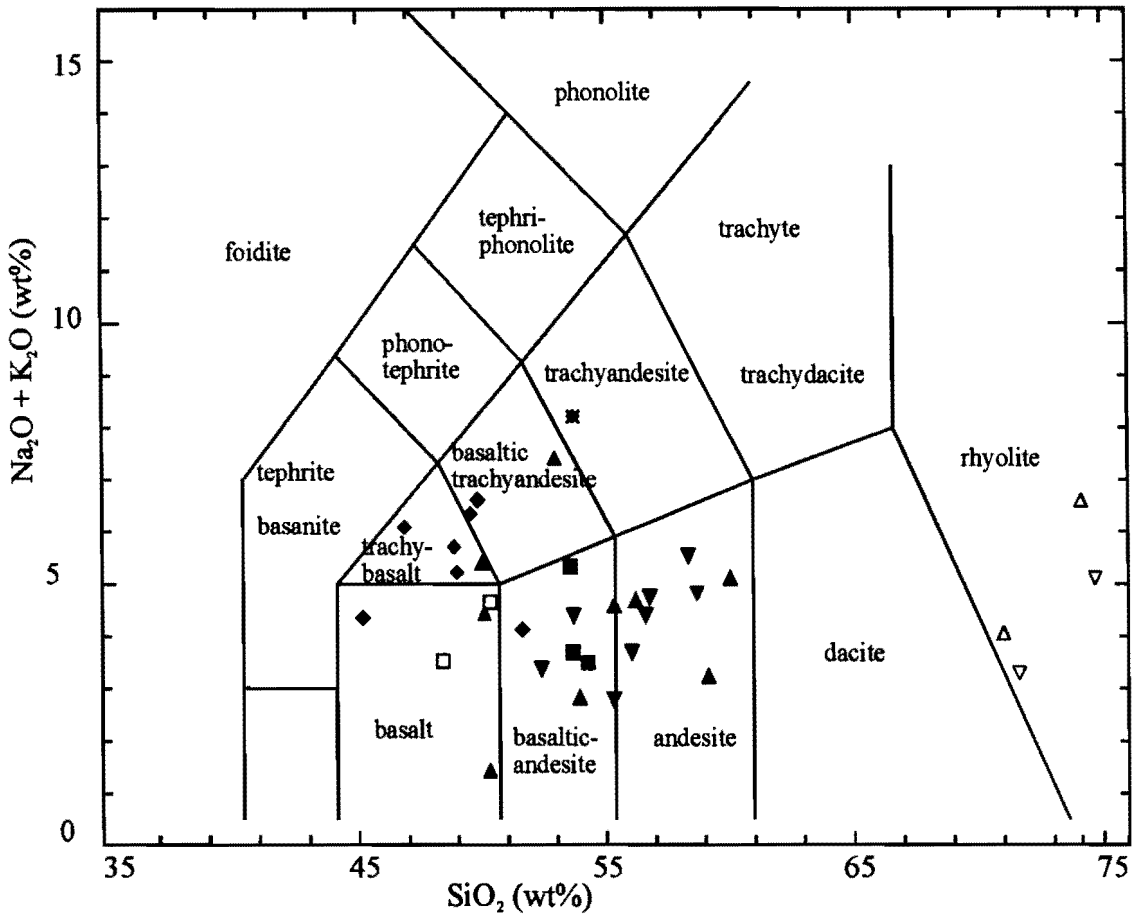

Figure 5.1: Studied data plotted on the TAS (total alkalis/silica) diagram of Le Maitre (1989)

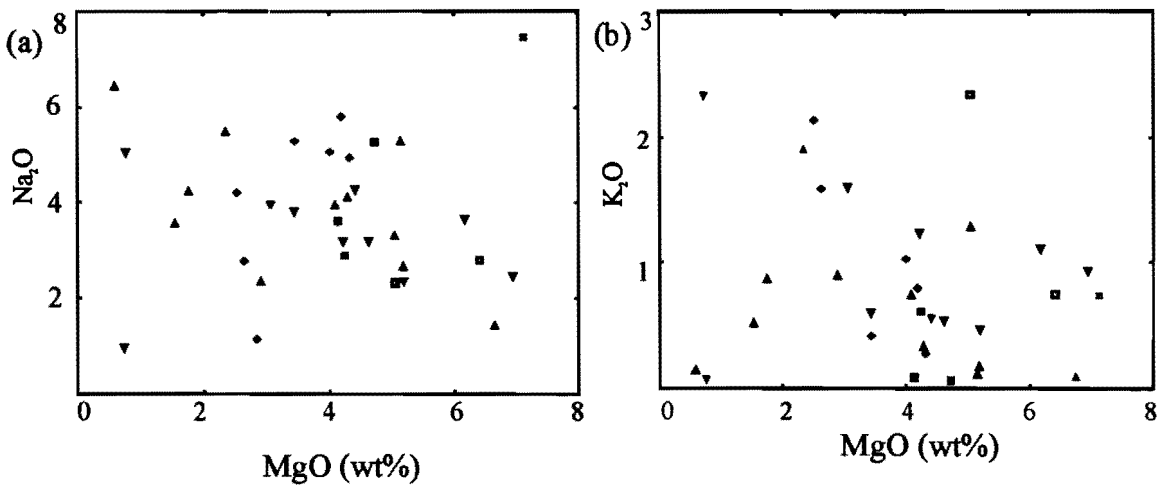

Figure 5.2: Harker variation diagrams of: (a) Na_2O vs MgO and (b) K_2O vs MgO

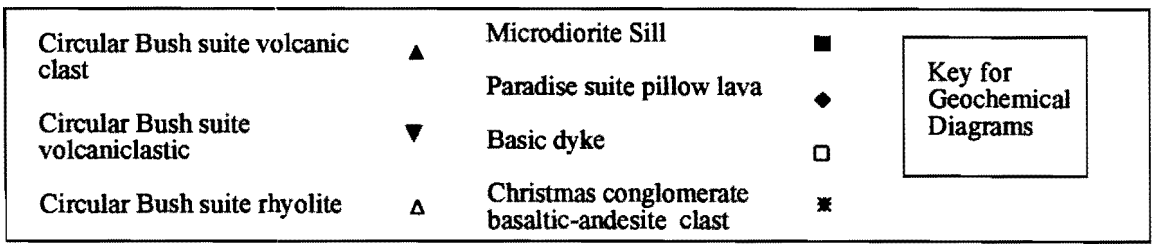

5.5 Major Elements

Figures (5.2, 5.3) show Harker variation diagrams of selected major elements (K_2O, Na_2O, Al_2O_3, FeO, TiO_2, P_2O_5) versus MgO, which is used as an inverse index of differentiation. K_2O and Na_2O both exhibit diffuse scattered plots as a result of their mobility during alteration (Figure 5.2a, 5.2b). Al_2O_3 shows a slight increase with fractionation, then decreases rapidly toward the evolved rhyolitic compositions (Figure 5.3a). Paradise suite basalts are high in Al_2O_3 (20 to 24 wt%) as a result of their high plagioclase content, and can be regarded as high-alumina basalts.

Circular Bush suite rocks initially show a gradual increase in TiO_2 with increasing fractionation, but at around 3 wt% MgO the trend reverses and TiO_2 decreases rapidly (Figure 5.3b). Similar trends can be observed for FeO (Figure 5.3c). This is typical of calc-alkaline rocks and suggests fractionation has taken place under relatively wet, oxidising conditions (high P_{H_2O} and f_{O_2}). Magnetite crystallises from the outset, rapidly depleting the residual liquids in Fe and TiO_2. In contrast, the Paradise suite basalts show a rapid increase in TiO_2 with decreasing MgO. This is a typical tholeiitic trend and is caused by fractionation under relatively dry, reducing conditions (low P_{H_2O} and f_{O_2}). The crystallisation of magnetite is suppressed, and thus Fe and TiO_2 are enriched in the melt during early stages. The basic dykes have very high TiO_2 (2.23-2.67 wt%), plotting well above the other suites, indicative of their different geochemical evolution.

In the Circular Bush suite, P_2O_5 gradually increases then decreases, whereas it increases rapidly in the Paradise suite (Figure 5.3d). The late stage decrease in P_2O_5 in the Circular Bush suite is attributed to the crystallisation of apatite. The basic dykes have much higher P_2O_5 than the other suites, again showing their differing geochemical affinity.

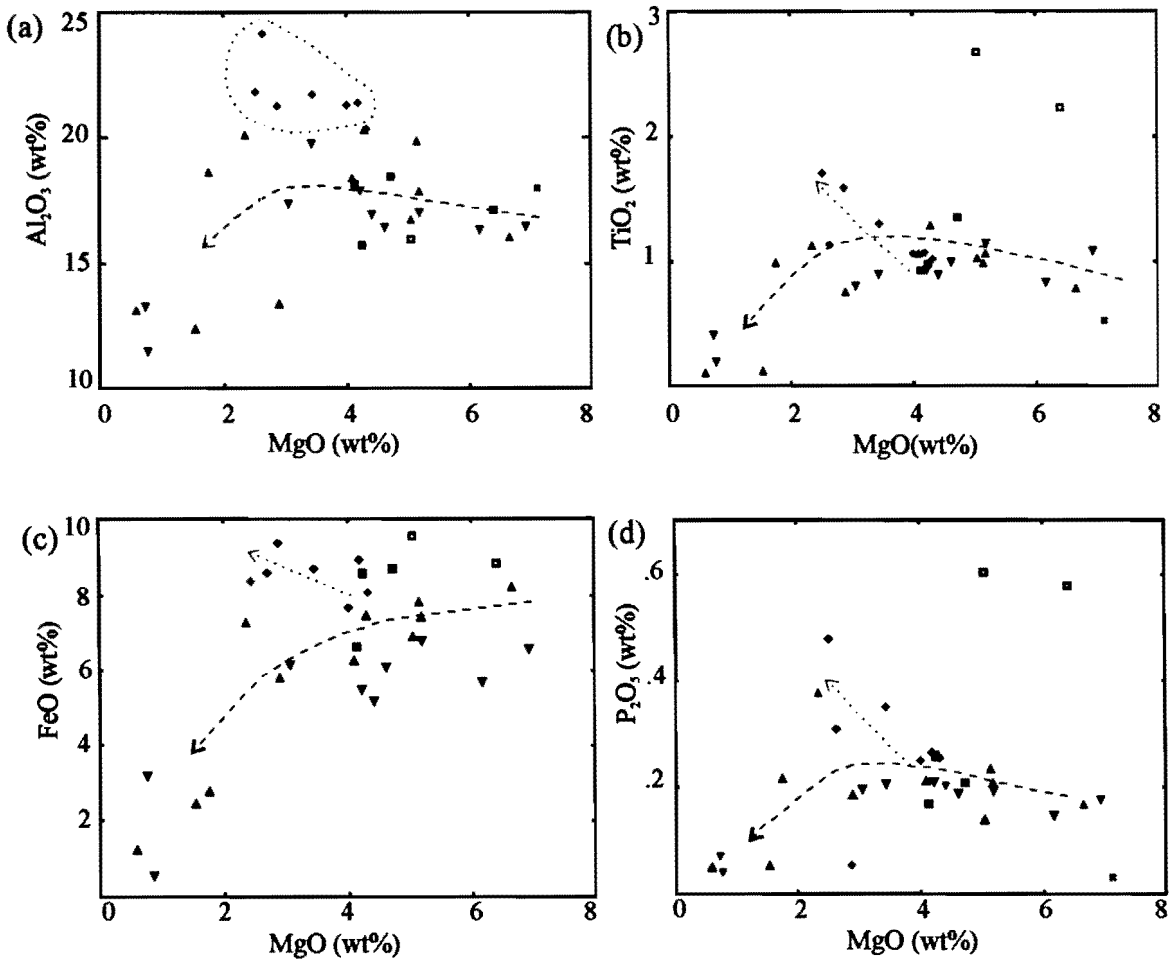

Figure 5.3: Harker variation diagrams for: (a) Al_2O_3 (b) TiO_2 (c) FeO (d) P_2O_5. All plotted against MgO. Fractionation trends for Circular Bush suite shown as dashed line, Paradise suite indicated by dotted line.

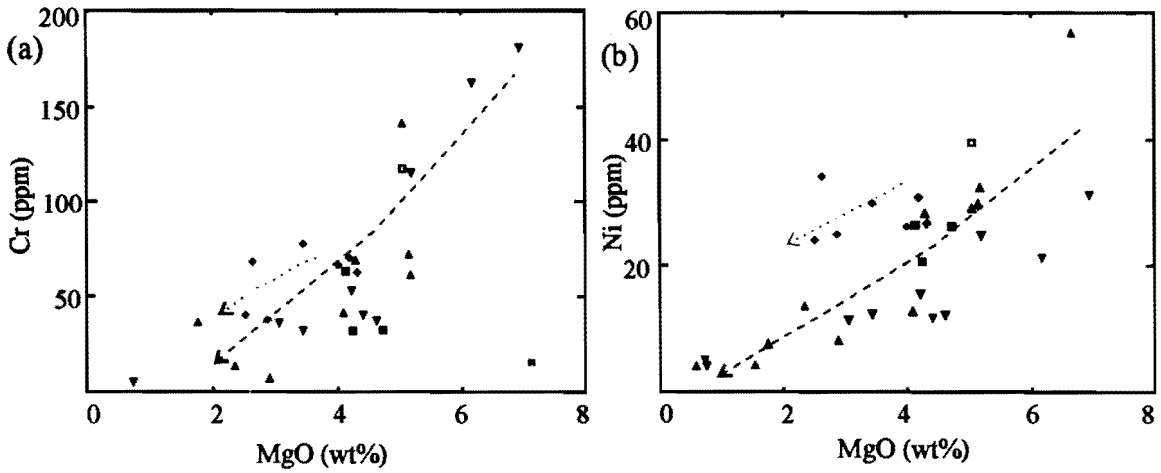

Figure 5.4: Harker variation diagrams: (a) Cr vs MgO (b) Ni vs MgO. Circular Bush suite fractionation trend indicated by dashed line, Paradise suite trend by dotted line.

5.6 Trace Elements

Figures (5.4, 5.5) show selected plots of trace elements against MgO. Ni (3-40 ppm) and Cr (5-200 ppm) concentrations are low in both suites of volcanics, a typical feature of island arc volcanics (Figure 5.4). Figure(5.4b) shows a good correlation between Ni and MgO. This suggests olivine fractionation en route to the surface, as Ni is the most compatible trace element in olivine. Figure (5.4a) shows a similar correlation for Cr. Cr is removed either by clinopyroxene, chrome-spinel or chromite. Clinopyroxene fractionation is probably the most dominant control on this trend.

The Circular Bush suite exhibits increasing Zr with fractionation, which then decreases toward the rhyolitic compositions, as zircon crystallises out (Figure 5.5a). The Paradise suite shows a rapid increase in Zr because zircon has not crystallised from these mafic compositions. Ba concentrations have been severely affected by low grade metamorphism and metasomatism as can be seen from the very scattered nature of Figure 5.5b. Y concentrations are low (15-40 ppm) in both the Circular Bush suite and Paradise suite (Figure 5.5c). This may indicate that garnet is present in the source (suggesting a deep mantle origin), as Y has a high partition co-efficient in garnet. The basic dykes have higher (30-50 ppm) concentrations of Y. Ce values range from 20 to 55 ppm for both suites, and are again higher for the basic dykes (50-70 ppm), suggesting higher degrees of LREE enrichment in the later (Figure 5.5d).

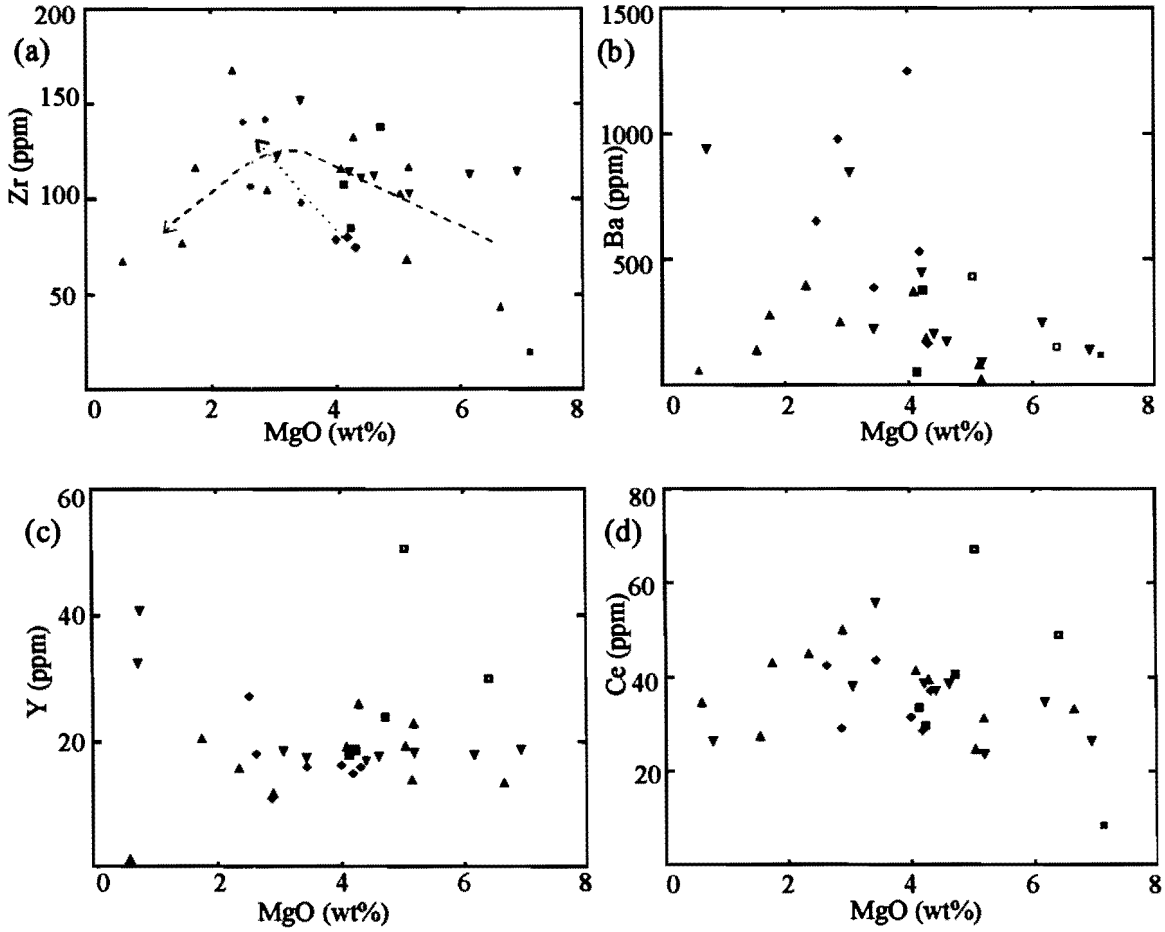

Figure 5.5: Harker variation diagrams for: (a) Zr (b) Ba (c) Y (d) Ce. All plotted against MgO. Fractionation trends of Circular Bush suite shown by dashed line, Paradise suite by dotted line.

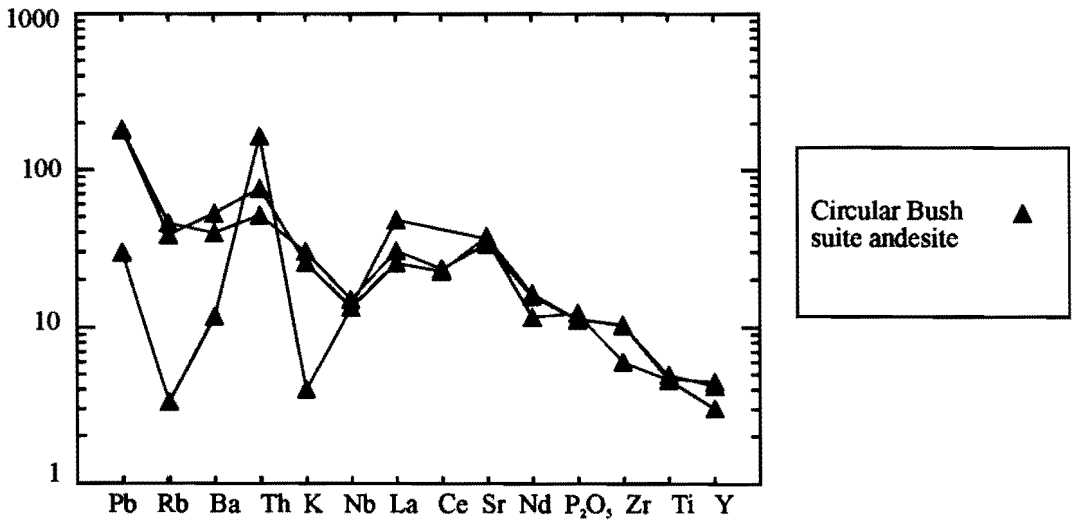

Figure 5.6: PRIM normalised spider diagram showing selected samples of Circular Bush suite andesite.

5.7 Spider Diagrams

Comparison of trace element compositions between different volcanic suites is best made by using multi-element mantle or MORB normalised diagrams or *spider diagrams*. Elements are arranged in order of increasing incompatibility (from right too left) for a normal upper mantle spinel peridotite mineral assemblage (Sun and McDonough, 1989, Saunders et al, 1991). Figures 5.6 and 5.7 show selected PRIM (primordial mantle) normalised spider diagrams of representative samples from each suite.

Circular Bush Suite andesites (Figure 5.6) show enrichment in LILE elements and low abundances of elements with high ionic potentials relative to primitive mantle. However, as mentioned earlier, LILE elements (K, Sr, Ba, Rb) are mobile under low grade metamorphism, and therefore do not reflect primary values. Th may be close to its original value, and is clearly enriched relative to primitive mantle. HFS elements (Nb, La, Ce, Nd, Zr, Ti, Y) are relatively immobile, and can be observed to be depleted. Nb is anomalously low, which is typical of subduction-related volcanism. The microdiorite sills show very similar trends for HFS elements, but LILE concentrations are more dispersed (Figure 5.7b).

Circular Bush suite rhyolites have high Th, low Nb, and are more highly depleted in high ionic potential elements, with the notable exception of a strong peak in Zr (Figure 5.7a). Their greater depletion in HFS elements is due to their more evolved composition. The Th anomaly may be more apparent than real because of losses of the elements adjacent to it on the spider diagram during low grade metamorphism (losses of Rb, Ba, K).

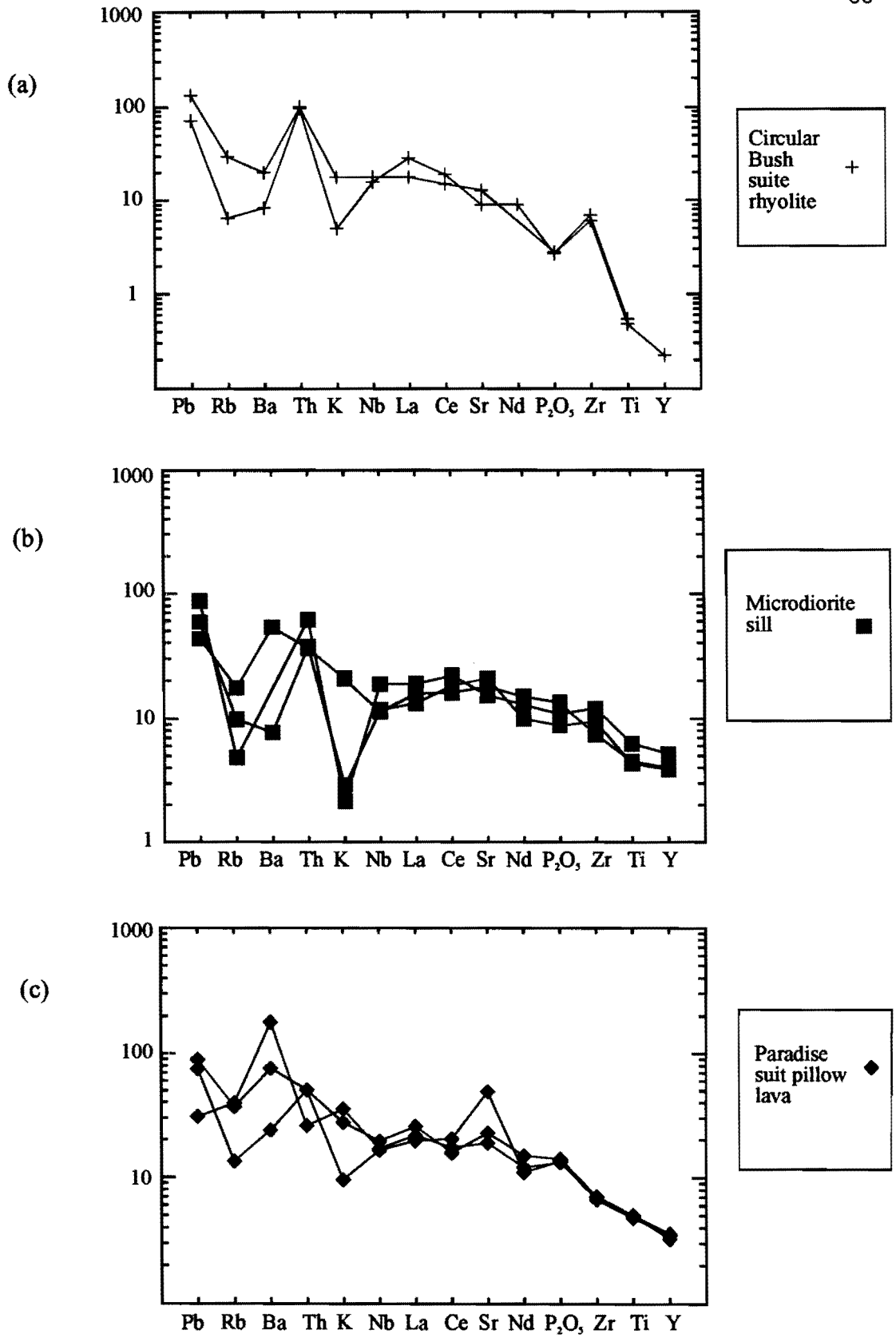

Figure 5.7: PRIM normalised spider diagrams for (a) Circular Bush suite rhyolite (b) Microdiorite sills (c) Paradise suite pillow lava.

Paradise suite basalts also shows erratic behaviour of Ba, K, Rb and Sr. HFSE abundances are again low, and there is a small negative Nb anomaly suggestive of subduction-related generation (Figure 5.7c).

The basic dykes show rather different trends from the other suites. The dykes are enriched in Y, Ti, Zr, Ce, P_2O_5 and Nd (Figure 5.8). One sample shows a small Nb anomaly.

Island arc volcanics are commonly divided into four main series on the basis of their K_2O contents (Figure 5.9): low K tholeiite, medium K calc-alkaline, high K calc-alkaline and shoshonitic series. Due to the erratic behaviour of K_2O in the rocks studied, classification on this basis can not be made. Instead, selected samples from the different suites have been compared on spider diagrams with calculated average compositions for Tertiary to Recent low-K to shoshonitic series (averaged compositions from Ewart, 1982). Care has been taken to ensure samples compared have similar SiO_2 and MgO values (i.e., they have undergone similar amounts of differentiation). However, it must be noted that this can only provide an estimate, as classification is normally strictly based on K_2O content.

Circular Bush suite andesites most closely fit medium-K calc-alkaline series trace elemental abundances (Figure 5.10a). Obviously, mobile elements K, Rb, Ba and Sr deviate significantly, but immobile element concentrations are almost identical. Sills believed to be related to the Circular Bush suite clearly are calc-alkaline as well (Figure 5.10b).

Interestingly, although Paradise suite rocks show tholeiitic trends in TiO_2 and FeO, their immobile trace element concentrations are much higher than low-K tholeiitic series rocks. Their immobile element abundances best fit that of medium-K calc-alkaline series (Figure 5.10c). The significance of this will be discussed in a following section.

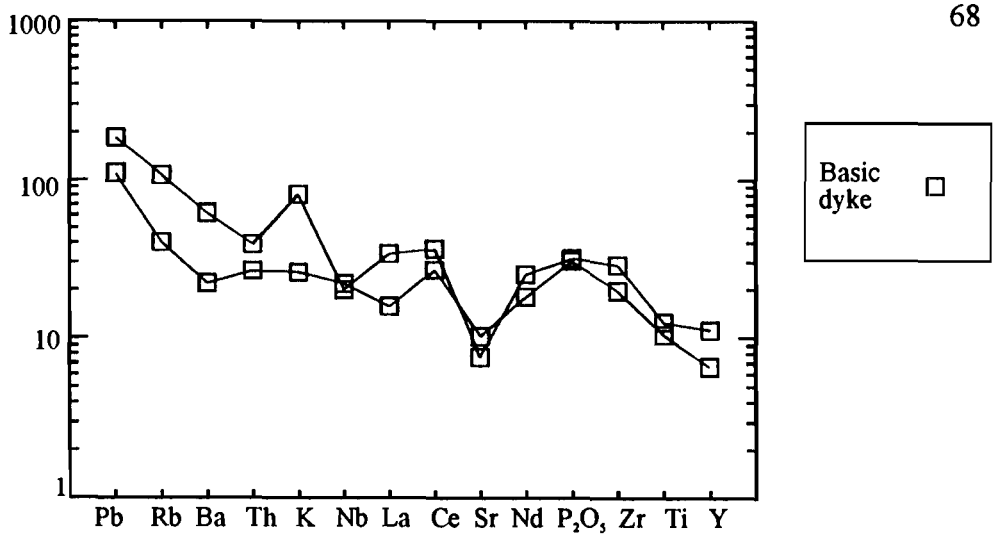

Figure 5.8: PRIM normalised spider diagram of basic dykes.

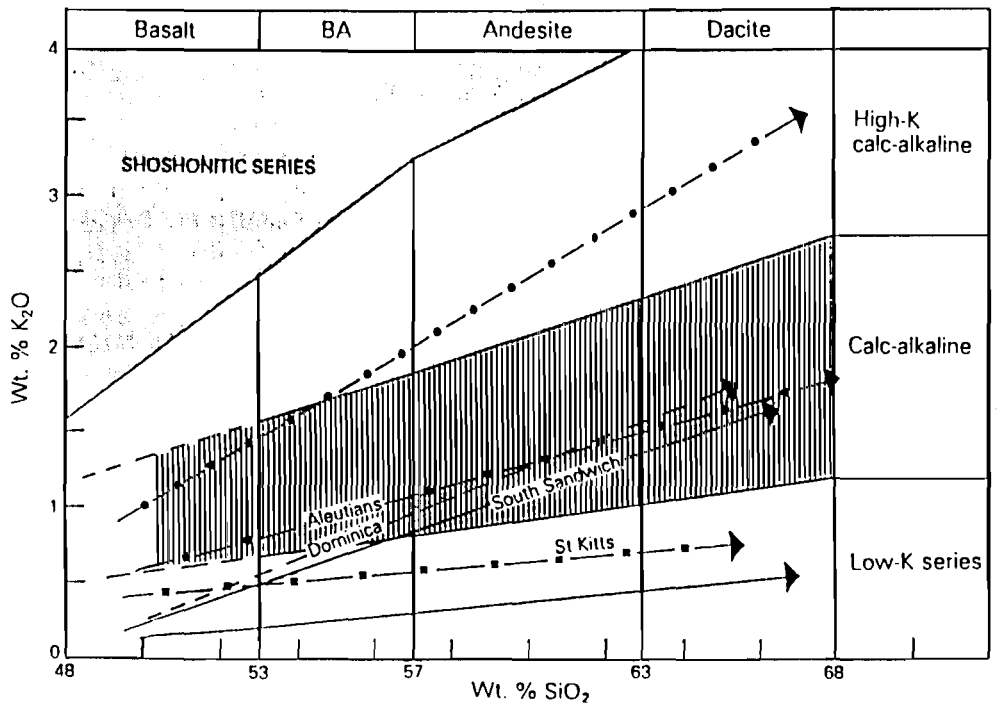

Figure 5.9: Plot of wt% K_2O versus wt% SiO_2 showing the major divisions of the island arc volcanic rock suites (after Wilson, 1989).

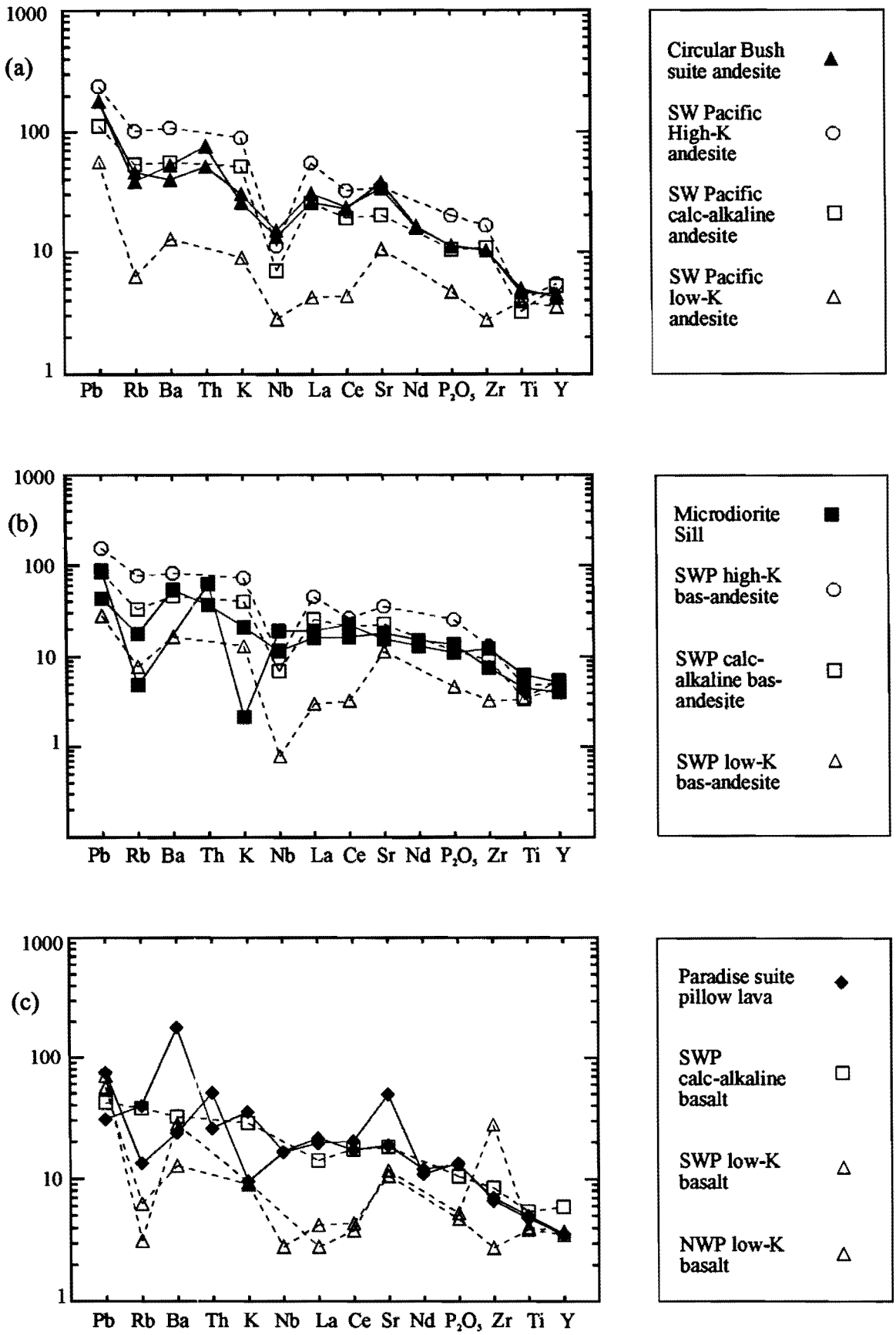

Figure 5.10: PRIM normalised spider diagrams of averaged composition SW Pacific low-K, calc-alkaline and high-K series plotted against the various suites (average compositions from Ewart, 1982).

5.8 Christmas Conglomerate

One volcanic clast from the Christmas Conglomerate Member (stratigraphically underlying the Circular Bush suite and Paradise suite was geochemically analysed (DRM 142). The sample has high MgO (7.12 wt%), and looks at first to have a boninitic affinity. However closer examination reveals that the rock has anomalously low CaO (0.67 wt%), and anomalously high Na_2O (7.48 wt%). This suggests that the rock has been metasomatised, losing CaO and gaining Na_2O and MgO. Its trace element geochemistry when compared with averaged Low-K to high-K series basaltic-andesites most closely fits that of low-K tholeiites (Figure 5.11). This may indicate that the Christmas Conglomerate contains volcanic material from an earlier primitive low-K tholeiitic arc. Further sampling and geochemical analyses are required to support this idea.

5.9 CIPW Norms

CIPW normative calculations for the samples analysed are given in Appendix Three. CIPW norm calculations are less appropriate for altered rocks, as element transfer during alteration will significantly affect recalculated compositions. However, they prove useful in a general sense.

Circular Bush suite basaltic andesites and andesites typically contain normative quartz and large amounts of hypersthene. Many have normative corundum. The rhyolites, as expected show high amounts of normative quartz. In contrast most of Paradise suite basalts have normative olivine and nepheline, and do not contain normative quartz. Rocks from both suites contain small amounts of normative zircon, whereas the basaltic-andesite clast from the Christmas Conglomerate Member has none. The basic dykes have higher concentrations of normative apatite, zircon and ilmenite than the other suites.

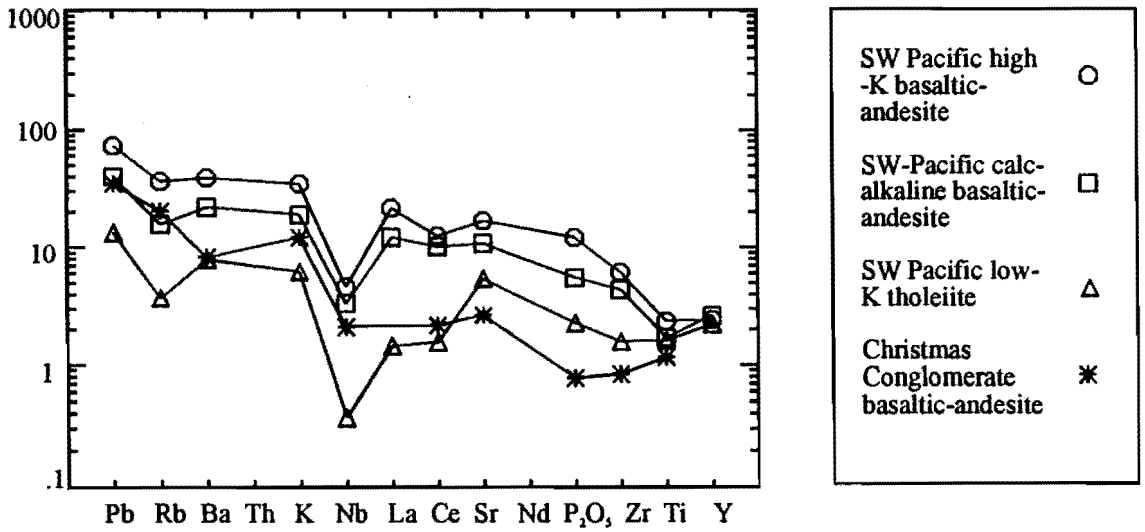

Figure 5.11: PRIM normalised spider diagram of averaged composition SW-Pacific series rocks compared to a basaltic andesite clast from the Christmas Conglomerate (averaged compositions from Ewart, 1982).

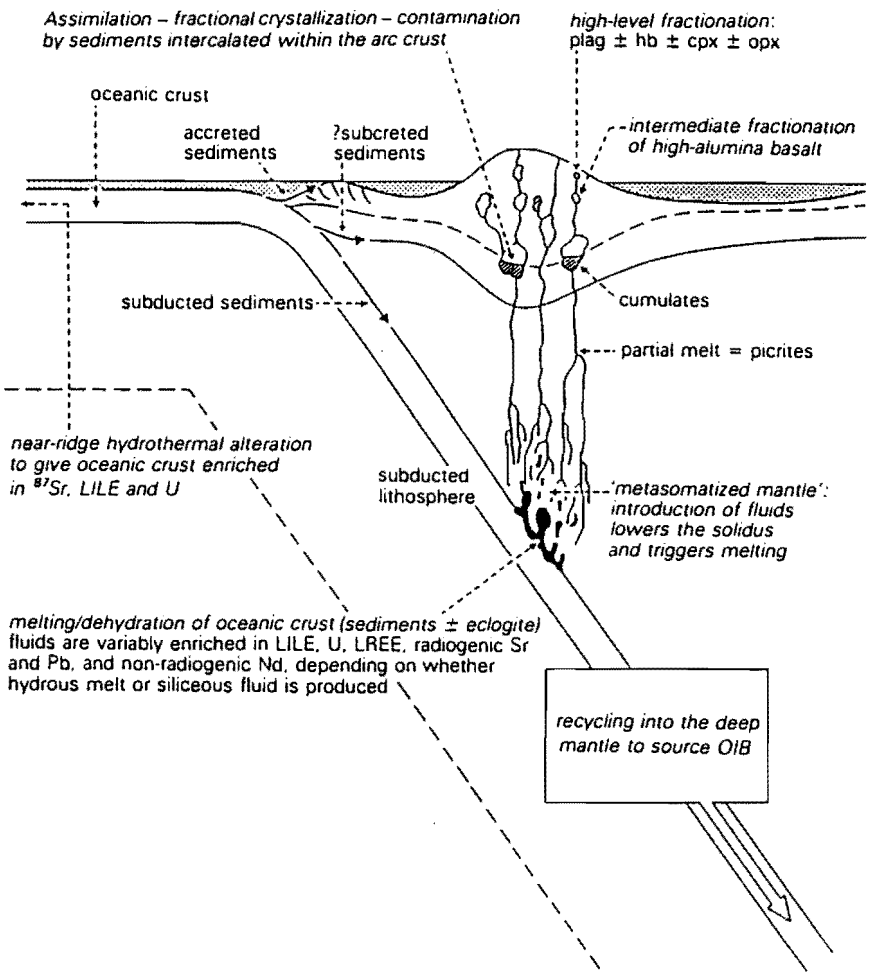

Figure 5.12: Summary of the magma generation processes in an ocean-ocean collision zone (after Davidson, 1984)

5.10 Tectonic Setting

The data set were plotted on commonly used tectonomagmatic discrimination diagrams (eg. Pearce and Cann, 1973, Pearce, 1975, Pearce and Norry, 1979, Wood, 1980). However, these proved to be inconclusive, as they are designed for fine grained, fresh, unaltered basic volcanic rocks.

Trace element abundances (high LILE, low HFSE) suggest that the Circular Bush suite and the Paradise suite are subduction-related. The question arises as to whether they were formed in an intra-oceanic arc or on a continental margin. The low-K tholeiitic to medium-K calc-alkaline affinity of the suites is more characteristic of an intra-oceanic setting (continental arcs are usually dominated by more evolved high-K calc-alkaline andesites, dacites and rhyolites). However, no unequivocal conclusion can be drawn from the data. Detailed isotopic work is required to resolve the question.

5.11 Petrogenesis

It is generally accepted that island arc basaltic magmas are generated by the partial melting of the mantle wedge above the slab of subducted oceanic lithosphere (Wilson, 1989). LILE (Rb, Ba, Th, Sr, K) and LREE elements are transferred from the subducting slab by hydrous fluids and melts and are concentrated in the mantle wedge where they are stabilised by hydrous phases such as hornblende and phlogopite (Wilson, 1989, Saunders et al, 1991). HFS elements are insoluble in hydrous fluids and are relatively insoluble in hydrous melts, and therefore remain in the subducted slab (Saunders et al, 1991). This gives subduction-related magmas their characteristic LILE enrichment and HFSE depletion. Slab induced convection is believed to drag down metasomatised mantle, allowing the continual breakdown of hornblende, releasing the fluids required to initiate melting or to further metasomatize the mantle wedge. Subducted sediment may be involved in magma genesis, but only to a small extent as the

majority is thought to be carried into the mantle (Saunders et al, 1991). Fractionation of olivine + clinopyroxene + orthopyroxene + magnetite + plagioclase is thought to play the major role on the variation of eruptive products in subduction settings (Powell, 1978).

It is envisaged that the primitive melts for both suites were formed by the source conditioning and melting processes outlined above. Where the two suites differ is in the conditions and environment in which high level fractionation took place. Circular Bush suite rocks have evolved from the fractionation of olivine + clinopyroxene + magnetite + plagioclase under wet, oxidising conditions, giving them a typical calc-alkaline trend.

The Paradise suite shows immobile trace element concentrations similar to calc-alkaline basalts. Their high plagioclase content and as a consequence, high Al_2O_3, is suggestive of fractionation under high P_{H_2O} and high P. Under such conditions the crystallisation of plagioclase is suppressed until it nucleates at near surface pressures. However, this is clearly at odds with the tholeiitic trend of Fe-enrichment observed in the suite, which suggests fractionation under low P_{H_2O}. A possible solution is that the source was particularly rich in plagioclase i.e., plagioclase peridotite-garnet peridotite transition (depth 80-100 km). The suite may therefore represent magmas derived from higher pressure source than the Circular Bush suite, further from the trench.

The basic alkaline dykes show different spider and trace element properties. They have higher Zr, Ce, Ti, Y and Nd, and probably have a deeper mantle source than the Circular Bush suite and Paradise suite. They show broad similarities to continental flood basalts and therefore may have been emplaced in an extensional crustal setting.

CHAPTER SIX: DISCUSSION

6.1 Introduction

The aim of this chapter is to examine volcanic facies models for the suites within the Devil River Volcanics, and to compare their geology and geochemistry with other volcanic suites in the Central Sedimentary Belt of the Takaka Terrane. General comparisons will be made with Cambrian volcanics from throughout the dismembered fragments of South-east Gondwana.

6.2 Volcanic Facies Analysis

Careful documentation of characteristic volcanic facies can provide important clues to the mode of deposition, environmental conditions and paleotectonic setting of ancient volcanic rocks (Cas and Wright, 1987).

Island arcs typically contain a high percentage of volcaniclastic material. Figure 6.1 shows a diagrammatic section through a typical island arc. Close to the volcanic centre a *proximal* facies is recognised, characterised by massive lava flows, domes, agglomerates, coarse volcaniclastics and pyroclastic flows (if emergent). If the arc is submerged, pillow lavas and hyaloclastites are common. The *medial* facies is composed predominantly of reworked pyroclastics, debris flows, turbidites, volcanic conglomerates and volcanic sandstones. Resedimented finer volcaniclastics, dilute subaqueous debris flows and turbidity current deposits intercalated with 'non-volcanic' background sedimentation form the *distal* facies. Pelagic and hemipelagic background sedimentation is more characteristic of an intra-oceanic arc setting, whereas terrigenous background sediment suggests proximity to a major landmass (Cas and Wright, 1987).

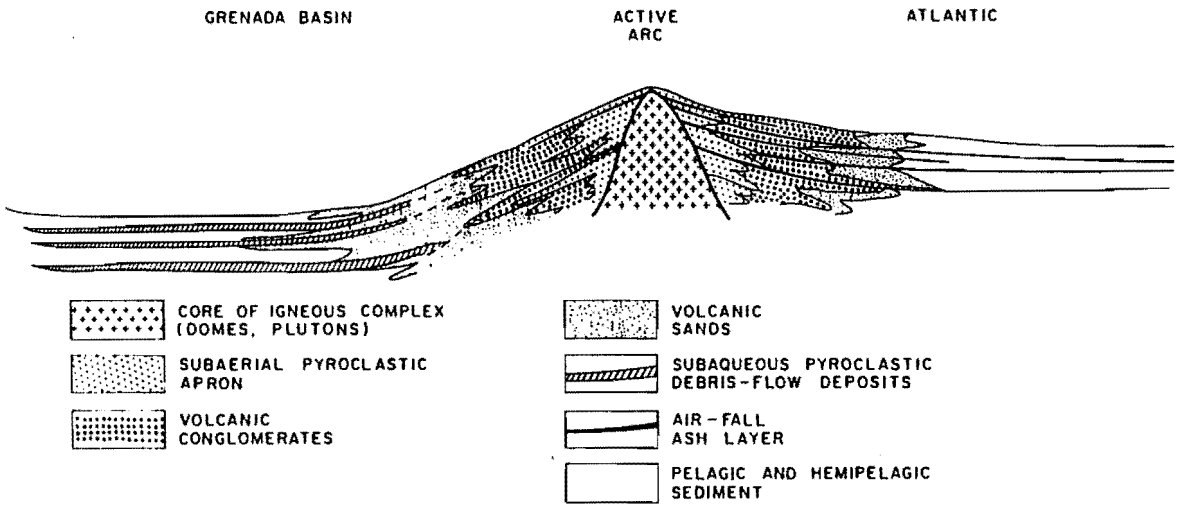

Figure 6.1: Schematic section through a modern volcanic arc (Lesser Antilles volcanic arc) showing the distribution of volcanigenic sediments in and around the arc (after Sigurdsson et al, 1980).

6.2.1 Circular Bush Suite

In the Anatoki Range area, the Circular Bush suite is composed of a thick sequence of subaqueous mass flow deposited tuff-breccias, lapilli-tuffs, reworked tuffs and volcanic conglomerate (Figure 3.2). No lava flows, ignimbrites or agglomerates were observed. Cuspate vitric shards are present in some of the tuff layers, indicative of subaerial phreatomagmatic eruption (see section 4.1.2). Other tuffs (see section 4.1.2) contain angular and blocky shards which are typical of hydroclastic (submarine erupted) fragmentation. The presence of a thick sequence of reworked volcaniclastics and the absence of lava flows, suggest that the rocks of the Circular Bush suite occupy a medial facies relative to the eruptive centre (Figure 6.2). From the presence of both submarine and subaerially erupted volcanic material, it is probable that the rocks formed on the flanks of an emergent, mature, marine stratovolcano (Figure 6.2). Such volcanoes may be tens of kilometres across, and have high rates of subaerial mass wastage and shoreline erosion, accompanied by major submarine mass flow processes. These processes produce coarse sediment aprons, built up largely of mass-flow deposits (debris flows, rubble avalanches, turbidity currents, slumps and slides) (Cas and Wright, 1987, Fisher, 1984). Emergent marine stratovolcanoes are normally characterised by relatively evolved compositions, which is consistent with the geochemistry of the Circular Bush suite (basaltic-andesite to andesite of a medium-K calc-alkaline affinity with subordinate basalt and rhyolite).

In the Anatoki River, the Circular Bush suite is composed of thin tuffaceous sandstones and siltstones and fine grained lapilli-tuff (Figure 3.3a), interpreted to have been deposited from dilute turbidity currents and subaqueous debris flows. This suggests these rocks have formed in a more distal facies relative to the eruptive centre (Figure 6.2). Interbedded with the volcanics are laminated siltstones and fine to medium sandstones with relatively little volcanic content, which probably represent the background sedimentation from within the depositional basin. The sandstone-siltstone dominated

background sedimentation, rather than pelagic sediment, may indicate proximity to a continental landmass.

6.6.2 Paradise Suite

The Paradise suite is composed of basaltic pillow lava, massive flows and rare pillow breccia and tuffs. The lavas show a rapid lateral variation in thickness, which suggests that they have been erupted onto an irregular topography. This was most probably caused by eruption into small fault controlled basins (Figure 6.3), producing locally thick ponded basaltic piles (Cas and Wright, 1987). In the Anatoki River, the Paradise suite is very thick (hundreds of metres) suggesting a proximal setting relative to the eruptive centre (Figure 6.3, A). In the Anatoki Range, the Paradise suite is relatively thin (only 50m), suggesting it is a greater distance from the eruptive centre (Figure 6.3, B).

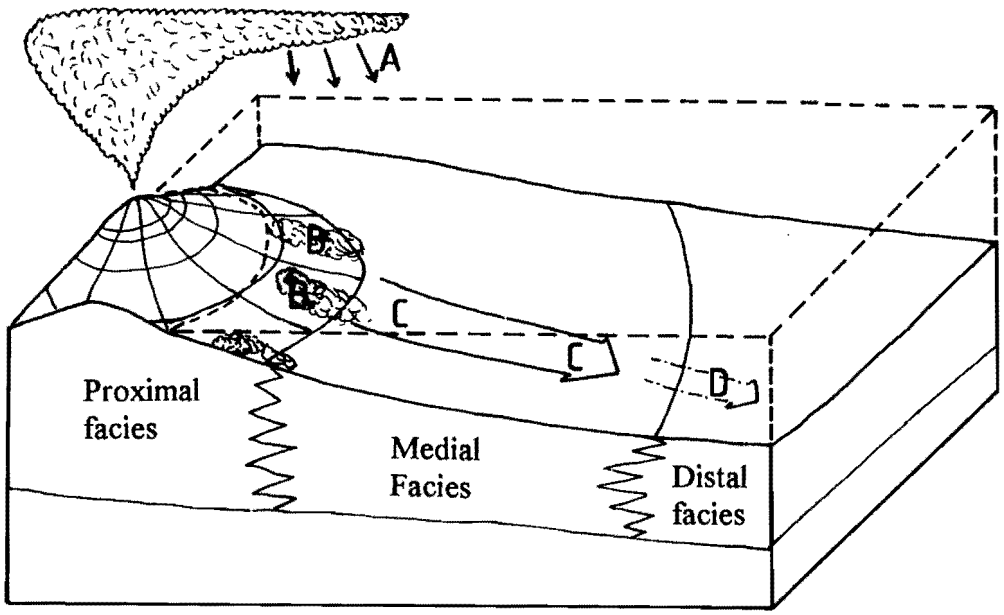

Figure 6.2: Inferred depositional environment of the Circular Bush suite. A = subaerial volcaniclastics, B = submarine erupted volcaniclastics, C = Volcanic rich debris flows, D = dilute turbidity currents.

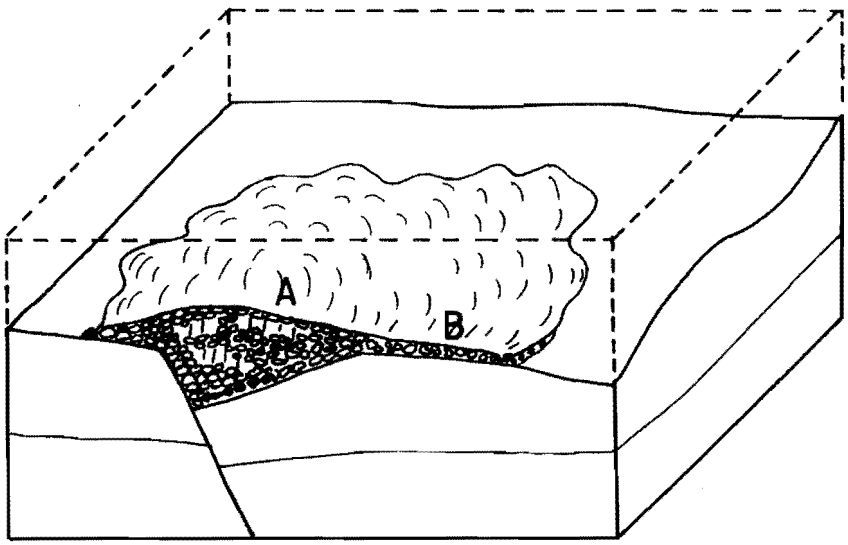

Figure 6.3: Inferred depositional setting of the Paradise suite. A = section in Anatoki River, B = section in Anatoki Range.

6.3 Comparison With Other Cambrian Volcanics of Northwest Nelson

6.3.1 Waingaro Fault-bounded Slice

Middle-Late Cambrian Volcanics within the Waingaro Fault Bounded slice in the Cobb Valley area have been studied by Munker (1993). The Waingaro Slice was found consists of a collage of smaller fault slices (termed subslices), containing different parts of the succession.

Three suites of volcanics were identified: Benson (basaltic andesites), Cobb Flat (basalt-basaltic andesites) and Peel Volcanic suites (basaltic andesites). All suites are submarine, and are intercalated with large amounts of volcanogenic sediment, consistent with an island arc origin. The Benson Volcanic suite is interbedded with sandstone turbidites, which Munker (1993) inferred to represent proximity to a continental landmass.

The oldest suite (Benson Volcanic suite) has immobile and REE elemental concentrations similar to low-K island arc tholeiitic suites, whereas the two younger suites (Cobb Flat and Peel Volcanic suites) show more evolved calc-alkaline to high-K affinities. Munker (1993) notes that the type of basement (continental or oceanic) onto which the volcanics were deposited can not be determined.

Figures 6.4a and 6.4b show Waingaro Slice volcanic suites compared with the Circular Bush suite, Christmas Conglomerate Member basaltic-andesite and the Paradise suite. The Circular Bush suite appears to fit most closely with the Peel Volcanic suite in terms of its immobile and trace element characteristics (Figure 6.4a). The Circular Bush suite contains andesites and rhyolite which suggest it is more evolved than the Peel suite, which is basaltic to basaltic andesitic in composition. The Benson Volcanic suite is clearly much more primitive than the Circular Bush and Paradise suites, but show similarities to the basaltic-andesite clast from the Christmas Conglomerate (Figure 6.4b).

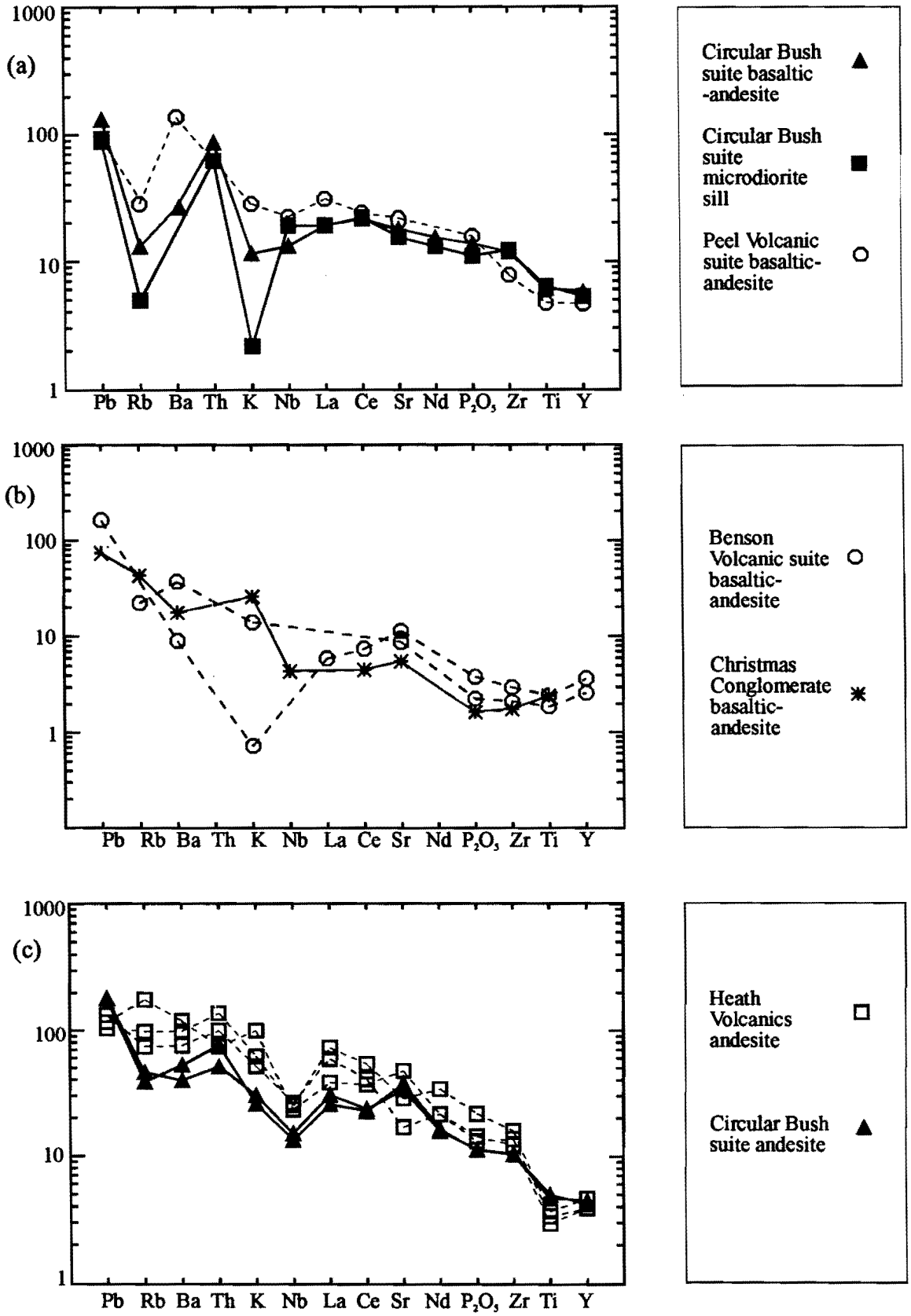

Figure 6.4: PRIM normalised spider diagrams of: (a) Circular Bush suite compared with the Peel Volcanic suite (basaltic andesite compositions) (b) Benson Volcanic suite basaltic andesite compared with a basaltic andesite clast from the Christmas Conglomerate. (c) Heath Volcanics horneblende andesites compared with Circular Bush suite andesites.

The Circular Bush suite and the Paradise suite may have formed in the same arc as the Benson, Cobb-Flat and Peel Volcanic suites. Their difference in compositions may reflect the evolution of an arc through time from primitive low-K tholeiitic (Benson Volcanic suite, Christmas Conglomerate Member basaltic andesite) to more evolved medium to high-K suites (Cobb-Flat, Peel, Circular Bush, and Paradise suites). Such trends are often observed in island arcs, and have been attributed to changing primary magma chemistry combined with varying conditions of low-pressure fractionation (Wilson, 1989). During the early stages of arc development the overlying crust is thin and rising basaltic magmas will not be impeded in their ascent. As the arc develops the thickening pile of magma and crustal underplating serves as a density filter, causing primary magmas to pond and fractionate in high level magma chambers (Wilson, 1989). Fractional crystallisation results in the generation of lower density andesites, which are more easily erupted.

6.3.2 Heath Fault-bounded Slice

Andesitic to dacitic sills intruding the Balloon Formation (Heath Volcanics) are classified as convergent margin (subduction) related by Stewart (1988). Comparison of the Heath Volcanics with the studied rocks is made in Figure 6.4c. Their immobile element concentrations are more characteristic of high-K calc-alkaline series rocks, indicating that they are more evolved than the Circular Bush suite, which is in agreement with their more fractionated compositions.

6.3.3 Mataki/Salisbury Fault-bounded Slice

Figure 6.5 shows basalts from the Paradise suite compared to Mataki/Salisbury Basalts of similar composition. They show very different geochemical trends, indicating they have a different petrogenetic evolution. Stewart (1988) suggests the basalts are of seamount origin, whereas Pound (1993) postulates they are of back-arc origin. Clearly the Mataki/Salisbury Basalts are different from Devil River Volcanics.

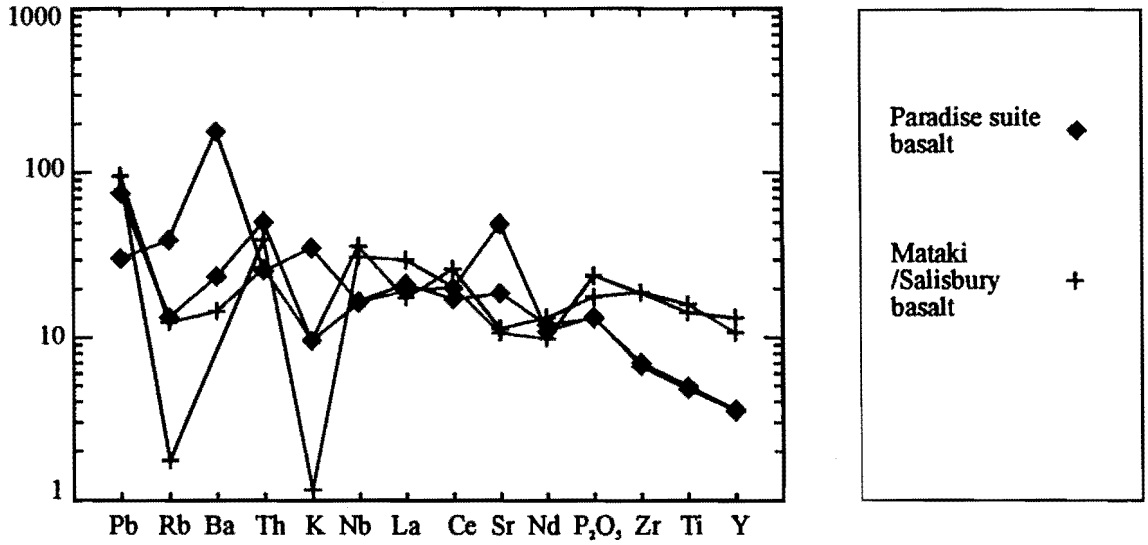

Figure 6.5: PRIM normalised spider diagram of Mataki/Salisbury basalt compared with Paradise suite basalt.

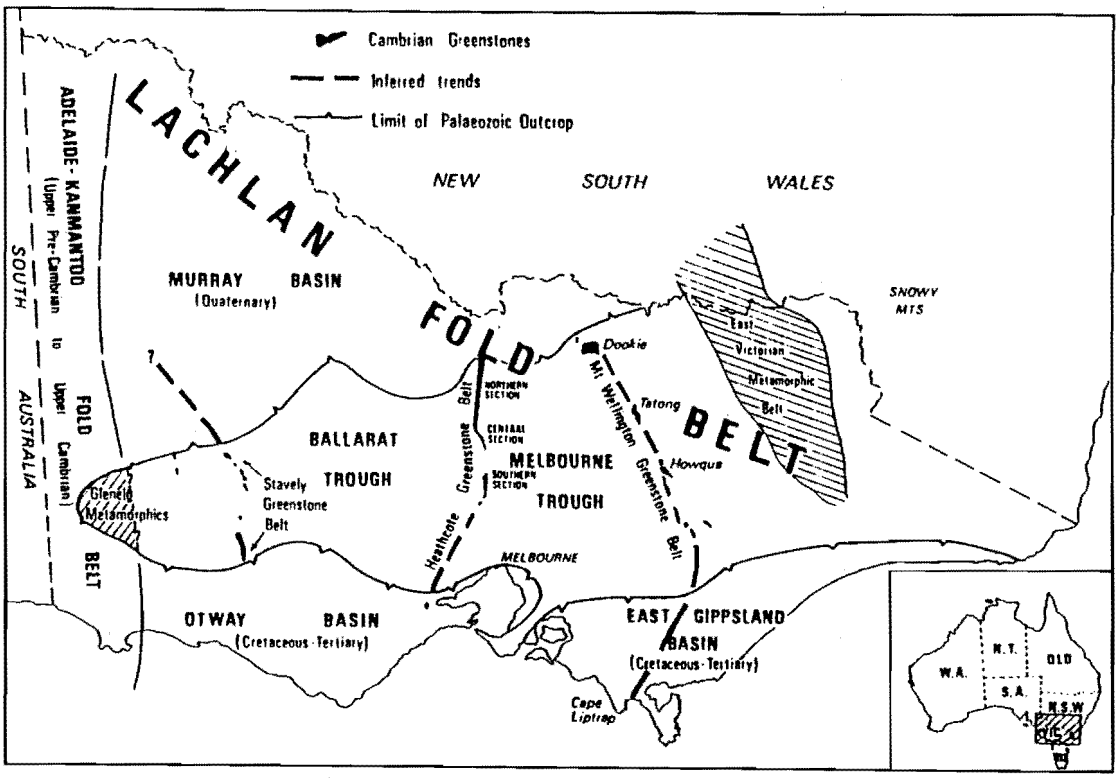

Figure 6.6: Location of Cambrian greenstone belts within the Lachlan Fold Belt, SE Australia (after Crawford and Keays, 1978).

6.3.4 Basic Alkaline Dykes and Sills

Mildly alkaline doleritic sills and dykes of similar mineralogy and geochemistry to those identified in this study have been documented in the Waingaro Slice (Benson doleritic sills - Munker, 1993), Balloon, Heath, Junction and Salisbury/Mataki fault bounded slices (Stewart, 1988). Hickey (1986) describes *carbonate altered* dykes within the Wangapeka Formation (Eastern Sedimentary Belt), and Grindley (1980) and Coleman (1981) also describe intrusives of similar mineralogy from throughout the Central and Eastern Belts. Basic dykes are also found in the Buller Terrane.

The basic intrusives crosscut penetrative fabrics related to the F_1 event (Munker, 1993, Stewart, 1988, Grindley, 1980). All have a greenschist facies metamorphic mineral assemblage, which probably constrains the age of emplacement to pre-Cretaceous (see section 4.5). Coleman (1981) correlates the dykes with the Riwaka Complex and assigns them a Late Devonian to Early Carboniferous age. However, the Riwaka Complex does not possess alkaline chemistry and this correlation therefore is untenable.

The intrusives show broad similarities to continental flood basalts in terms of their Th, La, Ce and Nb concentrations, suggesting they may have been erupted in an extensional tectonic setting. Whether they represent a single event is unclear. Further geochemical characterisation, isotopic work, dating, and comparison of Takaka and Buller Terrane basic intrusives is required

6.4 Age of the Devil River Volcanics

No direct age control (from fossils or isotopic dating) is available for the Devil River Volcanics on the Anatoki Range. One sample of conglomerate with limestone clasts from *Tasman Formation-like* lithologies overlying the volcanic pile was dissolved in acetic acid, but proved unfossiliferous. The age must therefore be determined by indirect means. The *Tasman Formation-like* unit overlying the Devil River Volcanics may be

correlate with the Tasman Formation in the Cobb Valley, which has been dated from fossil fauna as Undillan to Boomerangian (Cooper, 1993). Therefore the age of the Devil River Volcanics is tentatively inferred to be Middle Cambrian.

6.5 Comparison with other Cambrian Volcanics in Gondwana Fragments

Cambrian metavolcanics of similar age to the Devil River Volcanics occur in suspect terranes throughout southeastern Australia and in Northern Victoria Land, Antarctica.

6.5.1 Australia

Cambrian greenstones of Victoria form three narrow, linear belts (Figure 6.6). The Stavely Greenstone belt is composed of andesites, dacites, with minor cherts, serpentinite and shale. The Mount Wellington and Heathcote Greenstone Belts show very similar stratigraphic and geochemical sequences (Crawford, 1984), characterised by boninites and low-Ti andesites, overlain by thick piles of evolved tholeiitic basalts. The Heathcote greenstone belt is divisible into three segments. The northern and eastern segments are dominated by tholeiitic metabasalts and metadolerites with MORB affinities The central section contains tholeiitic basalts, low Ti andesites and boninites.

The Middle to Late Cambrian Mount Read Volcanics form a 200 by 20 km belt in western Tasmania (Figure 6.7). Crawford et al. (1992) recognise five major suites within the belt. Suites I and II are dominated by andesites, dacites and rhyolites which have

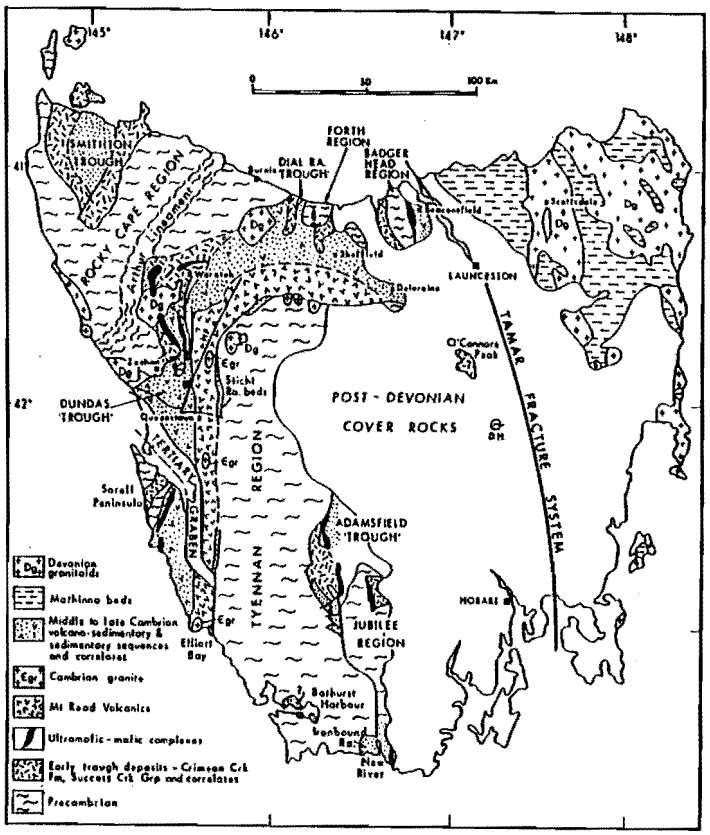

Figure 6.7: Simplified geological map showing the present distribution of major early Palaeozoic tectonic elements of western Tasmania (after Crawford et al. 1992).

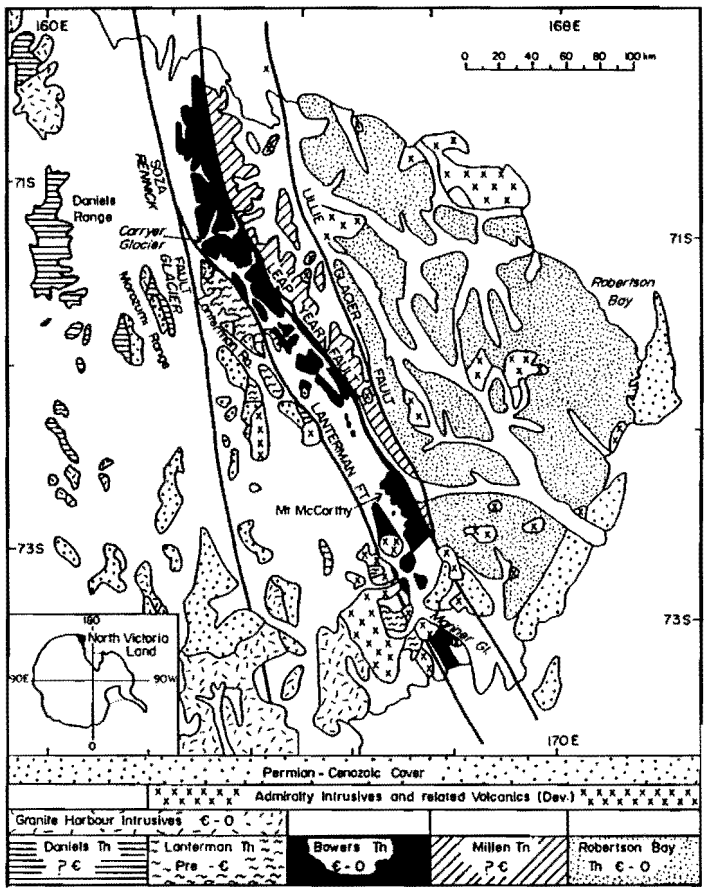

Figure 6.8: Tectonostratigraphic terranes of northern Victoria Land, Antarctica. The Glasgow Volcanics occur in the Bowers Terrane (after Bradshaw et al., 1985).

transitional medium-K/high-K to high K affinities. Suite III is characterised by basaltic to andesitic lavas which have geochemistry ranging from high-K to shoshonitic. Suite IV contains tholeiitic basaltic to andesitic sills and a genetically related transitional tholeiitic-alkaline dyke swarm. Suite V contains low Ti basalts and lava breccias (thought to be rift tholeiites in a window of Eocambrian basement).

Berry and Crawford (1991) and Crawford et al. (1992) have postulated a model for the Mount Read Volcanics whereby emplacement of ophiolites onto a passive margin produced crustal thickening. Relaxation rifting led to the formation of major grabens along the collision zone. Post-collision calc-alkaline and shoshonitic lavas were erupted into these grabens (suites I to III). Continuing extension led to incipient rifting, forming the tholeiitic dyke swarm (Suite IV), but was insufficient to lead to back arc rifting.

6.5.2 North Victoria Land

The Sledgers Group, within the Bowers Terrane of northern Victoria Land (Figure 6.8), consists of interfingering volcanics (Glasgow Volcanics) and mudstones and thin sandstones intercalated with conglomerate (Molar Formation) (Weaver et al., 1984, Bradshaw et al., 1985). The Lower Sledgers Group and the western Upper Sledgers Group are dominated by andesites and dacites with subordinate basalts, rhyolites and ignimbrites. In the eastern portion of the Upper Sledgers Group basalts dominate and andesitic rocks are subordinate. Most volcanism in subaqueous, but the presence of ignimbrites in the Lower Sledgers group suggests periodically emergent conditions (Weaver et al., 1984). The basalts have geochemistry of island arc tholeiites, and the andesites show geochemical affinities to boninites. The volcanic rocks interfinger with and are overlain by continental derived sediments, which suggests that the arc ended up very close to a continental margin (Dr J.D. Bradshaw, pers. comm.).

6.5.3 Comparison

The Mount Read Volcanics, Heathcote Greenstone Belt and Glasgow Volcanics are all of similar age to the Devil River Volcanics (Middle Cambrian). Selected analyses of the Devil River Volcanics and similar composition andesites and basalts from the Mount Read, Heathcote and Glasgow Volcanics are included in Table 6.1. Figures 6.9 and 6.10 show a broad similarity between the these Cambrian Volcanics, but there is a great deal of scatter. Suite I andesites from the Mount Read Volcanics show the greatest similarity to the Circular Bush suite andesite. Suite II andesites have higher concentrations of La, Ce, P_2O_5, and Zr, consistent with their more fractionated compositions (high-K calc-alkaline). The low-Ti andesites from the Heathcote and Glasgow Volcanics appear to be more primitive than the Circular Bush suite andesites, and have lower P_2O_5, Zr, Ti, and Y. Paradise suite basalts have different geochemistry to basalts in the Glasgow and Mount Read Volcanics (Figure 6.10). Suite III basalts are more evolved, with high K to shoshonitic affinities, and correspondingly higher La, Ce, Zr and P_2O_5. Suite IV and suite V basalts from the Mount Read Volcanics and basalt from the Upper Sledgers Group of the Glasgow Volcanics appear more primitive than the Paradise suite, and have lower concentrations of La, Ce, P_2O_5 and Ti.

The amount of variation seen between the Devil River Volcanics and Mount Read, Heathcote and Glasgow Volcanics is not suprising, as magma chemistry is very much dependant on the source characteristics, the component of LILE enrichment from the subducted slab and the degree of fractionation, which are all highly variable along a convergent margin. Subsequent alteration by low grade metamorphism creates further complication.

SAMPLE	Circular Bush suite andesite (DRM 74)	Paradise suite basalt (DRM 138)	MRV suite I andesite (MR644)	MRV suite II andesite (AR6)	MRV suite III basalt (482080)	MRV suite IV basalt (STP234)	MRV suite V basalt (C3)	GV low-Ti andesite (F1/81)	GV basalt (81/104)	HGB low-Ti andesite (HR2)	HGB type B boninite (HR15)
SiO_2	61.98	50.18	60.70	58.5	52.10	50.80	50.50	58.70	49.41	63.95	58.32
TiO_2	.99	1.02	.78	.46	.57	1.14	2.56	.32	.72	.26	.18
Al_2O_3	18.65	20.37	16.40	16.00	17.50	17.30	14.20	16.00	17.28	15.05	11.39
Fe_2O_3	.96	2.08	-	-	-	-	-	6.29	8.75	-	-
FeO	2.78	8.09	6.64	7.41	12.50	8.91	15.40	-	-	6.25	13.28
MnO	.12	.18	.12	.11	.15	.24	.26	.08	.14	.16	.17
MgO	1.76	4.32	2.97	4.37	6.16	7.81	5.97	5.45	6.41	3.82	6.00
CaO	7.44	7.56	7.90	6.26	4.53	8.90	4.40	7.11	10.04	4.59	4.36
Na_2O	4.23	4.95	3.90	6.75	4.28	3.98	5.45	4.42	3.14	4.42	5.79
K_2O	.87	.28	.39	.37	1.83	.74	.34	.86	.07	1.42	.44
P_2O_5	.22	.26	.15	.33	.36	.15	.26	.07	.09	.08	.07
LOI	-	-	3.26	1.65	3.41	7.98	3.71	.67	4.07		
Ni	7	59	14	40	70	70	42	49	70	50	59
Cr	34	25	77	142	85	175	26	91	50	52	103
V	129	342	163	206	294	223	814	-	-	86	232
Sc	-	-	13	27	33	30	33	-	-	17	33
Zr	108	70	146	160	168	71	132	44	47	106	55
Y	19	15	30	23	22	25	48	11	20	13	19
Sr	656	975	31	516	372	184	33	221	114	259	196
Rb	27	8	10	14	41	30	8	14	3	25	20
Ba	258	157	151	188	1052	173	136	-	-	-	178
Ce	40	13	50	-	186	24	21	-	-	-	-
La	20	35	22	-	84	10	8	-	-	-	-
Nb	10	11	9	8	9	< 3	8	1	3	-	-

Table 6.1: Selected geochemical analyses from the Devil River Volcanics, Mount Read Volcanics(MRV) (Crawford et al. 1992), Glasgow Volcanics (GV) (Weaver et al. 1984), and Heathcote Greenstone Belt (HGB) (Crawford and Cameron, 1985). (Major element values are volatile-free).

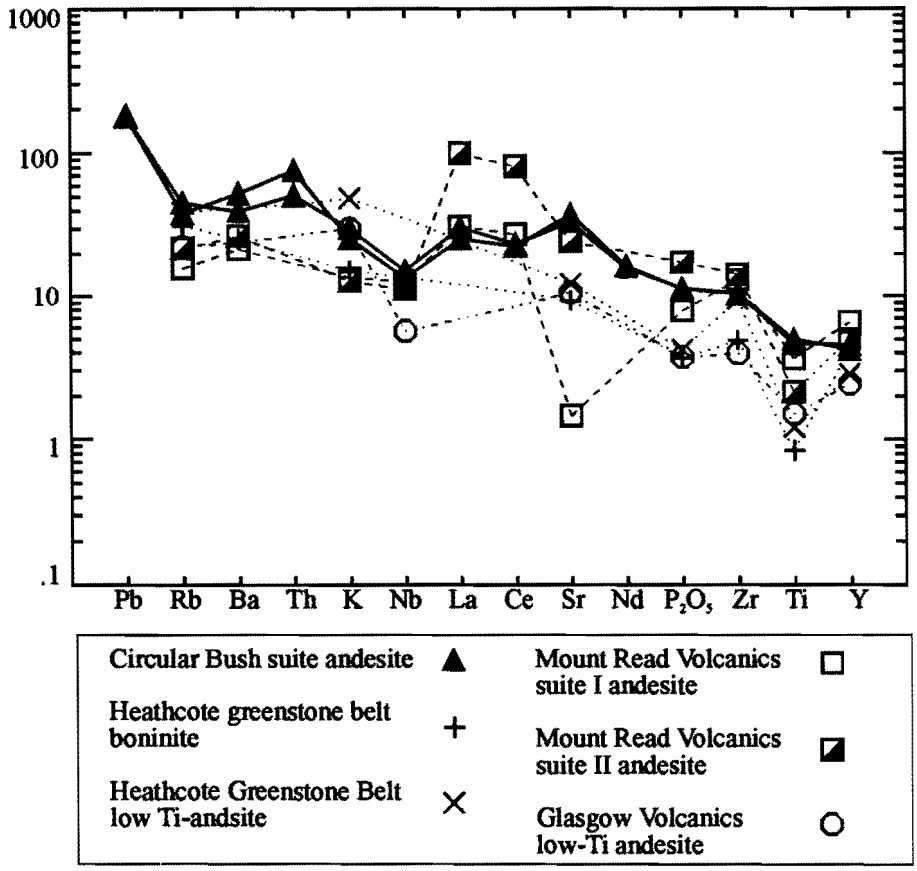

Figure 6.9: PRIM normalised spider diagram comparing Circular Bush suite andesites to andesites from the Glasgow, Heathcote and Mount Read Volcanics.

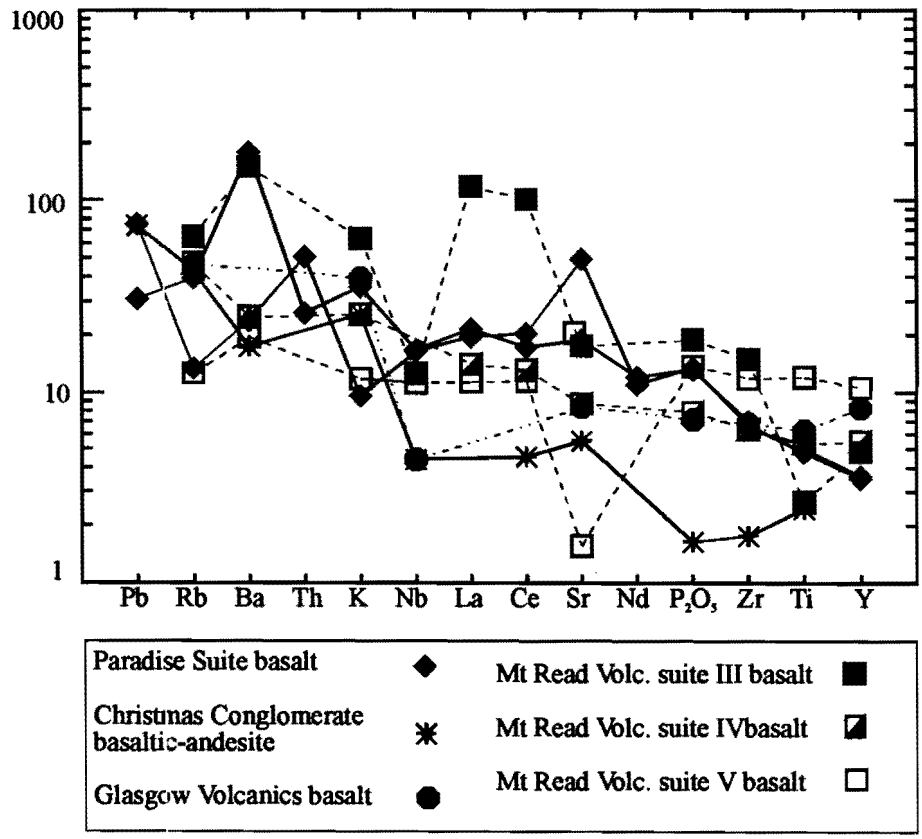

Figure 6.10: PRIM normalised spider diagram comparing Paradise suite basalts with basalts from the Mount Read, Glasgow and Heathcote Volcanics. Christmas conglomerate basaltic-andesite clast also shown.

CHAPTER SEVEN: CONCLUDING SUMMARY

- The Middle Cambrian Devil River Volcanics are composed of a highly strained conglomerate, the *Christmas Conglomerate Member*, overlain by two volcanic suites, the *Circular Bush suite* and the *Paradise suite*. Overlying these is a post-arc sedimentary sequence of sandstones and siltstones which progressively grade into *Tasman Formation-like* lithologies.

- The Christmas Conglomerate Member is at least 300 metres thick, and contains chert, sandstone and volcanic clasts. The volcanic clasts have a basaltic-andesitic composition, and immobile element abundances similar to low-K tholeiitic rocks.

- The Circular Bush suite is composed of reworked tuff, tuff-breccia, lapilli-tuff, tuffaceous sandstones and siltstones, volcanic conglomerate and rare chert lenses. In the Anatoki Range the suite is at least 1200 metres in thickness. Volcanic clasts are predominantly andesite and basaltic andesite, with subordinate rhyolite and basalt. The tuffs contain both subaerially erupted and submarine erupted volcaniclastics. The suite is inferred to have formed on the flanks of an emergent marine stratovolcano.

- The Paradise suite contains a variable thickness (50m to 400m+) of basaltic pillow lavas and rarer massive flows, pillow breccias and tuffaceous sandstones and siltstones. Lateral variation in thickness may reflect eruption onto an irregular seafloor topography.

- The Circular Bush Suite shows calc-alkaline trends in TiO_2 abundance, suggesting fractionation under high P_{H_2O} and fO_2. The suite has immobile element abundances similar to medium-K calc-alkaline rocks.

- The Paradise Suite contains basalts which have a tholeiitic trend of Fe enrichment. They have high Al_2O_3 and have immobile element abundances similar medium-K calc-alkaline rocks. Their high plagioclase content may reflect melting of a plagioclase rich source (i.e., plagioclase peridotite - garnet peridotite transition).

- Both the Circular Bush Suite and the Paradise Suite have LILE and HFSE which suggest they are subduction-related. It is unclear whether they formed in a continental margin or an intra-oceanic island arc.

- The succession is folded into a series of north-south striking, tight to isoclinal folds (F_1), which have been refolded by two subsequent phases of folding of unknown orientation (F_2 and F_3).

- Analysis of calcite c-axes on a calc-mylonite from the Haupiri Fault suggests that the latest movement on this fault had a normal sense of shear.

- Basic alkaline dykes cross-cut F_1 fabrics. The dykes show broad geochemical similarities to continental flood basalts, suggesting they were emplaced in an intra-plate setting. Similar intrusives are documented throughout the Takaka Terrane.

CHAPTER EIGHT: FUTURE WORK

Recommendations for further work include:

- Isotopic characterisation of Central Belt volcanics in order to determine affinities between the various suites.

- Mapping and geochemistry of Devil River Volcanics to the north (Haupiri Range, Hardy Ridge areas).

- Further study on the Christmas Conglomerate - clast population, depositional environment, petrology and geochemistry of clasts, strain analysis of deformed clasts.

- Mapping and geochemistry of volcanics in the Anatoki Formation to the east and southeast of Boulder lake to determine affinity to other Central Belt volcanic suites.

- Detailed geochemical characterisation and dating of basic intrusives throughout the Takaka Terrane.

REFERENCES

Bell, J.M., Webb, E.J.H., and Clarke, E. de C., 1907, The Geology of the Parapara Subdivision, Karamea, Nelson., *New Zealand Geological Survey Bulletin* 3

Bishop, D.G., 1971, Sheet S1 and S3 - Farewell - Collingwood (1st ed.). Geological Map of New Zealand 1:63 360. DSIR, Wellington, New Zealand

Bishop, D.G., Bradshaw, J.D., and Landis, C.A., 1985, Provisional terrane map of the South Island, New Zealand. In: D.G. Howell (Ed.): *Tectonostratigraphic Terranes of the Circum-Pacific Region*, pp 515-521. Circum-Pacific Council for Energy and Mineral Resources, Earth Sciences Series, 1

Bradshaw, J.D., 1982, S13 - Cobb: a review of the new map and the structural interpretation of the Central Belt rocks of S13 and S8. *New Zealand Journal of Geology and Geophysics* 25: 371-379

Bradshaw, J.D., Weaver, S.D., and Laird, M.G., 1985, Suspect terranes and Cambrian tectonics in northern Victoria Land, Antarctica. In: Howell, D.G.(Ed.), *Tectonostratigraphic Terranes of the Circum Pacific Region.* Circum-Pacific Council for Energy and Mineral Resources, Earth Sciences Series 1: 467-497

Braithwaite, R.L., 1968, The Geology of the Boulder Lake Area, North-west Nelson. Part 1 - The Anatoki Formation. *New Zealand Journal of Geology and Geophysics* 11(1): 78-91

Busby-Spera, C.J., 1988, Evolution of a middle Jurassic back-arc basin, Cedros Island, Baja California: evidence for a marine volcaniclastic apron. *Geological Society of America Bulletin* 100: 218-233

Cas, R.A.F., and Wright, J.V., 1987, *Volcanic successions: modern and ancient.* Allan and Unwin, London

Coleman, A.C., 1971, Geology of the Middle Cobb Area, Northwest Nelson. B Sc(Hons) Thesis, University of Otago, Dunedin, New Zealand

Coleman, A.C., 1981, Part sheets S18, S19, S25, S26 Wangapeka. 1:63 360 Geological Map of New Zealand and accompanying notes. DSIR Wellington, New Zealand

Cooper, R.A., 1979, Lower Palaeozoic rocks of New Zealand. *Journal of the Royal Society of New Zealand* 9(1): 29-84

1984, Lower Palaeozoic terranes. *Geological Society of New Zealand Miscellaneous Publication* 31A

1986, Central Belt structure: an alternative interpretation. *Geological Society of New Zealand Miscellaneous Publication* 34: 11-13

1989, Early Palaeozoic terranes of New Zealand. *Journal of the Royal Society of New Zealand* 19(1): 73-112

1993, Northwest Nelson basement geology: Part 1 - the Takaka Terrane - background and introduction. *Geological Society of New Zealand Miscellaneous Publication* 79B: 77-84

Cooper, R.A., and Tulloch, A.J., 1992, Early Palaeozoic terranes in New Zealand and their relationships to the Lachlan Fold Belt. *Tectonophysics* 214: 129-144

Crawford, A.J., 1984, Geochemistry of Cambrian volcanics in dispersed fragments of Gondwana foldbelts. Seventh Australian Geological Convention, Sydney, *Geological Society of Australia, Abstracts*: 12.

Crawford, A.J., and Cameron, W.E., 1985, Petrology and geochemistry of Cambrian boninites and low-Ti andesites from Heathcote, Victoria. *Contributions to Mineralogy and Petrology* 91: 93-104

Crawford, A.J., Corbett, K.D., and Everard, J.L., 1992, Geochemistry of the Cambrian volcanic hosted massive sulphide-rich Mount Read Volcanics, Tasmania and some tectonic implications. *Economic Geology* 87: 597-619

Crawford, A.J., and Keays, R.R., 1978, Cambrian greenstone belts in Victoria: marginal sea-crust slices in the Lachlan Fold Belt of southeastern Australia. *Earth and Planetary Science Letters* 41: 197-208

Crook, 1980, Fore-arc evolution and continental growth: a general model. *Journal of Structural Geology* 2: 289-303

Crook, K.A.W. and Feary, D.A., 1982, Development of New Zealand according to the fore-arc model of crustal evolution. *Tectonophysics* 87: 65-107

Ewart, A., 1982, The mineralogy and petrology of Tertiary-Recent orogenic volcanic rocks: with special reference to the andesitic-basaltic compositional range. In: Thorpe, R.S. (Ed.), *Andesites.* John Wiley and Sons

Fisher, R.V., 1984, Submarine volcaniclastic rocks. In: Kokelaar, B.P., Howells, M.F. (Eds), Marginal basin geology: volcanic and associated sedimentary and tectonic processes in

modern and ancient marginal basins. *Geological Society of London Special Publication* 16: 5-27

Grindley, G.W., 1961, Sheet 13-Golden Bay (1st ed.). Geological map of New Zealand 1:250 000. DSIR, Wellington, New Zealand

1971, Sheet S8 - Takaka (1st ed.). Geological Map of New Zealand 1:63 360. DSIR, Wellington, New Zealand

1978, in Suggate, R.P., Stevens, G.R., and Te Punga, M.T., (Eds) 1978, *The Geology of New Zealand.* Government Printer: Wellington. 2 vols: 820 pp.

1980, Sheet S13 - Cobb (1st ed.) Geological Map of New Zealand 1:63 360. DSIR, Wellington, New Zealand

1982, S13 - Cobb. A review of the new map and the structural interpretation of the Central Belt Rocks of S13 and S8 - Reply. *New Zealand Journal of Geology and Geophysics* 25: 371-379

Harrison, I.S., 1993, The structure of the Buller Terrane west of the Anatoki Thrust, upper Cobb Valley, Northwest Nelson, New Zealand. Unpublished M.Sc. Thesis, University of Canterbury, Christchurch.

Henderson, J., Notes to accompany a Geological Sketch-map of the Mount Arthur District. *Journal of Science and Technology* 6: 174-190

Houghton, B.F., and Landis, C.A., 1989, Sedimentation and volcanism in a Permian arc-related basin, southern New Zealand. *Bulletin of Volcanology* 51: 433-450

Keble R.A., and Benson, W.N., 1929, Ordovician Graptolites of North-west Nelson. *Transactions of the New Zealand Institute* 59: 840-863.

Le Maitre, R.W., (Ed.), 1989, *A Classification of Igneous Rocks and Glossary of Terms.* Blackwell, Oxford. 193 pp.

McDonough, W.F., Sun, S-s, Ringwood, A.E., Jagoutz, E., and Hofmann, A.W., 1992, K, Rb and Cs in the earth and moon and the evolution of the earth's mantle. *Geochimica et Cosmochimica Acta.* 56: 1001-1012

Munker, C., 1993, Geology and geochemistry of metavolcanic rocks west of Cobb Reservoir, Northwest Nelson, New Zealand., Diploma Thesis, Institut fur Geologie und Dynamik der Lithosphare der Georg August Universitat, Gottingen, Germany

Norrish, K., and Hutton, J.T., 1969, An accurate X-ray spectrographic method for the analysis of a wide range of geologic samples. *Geochimica et Cosmochimica Acta* 33: 431-454

Pearce, J.A., 1975, Basalt geochemistry used to investigate past tectonic environments on Cyprus. *Tectonophysics* 25: 41-67

Pearce, J.A., and Cann, J.B., 1973, Tectonic setting of basic volcanic rocks using trace element analyses. *Earth and Planetary Science Letters* 19: 290-300

Pearce, J.A., and Norry, M.J., 1979, Petrogenetic implications of Ti, Zr, Y and Nb variations in volcanic rocks. *Contributions to Mineralogy and Petrology* 69: 33-47

Pound, K., 1993, Haupiri Group rocks of Northwest Nelson. *Geological Society of New Zealand Miscellaneous Publication* 79B: 85 -105

Powell, M., 1978, Crystallisation conditions of low-pressure cumulate nodules from the Lesser Antilles island arc. *Earth and Planetary Science Letters* 39: 162-172

Powell, N.G., 1984, Metamorphism within part of the Waingaro Schist Zone, Northwest Nelson, New Zealand. Unpublished M.Sc. Thesis, University of Auckland, New Zealand

1985, Devil River Fault and Anatoki Thrust: Thin associated structures, mechanisms and senses of movement. *Geological Society of N.Z. Miscellaneous Publication* 32A

1986a, On some aspects of the Devil River Volcanics. *Geological Society of New Zealand Miscellaneous Publication* 34: 32

1986b, Timing of metamorphism and deformation in the Takaka Terrane, with notes on metamorphic zonation. *Geological Society of New Zealand Miscellaneous Publication* 34: 33-35

Rennison, M.W., 1992, The petrology, structure and geochemistry of the eastern margin of the Mount Olympus Pluton, Northwest Nelson, New Zealand. Unpublished B.Sc.(Hons) thesis, University of Canterbury, New Zealand

Saunders, A.D., Norry, M.J., and Tarney, J., 1991, Fluid influence on the trace element compositions of subduction zone magmas. *Philosophical Transactions of the Royal Society of London SERIES A* 335: 377-392

Shelley, D., 1975, Metamorphic belt and volcanic arc migration in New Zealand. *Nature* 258: 668-672

1981, The Pikikuruna nappe, Northwest Nelson. *N.Z. Journal of Geology and Geophysics* 27: 139-149

1993, *Igneous and metamorphic rocks under the microscope: classification, textures, microstructures and mineral preferred orientations*. Chapman and Hall pp 445.

Sigurdsson, H., Sparks, R.S.J., Carey, S.N., and Huang, T.C., 1980, Volcanogenic sedimentation in the Lesser Antilles arc. *Journal of Geology* 88: 523-540

Stewart, M., 1988. The geology of the Cobb Reservoir area, Northwest Nelson. Unpublished M. Sc. Thesis, University of Canterbury, New Zealand

Sun, S-s, and McDonough, W.F., 1989, Chemical and isotopic systematics of oceanic basalts: implications for mantle composition and processes. In: Saunders, A.D., and Norry, M.J., (eds.), *Magmatism in the ocean basins*. Geological Society of London Special Publication 42: 313-345

Turner, F.J., 1953, Nature and dynamic interpretation of deformation lamellae in calcite of three marbles. *American Journal of Science* 251: 276-298

Ward, C.M., 1986a, The Fanny and Goodyear terranes of southern Fiordland and their relations with west Nelson. *Geological Society of New Zealand Miscellaneous Publication* 34: 46-47

Weaver, S.D., Bradshaw, J.D., and Laird, M.G., 1984, Geochemistry of Cambrian volcanics of the Bowers Supergroup and implications for the Early Palaeozoic tectonic evolution of northern Victoria Land, Antarctica. *Earth and Planetary Science Letters* 68: 128-140

Weaver, S.D., Gibson, I.L., Houghton, B.F., and Wilson, C.J.N., 1990, Mobility of rare earth and other elements during the crystallisation of peralkaline silicic lavas. *Journal of Volcanology and Geothermal Research* 43: 57-70

Wilson, M, 1989, *Igneous Petrogenesis: a global tectonic approach*. Harper Collins, London, pp 466

Wood, D.A., 1980, The application of a Th-Hf-Ta diagram to the problems of tectonic classification and to establishing the nature of crustal contamination of basaltic lavas of the British Tertiary volcanic province. *Earth and Planetary Science Letters* 50: 11-30

APPENDIX ONE: SAMPLE LOCATIONS

(CBS = Circular Bush suite, PS = Paradise suite, CCM = Christmas Conglomerate Member, UOC = University of Canterbury)
All grid references taken from NZMS 260: M26 Cobb.

Field No.	UOC No.	Grid Ref	Description
DRM 3	14607	782285	CBS tuff-breccia (matrix)
DRM 4	14608	782285	CBS andesite clast
DRM 5	14609	783284	CBS rhyolite clast
DRM 8	14610	784283	CBS lapilli tuff-tuff
DRM 10	14611	789283	Chert lens
DRM 12	14612	791283	CBS lapilli-tuff
DRM 13	14613	792283	CBS sheared tuffaceous sandstone
DRM 14	14614	793283	CBS lapilli-tuff
DRM 15	14615	793283	Tuffaceous sandstone/siltstone
DRM 16	14616	794283	CBS lapilli-tuff, tuff-breccia
DRM 17	14617	794283	CBS tuff
DRM 18	14618	795284	Tuffaceous sandstone
DRM 19	14619	794284	CBS lapilli-tuff
DRM 20	14620	795283	CBS lapilli-tuff, tuff-breccia
DRM 21	14621	795283	CBS basaltic andesite clast
DRM 23	14622	795285	CBS basaltic-andesite clast
DRM 25	14623	786305	PS pillow lava
DRM 26	14624	787305	PS pillow lava
DRM 27	14625	787281	CBS sericite-pyrite lens
DRM 28	14626	787279	CBS highly altered andesite clast
DRM 29	14627	789273	Devil Volcanic Conglomerate
DRM 30	14628	785275	CBS basalt?
DRM 31	14629	783275	PS pillow basalt
DRM 38	14630	797286	CBS tuffaceous sandstone
DRM 39	14631	797286	Recrystallised carbonate lens
DRM 41	14632	798286	CBS tuff
DRM 62	14633	803284	CBS tuffaceous sandstone
DRM 63	14634	805284	Tuffaceous sandstone
DRM 65	14635	820285	Tuffacous sandstone/siltstone
DRM 66	14636	804284	CBS basalt ?
DRM 70	14637	782285	CBS andesite clast
DRM 71	14638	783284	CBS rhyolite clast
DRM 72	14639	783284	CBS rhyolite clast
DRM 73	14640	784283	CBS tuff-breccia (matrix)
DRM 74	14641	784283	CBS andesite clast
DRM 75	14642	786283	CBS carbonate-rich tuff
DRM 76	14643	786283	CBS carbonate-rich tuff
DRM 78	14644	786283	CBS tuffaceous sandstone
DRM 79	14645	786282	CBS carbonate-rich tuff
DRM 83	14646	797283	CBS tuffaceous sandstone
DRM 89	14647	777296	Chert-lithic coarse sandstone
DRM 91	14648	792303	PS pillow breccia

Field No.	UOC No.	Grid ref	Description
DRM 92	14649	792303	PS pillow lava
DRM 93	14650	792302	PS pillow lava
DRM 94	14651	792300	PS tuffaceous sandstone
DRM 95	14652	792299	Fine grained tuffaceous sandstone
DRM 97	14653	771297	Calc-mylonite
DRM 98	14654	773299	Sheared quartz-rich sandstone
DRM 111	14655	803305	Microdiorite sill
DRM 112	14656	803304	Basic dyke
DRM 115	14657	790305	PS pillow lava
DRM 118	14658	783284	CBS rhyolite
DRM 122(a)	14659	771297	Orientated calc-mylonite
DRM 122(b)	14660	771297	Orientated calc-mylonite
DRM 124	14661	789283	Chert lens
DRM 136	14662	789259	Tuff-breccia
DRM 137	14663	780262	Chert lens
DRM 138	14664	783275	PS pillow lava
DRM 139	14665	808288	Basic dyke
DRM 141	14666	808287	CCM sandstone clast
DRM 142	14667	807287	CCM basaltic andesite clast
DRM 143	14668	803282	Laminated grey siltstone/fine sandstone
DRM 145	14669	802285	Microdiorite sill
DRM 146	14670	785280	CBS andesite clast
DRM 147	14671	798305	CBS lapilli-tuff
DRM 148	14672	799305	Microdiorite sill
DRM 153	14673	785300	Grey sandstone and laminated siltstone
DRM 154	14674	801302	Grey sandstone and laminated siltstone
DRM 160(a)	14675	803307	CCM pebble conglomerate
DRM 160(b)	14676	803307	CCM pebble conglomerate

APPENDIX TWO: THIN SECTION DESCRIPTIONS OF THE VOLCANIC ROCKS

SAMPLE No.	COMPOSITION	DESCRIPTION/TEXTURE	INTERPRETATION
DRM 5	plagioclase (sericitized), quartz, biotite, chlorite, apatite, zoisite, albite , calcite.	Bipyramidal embayed quartz (1-3mm) phenocrysts and sericitized and carbonate/albite altered plagioclase phenocrysts in a fine grained felsitic groundmass of quartz, albite, zoisite, sericite and chlorite. Small biotite microphenocrysts degraded to carbonate and a dark-grey isotropic mineral. Small apatite crystals within the biotite.	Rhyolite clast
DRM 71	plagioclase (sericitized), quartz, K-feldspar?, biotite, chlorite, apatite, zoisite, albite , calcite.	1-5 mm bipyramidal embayed quartz phenocrysts (often with small rounded inclusions) and sericitized and carbonate/albite altered plagioclase phenocrysts (An 5-10%) in a fine grained felsitic groundmass of quartz, albite, zoisite, sericite and chlorite. Thin (1-3mm) slightly more felsic layers alternating with darker, slightly more basic layers - primary flow banding. Thin styolitic layers and pressure solution seams. Degraded biotite microphenocrysts.	Flow banded rhyolite clast
DRM 72	plagioclase (sericitized), quartz, K-feldspar?, biotite, chlorite, apatite, zoisite, albite , calcite.	1-5 mm bipyramidal embayed quartz phenocrysts (often with small rounded inclusions) and sericitized and carbonate/albite altered plagioclase (An 5 - 9%) phenocrysts in a fine grained felsitic groundmass of quartz, albite, zoisite, sericite and chlorite. Ground mass sometimes shows a poikilomosaic texture of albite enclosing tiny grains of sericite and chlorite. Possibly some K-feldspar phenocrysts.	Rhyolite clast
DRM 28	plagioclase (highly saussuritized and sericitized), chlorite, calcite, magnetite, zoisite, quartz	Highly altered plagioclase in an altered felsitic matrix. Abundant carbonate.	Andesite clast
DRM 70	plagioclase (saussuritized and sericitized), chlorite, calcite, albite, zoisite, quartz, magnetite, ilmenite	Porphyritic texture of 2-5mm tabular plagioclase phenocrysts and chlorite (after clinopyroxene and amphibole) in a fine grained felsitic groundmass of sericite, albite, quartz, chlorite, ilmenite and magnetite. Plagioclase shows relic zoning preserved by alternating sericitized and saussuritized layers. Amygdales are infilled with quartz and chlorite.	Andesite clast
DRM 74	plagioclase (saussuritized and sericitized), chlorite, calcite, albite, zoisite, quartz, magnetite, ilmenite	Porphyritic texture of 2-5mm tabular plagioclase phenocrysts and chlorite (after clinopyroxene and amphibole) in a fine grained felsitic groundmass of sericite, albite, quartz, chlorite, ilmenite and magnetite. Plagioclase shows relic zoning preserved by alternating sericitized and saussuritized layers. Amygdales are infilled with quartz and chlorite.	Andesite clast
DRM 23	Plagioclase (highly saussuritized and sericitized), chlorite, epidote, calcite, zoisite, quartz, magnetite, ilmenite.	Intergranular texture of interlocking variably altered plagioclase in a groundmass of albite, chlorite, epidote, carbonate and magnetite.	Basaltic andesite clast
DRM 146	Plagioclase, chlorite, calcite, epidote, magnetite	Intergranular texture of interlocking variably altered plagioclase in a groundmass of albite, chlorite, epidote, carbonate and magnetite.	Basaltic-andesite clast
DRM 30	Plagioclase (saussuritized and sericitized), epidote, zoisite, chlorite, ilmenite, magnetite	Intersertal texture. Altered plagioclase (1-3mm) laths in a groundmass of chlorite, albite, epidote, zoisite and ilmenite.	Basalt clast
DRM 66	Plagioclase (saussuritized and sericitized), epidote, zoisite, chlorite, ilmenite, magnetite	Intersertal texture. Altered plagioclase (1-3mm) laths in a groundmass of chlorite, albite, epidote, zoisite and ilmenite.	
DRM 136	chlorite, albite, zoisite, magnetite, chlorite	Volcanic breccia with clasts with porphyritic texture (7-20mm) clinopyroxene phenocrysts pseudomorphed by chlorite in a fine/medium grained groundmass of chlorite, albite+magnetite	Basalt clast

Brief thin section descriptions of selected Circular Bush suite volcanic clasts.

SAMPLE No.	COMPOSITION	DESCRIPTION/TEXTURE	INTERPRETATION
DRM 3	chlorite, saussuritized and sericitized plagioclase, albite, magnetite, calcite	Fragmental: abundant 1-2 mm saussuritized plagioclase (showing relic twinning and zoning), chlorite replacing clinopyroxene. Chlorite occurs in voids, which may reflect an original sorting. Numerous pressure solution seams.	tuff-breccia (matrix)
DRM 14	sericitized plagioclase, albite, chlorite, magnetite, ilmenite, quartz	Fragmental: 2-7 mm rock volcanic rock fragments (andesite?), altered plagioclase, chlorite and calcite infilling voids. Numerous pressure solution seams. Minor amount of quartz grains.	Lapilli-tuff
DRM 16	saussuritized plagioclase, albite, chlorite, epidote, magnetite and quartz	Fragmental: saussuritized plagioclase (showing relic twinning and zoning). Equidimensional tachylytic shards. Epidote overgrowths. Pressure solution seams and chlorite + quartz veins.	Lapilli-tuff, tuff-breccia
DRM 17	calcite, chlorite, saussuritized plagioclase, rare quartz, magnetite	Fragmental : cuspate shaped vitric shards. Chlorite replacing clinopyroxene and amphibole. Abundant calcite.	Reworked tuff
DRM 20	saussuritized plagioclase, albite, chlorite, epidote, magnetite and quartz	Fragmental: saussuritized plagioclase (showing relic twinning and zoning). Equidimensional tachylytic shards. Epidote overgrowths. Pressure solution seams and chlorite + quartz veins.	Lapilli-tuff, tuff-breccia
DRM 41	calcite, chlorite, saussuritized plagioclase, rare quartz, magnetite	Fragmental : cuspate shaped vitric shards. Chlorite replacing clinopyroxene and amphibole. Abundant calcite.	Reworked tuff
DRM 73	chlorite, calcite, sericitized and saussuritized plagioclase, magnetite	Fragmental: coarse medium sand sized plagioclase (broken and subangular). Numerous pressure solution seams. Andesitic rock fragments (up to 2cm).	Tuff-breccia (matrix)
DRM 75	sericitized plagioclase, calcite, ankerite, chlorite, albite,	Fragmental: (highly altered) calcite and chlorite replacing ferromagnesian minerals, 1-2mm extremely altered plagioclase laths.	Carbonate-rich tuff
DRM 76	sericitized plagioclase, calcite, ankerite, chlorite, albite,	Fragmental: (highly altered) calcite and chlorite replacing ferromagnesian minerals, 1-2mm extremely altered plagioclase laths.	Carbonate-rich tuff

Brief thin section descriptions of selected Circular Bush suite volcaniclastic rocks

SAMPLE No.	COMPOSITION	DESCRIPTION/TEXTURE	INTERPRETATION
DRM 26	plagioclase (albitized/sericitized) 51%. chlorite 35%, magnetite 8%, calcite 4%, epidote 2%, quartz 1%.	Large (2-7mm) glomeroporphyritic masses of plagioclase (An 5 to ~15%) set in a fine grained groundmass of albite, chlorite and disseminated opaques. Swallow tailed and elongate albite microlites indicate rapid quenching. 1-2mm vesicles infilled by calcite and chlorite.	Plagioclase-phyric basaltic pillow lava
DRM 91	plagioclase (strongly saussuritized), chlorite, epidote, quartz, calcite, ilmenite.	Fragmental: 2-5 cm angular clasts, framework supported. Clasts contain highly-altered plag phenocrysts (2-4mm) set in a fine grained altered groundmass of albite, zoisite, epidote, and chlorite. Calcite and chlorite totally replacing clinopyroxene? Thin (<1mm) calcite + chlorite veins.	Basaltic hyaloclastite pillow breccia
DRM 92	plagioclase (strongly saussuritized), albite, chlorite, epidote, ilmenite, calcite	Large highly altered plagioclase phenocrysts (8%) (3-6mm) in an altered fine grained groundmass of chlorite, albite, ilmenite, zoisite, epidote. Relic albite microlites can be occasionally observed. Weak alignment of minerals in groundmass may reflect primary flow texture or a later tectonic overprint). Calcite and chlorite totally replacing clinopyroxene?	Plagioclase-phyric basaltic pillow lava.
DRM 115	plagioclase (variably sericitized, albitized and saussuritized), chlorite, calcite, ilmenite, magnetite	Variably altered glomeroporphyritic plagioclase (1-5mm) in a fine grained, intersertal texture, groundmass of albite. sericite and chlorite. 10-15% rounded 1-2 mm vesicles - infilled by calcite and chlorite. Thin (<1mm) calcite veinlets.	Vesicular, plagioclase-phyric basaltic pillow lava.
DRM 138	plagioclase (variably sericitized, albitized and saussuritized), chlorite, calcite, quartz ilmenite, magnetite	Variably altered glomeroporphyritic masses of plagioclase (1-5mm) (35-40%) in a fine grained groundmass of albite, chlorite, epidote, zoisite and ilmenite. 1-3mm vesicles infilled with calcite + carbonate, or more rarely, quartz.	Plagioclase-phyric basaltic pillow lava.

Brief thin-section descriptions of selected Paradise suite rocks.

SAMPLE No.	COMPOSITION	DESCRIPTION/TEXTURE	INTERPRETATION
DRM 111	quartz, plagioclase, chlorite, leucoxene, zoisite	Intergranular texture. Plagioclase albitized and sericitized or weakly saussuritized. Plagioclase is intergrown with chlorite, albite and quartz. Leucoxene has formed as a breakdown product of ilmenite.	Microdiorite sill
DRM 145	quartz, plagioclase, chlorite, leucoxene, epidote	Intergranular to sub ophitic texture. Plagioclase albitized and sericitized. Leucoxene has formed as a breakdown product of ilmenite.	Microdiorite sill
DRM 148	quartz, plagioclase, chlorite, leucoxene, hornblende, sericite, apatite?	Intergranular to sub ophitic texture. Plagioclase albitized and sericitized. Leucoxene has formed as a breakdown product of ilmenite. Small amount of fresh brown-green pleochroic hornblende.	Microdiorite sill
DRM 112	albite, chlorite, sericite, chlorite, apatite, calcite, ilmenite	Predominantly aphyric, fine grained texture of interlocking sericitized and albitized feldspar, often rimmed with ilmenite. Small apatite needles as inclusions in some feldspar. Small (1mm) rhombohedral shaped features replaced by chlorite, quartz and carbonate may either be altered clinopyroxene or sheared out vesicles.	Basic alkaline dyke
DRM 139	albite, chlorite, sericite, chlorite, apatite, calcite, ilmenite	Predominantly aphyric, fine grained texture of interlocking sericitized and albitized feldspar, often rimmed with ilmenite. Small apatite needles are found as inclusions in many feldspar crystals. Some feldspars have very high aspect ratios.	Basic alkaline dyke

Brief thin-section descriptions of selected intrusive rocks.

APPENDIX THREE: GEOCHEMICAL DATA

Major element data are presented as analysed, but for geochemical plots were recalculated on an anhydrous basis to eliminate the loss on ignition (LOI). Recalculated major element abundances are presented in the following table, as are CIPW normative values. For normative calculations an arbitrary ratio of $Fe_2O_3/FeO = 0.3$ was used.

Analytical precision and detection limits for XRF, and Primitive Mantle normalisation values used in this thesis are also given.

SAMPLE	DRM 12	DRM 16	DRM 17	DRM 20	DRM 23	DRM 25	DRM 26	DRM 28	DRM 30	DRM 31
SiO_2	58.07	53.47	48.48	52.81	53.25	43.24	46.94	52.48	48.35	47.96
TiO_2	.78	.87	.98	1.07	1.02	1.07	1.23	.65	.93	1.01
Al_2O_3	16.80	19.15	14.88	15.83	17.19	22.66	20.39	11.49	18.74	20.09
Fe_2O_3	6.66	8.77	6.64	7.08	8.00	7.03	9.16	5.60	8.27	12.22
MnO	.20	.16	.16	.14	.16	.11	.13	.17	.20	.15
MgO	2.95	3.33	6.25	4.81	4.97	2.47	3.23	2.49	4.85	3.93
CaO	4.15	6.48	8.18	6.79	6.90	11.43	5.20	9.07	5.97	3.02
Na_2O	3.81	3.69	2.21	2.17	2.55	2.60	4.97	2.01	5.00	5.46
K_2O	1.54	.58	.84	.43	.17	1.49	.39	.77	.11	.75
P_2O_5	.19	.20	.16	.18	.20	.29	.43	.16	.22	.25
LOI	3.11	3.21	9.22	6.77	3.56	5.70	5.70	13.12	4.98	4.81
TOTAL	100.26	99.91	99.99	100.19	100.37	100.17	100.29	99.68	100.11	99.65
Cr	35	31	163	107	59	64	73	6	68	66
Ni	11	12	28	23	31	32	28	7	28	29
V	87	89	151	171	238	358	408	115	308	386
Pb	8	8	8	9	10	5		9	2	6
Zn	94	103	81	81	85	109	154	79	105	107
K	12784	4815	6973	3570	1411	12369	3238	6392	913	6226
Rb	37	28	28	13	3	37	10	24	2	22
Ba	817	221	129	88	21	4802	364	217	78	499
Sr	430	147	147	237	537	787	590	309	720	449
Ga	17	19	19	17	14	8	18	11	5	20
Nb	14	14	8	10	8	13	16	7	9	13
Zr	118	147	103	95	112	100	92	90	64	75
Ti	4676	5216	5875	6415	6115	6415	7374	3897	5575	6055
Y	18	17	17	17	22	17	15	10	13	14
Th	6	4	4	2	5	3	4	3	2	4
La	15	24	7	6	12	11	15	17	8	17
Ce	37	54	24	22	30	40	41	43	32	27
Nd	<10	17	<10	<10	14	<10	16	14	<10	19
SiO_2	60.19	55.20	53.81	56.96	55.47	46.10	50.05	61.02	51.28	51.07
TiO_2	.81	.90	1.09	1.15	1.06	1.14	1.31	.76	.99	1.08
Al_2O_3	17.41	19.77	16.51	17.07	17.91	24.16	21.74	13.36	19.88	21.39
Fe_2O_3	2.13	9.05	2.27	2.35	2.57	2.31	3.01	2.00	2.70	3.09
FeO	6.15	.17	6.57	6.80	7.43	6.68	8.70	5.80	7.82	8.93
MnO	.21	.17	.18	.15	.17	.12	.14	.20	.21	.16
MgO	3.06	3.44	6.94	5.19	5.18	2.63	3.44	2.90	5.14	4.19
CaO	4.30	6.69	9.08	7.32	7.19	12.19	5.54	10.55	6.33	3.22
Na_2O	3.95	3.81	2.45	2.34	2.66	2.77	5.30	2.34	5.30	5.81
K_2O	1.60	.60	.93	.46	.18	1.59	.42	.90	.12	.80
P_2O_5	.20	.21	.18	.19	.21	.31	.35	.19	.23	.27
Total	100.00	100.00	100.00	100.00	100.00	100.00	100.00	100.00	100.00	100.00
qz	13.82	8.03	5.40	14.67	12.13	-	-	19.86	-	-
c	1.72	1.16	-	-	.71	-	3.23	-	-	5.66
z	.02	.03	.02	.02	.02	.02	.02	.02	.01	.02
or	9.45	3.58	5.52	2.75	1.05	9.40	2.46	5.30	.69	4.73
ab	33.41	32.51	20.75	19.80	22.47	13.23	44.83	19.77	44.87	49.19
an	20.45	32.24	31.31	34.73	34.51	49.11	25.54	23.33	30.14	14.53
di	-	-	10.26	.37	-	9.22	-	23.24	.05	-
hy	16.21	17.17	21.01	21.66	22.97	-	5.47	3.78	2.45	7.67
ol	-	-	-	-	-	7.92	10.90	-	15.57	11.19
mt	3.08	3.14	3.29	3.41	3.72	3.35	4.36	2.91	3.92	4.47
cr	.01	.01	.04	.02	.01	.01	.02	-	.02	.02
il	1.54	1.72	2.07	2.19	2.02	2.17	2.49	1.44	1.87	2.04
ap	.47	.49	.42	.46	.49	.75	.84	.44	.55	.64
ne	-	-	-	-	-	5.54	-	-	-	-

SAMPLE	DRM 41	DRM 66	DRM 70	DRM 71	DRM 73	DRM 74	DRM 75	DRM 83	DRM 91	DRM 92
SiO_2	53.10	49.21	54.51	75.54	52.01	57.53	52.54	54.40	48.87	46.49
TiO_2	.96	1.24	1.00	.10	.90	.92	.84	.79	1.47	1.57
Al_2O_3	15.65	19.47	17.33	12.84	14.85	17.31	16.17	15.36	19.61	20.01
Fe_2O_3	9.38	10.42	8.59	1.76	7.99	3.76	7.20	7.75	12.58	7.76
MnO	.17	.16	.13	.03	.14	.11	.14	.18	.05	.08
MgO	4.70	4.11	3.85	.58	4.16	1.63	3.80	5.82	2.65	2.31
CaO	5.56	7.53	4.77	.86	7.14	6.913	5.77	4.87	4.05	7.73
Na_2O	3.08	3.94	3.72	6.33	2.86	3.93	2.86	3.41	1.06	3.85
K_2O	1.20	.32	.70	.14	.48	.81	1.11	1.004	2.75	1.96
P_2O_5	.13	.24	.20	.05	.17	.20	.19	.14	.05	.44
LOI	6.45	3.24	4.70	1.68	8.49	6.71	9.18	5.84	7.16	8.17
TOTAL	100.38	99.87	99.51	99.92	99.20	99.83	99.78	99.60	100.29	100.36
Cr	132	66	39	< 3	34	34	48	154	35	37
Ni	27	27	12	4	11	7	14	20	23	22
V	184	221	158	16	139	129	130	123	248	246
Pb	3	9	12	5	6	12	5	8	11	10
Zn	89	103	104	25	91	36	76	106	109	112
K	9962	2656	5811	1162	3985	6724	9214	8716	22829	16271
Rb	46	8	23	4	18	27	45	32	87	66
Ba	4248	179	347	57	160	258	404	240	903	596
Sr	117	362	748	186	335	656	268	199	267	462
Ga	12	14	21	12	15	14	16	19	20	19
Nb	8	9	9	11	9	10	10	8	21	22
Zr	96	127	109	66	101	108	103	107	131	129
Ti	5755	7434	5995	600	5396	5515	5036	4736	8813	9412
Y	18	25	18	1	16	19	17	17	10	25
Th	4	7	6	8	3	4	4	5	5	7
La	6	13	17	20	15	20	17	11	10	23
Ce	23	38	39	34	35	40	35	33	27	80
Nd	11	20	21	12	12	20	14	<10	<10	24
SiO_2	56.97	51.34	57.90	77.01	57.73	61.98	58.33	58.51	53.02	50.05
TiO_2	1.03	1.29	1.06	.10	1.00	.99	.93	.83	1.59	1.31
Al_2O_3	16.79	20.31	18.41	1309	16.48	18.65	17.95	16.38	21.27	21.74
Fe_2O_3	2.39	2.58	2.16	.43	2.10	.96	1.90	1.97	2.01	3.01
FeO	6.91	7.46	6.26	1.23	6.09	2.78	5.49	5.69	5.82	8.70
MnO	.18	.17	.14	.03	.16	.12	.16	.19	.09	.14
MgO	5.04	4.29	4.09	.59	4.62	1.76	4.22	6.17	2.52	3.44
CaO	5.96	7.85	5.07	.88	7.93	7.44	6.41	5.36	8.44	5.54
Na_2O	3.30	4.11	3.95	6.45	3.17	4.23	3.18	3.65	4.20	5.30
K_2O	1.29	.33	.74	.14	.53	.87	1.23	1.11	2.14	.42
P_2O_5	.14	.26	.21	.05	.19	.22	.21	.15	.48	.35
Total	100.00	100.00	100.00	100.00	100.00	100.00	100.00	100.00	100.00	100.00
qz	8.76	-	11.82	35.46	12.10	16	12.32	9.34	15.74	-
c	-	-	2.28	.82	-	-	.18	-	8.18	-
z	.02	.03	.02	.01	.02	.02	.02	.02	.03	.03
or	7.63	1.98	4.40	.85	3.16	5.17	7.30	6.57	17.67	12.67
ab	27.96	34.78	33.43	54.60	26.86	35.82	26.87	30.84	9.73	32.08
an	27.47	36.03	24.14	4.10	29.18	29.35	30.64	25.07	21.82	34.47
di	2.05	1.14	-	-	7.44	5.32	-	.55	-	3.82
hy	20.90	17.85	18.40	3.27	15.94	4.67	17.76	22.89	19.16	-
ol	-	1.48	-	-	-	-	-	-	-	7.91
mt	3.46	3.74	3.14	.62	3.05	1.39	2.75	2.85	4.69	2.91
cr	.03	.01	.01	-	.01	.01	.01	.04	.01	.01
il	1.96	2.46	2.02	.19	1.90	1.88	1.77	1.58	3.03	3.25
ap	.34	.62	.51	.12	.45	.51	.50	.35	.13	1.14
ne	-	-	-	-	-	-	-	-	-	1.88

SAMPLE	DRM 111	DRM 112	DRM 115	DRM 118	DRM 124	DRM 136	DRM 137	DRM 138	DRM 139	DRM 142
SiO_2	52.74	44.49	43.98	69.82	75.93	46.28	72.98	47.07	46.94	52.97
TiO_2	1.30	2.00	.98	.11	.19	.70	.40	.96	2.43	.50
Al_2O_3	17.68	15.41	19.54	11.71	11.21	14.41	13.05	19.11	14.54	17.30
Fe_2O_3	12.13	11.55	10.25	3.37	4.55	10.74	2.69	11.06	12.64	10.52
MnO	.14	.16	.13	.06	.02	.18	.05	.17	.15	.05
MgO	4.52	5.75	3.67	1.46	.75	5.97	.72	4.05	4.59	6.83
CaO	2.86	7.61	8.15	4.61	.48	10.83	4.92	7.09	5.85	.64
Na_2O	5.05	2.50	4.65	3.36	4.93	1.28	.94	4.64	2.11	7.17
K_2O	.06	.67	.94	.49	.07	.01	2.29	.26	2.13	.71
P_2O_5	.20	.52	.23	.05	.04	.15	.07	.24	.55	.03
LOI	3.51	9.42	7.61	4.57	2.40	7.55	1.48	5.26	6.77	2.60
TOTAL	100.19	100.08	100.08	99.61	100.56	98.11	99.59	99.91	98.69	99.33
Cr	31	246	61	< 3	< 3	378	5	59	107	15
Ni	25	102	24	4	4	51	5	25	36	60
V	374	241	345	18	17	307	20	342	228	240
Pb	6	7	2	9	2	1	14	5	12	5
Zn	114	87	112	43	23	86	36	97	93	42
K	498	5562	7803	4068	581	83	19010	2158	17682	5894
Rb	3	23	23	18	4	< 1	106	8	62	26
Ba		138	1146	133	< 20	< 20	923	157	393	117
Sr	313	194	364	256	34	360	128	975	146	112
Ga	26	20	17	16	17	18	13	17	17	16
Nb	13	14	11	12	27	8	20	11	13	3
Zr	132	198	72	73	311	39	289	70	294	19
Ti	7793	11990	5875	659	1139	4197	2398	5755	14568	2998
Y	23	27	15		40	12	32	15	46	< 1
Th	5	2	2	8	12	1	16	4	3	< 1
La	13	10	14	12	21	6	36	13	22	< 5
Ce	39	44	29	26	43	30	85	35	61	8
Nd	17	22	15	<10	16	<10	38	14	31	<10
SiO_2	55.08	49.56	47.91	73.66	77.62	51.58	74.35	50.18	51.60	55.23
TiO_2	1.36	2.23	1.07	.12	.19	..78	.41	1.02	2.67	.52
Al_2O_3	18.46	17.16	21.31	12.35	11.46	16.06	13.29	20.37	15.98	18.04
Fe_2O_3	3.00	3.05	2.65	.84	1.10	2.84	2.74	2.080	3.29	2.60
FeO	8.70	8.83	7.67	2.44	3.19	8.22	.05	8.09	9.54	7.53
MnO	.15	.18	.14	.06	.02	.20	.05	.18	.16	.05
MgO	4.72	6.40	4.00	1.54	.77	6.65	.73	4.32	5.05	7.12
CaO	2.99	8.48	8.89	4.86	.49	12.07	5.01	7.56	6.43	.67
Na_2O	5.27	2.78	5.07	3.54	5.04	1.43	.96	4.95	2.32	7.48
K_2O	.06	.75	1.03	.52	.07	.01	2.33	.28	2.34	.74
P_2O_5	.21	.58	.25	.05	.04	.17	.07	.26	.60	.03
Total	100.00	100.00	100.00	100.00	100.00	100.00	100.00	100.00	100.00	100.00
qz	6.02	1.00	-	38.39	43.80	7.15	48.07	-	4.98	-
c	4.75	-	-	-	2.29	-	.16	-	-	3.73
z	.03	.04	.02	.02	.06	.01	.06	.01	.06	-
or	.37	4.42	6.07	3.06	.42	.07	13.83	1.64	13.87	4.39
ab	44.62	23.56	24.92	29.99	42.64	12.07	8.10	40.39	19.63	62.69
an	13.57	32.15	32.44	16.29	2.18	37.40	24.71	32.63	26.31	3.18
di	-	5.09	8.71	6.31	-	17.62	-	3.01	1.50	-
hy	23.27	23.81	-	4.43	6.58	19.73	1.83	-	22.51	-
ol	-	-	11.84	-	-	-	-	15.09	-	20.87
mt	4.35	4.42	3.84	1.22	1.60	4.11	2.74	4.05	4.78	3.77
cr	.01	.06	.01	-	-	.09	-	.01	.03	-
il	2.58	4.23	2.03	.22	.37	1.48	.22	1.94	5.07	.99
ap	.50	1.37	.60	.13	.10	.40	.29	.61	1.44	.07
ne	-	-	9.75	-	-	-	-	.79	-	.30

SAMPLE	DRM 145	DRM 146	DRM 148
SiO_2	52.35	51.94	54.26
TiO_2	.88	1.08	.95
Al_2O_3	17.26	19.18	15.31
Fe_2O_3	9.17	10.11	12.15
MnO	.14	.06	.17
MgO	3.92	2.24	4.12
CaO	8.20	4.16	7.48
Na_2O	3.42	5.25	2.80
K_2O	.08	1.82	.59
P_2O_5	.16	.36	.25
LOI	4.36	4.42	2.02
TOTAL	99.94	100.61	100.11
Cr	60	13	31
Ni	25	13	20
V	219	136	307
Pb	4	9	3
Zn	88	134	105
K	664	15108	4898
Rb	6	60	11
Ba	52	379	368
Sr	422	245	372
Ga	22	17	17
Nb	8	23	8
Zr	102	160	82
Ti	5276	6475	5695
Y	17	15	18
Th	3	8	3
La	9	21	11
Ce	32	43	29
Nd	13	16	20
SiO_2	55.18	54.43	55.85
TiO_2	.93	1.13	.98
Al_2O_3	18.19	20.10	15.76
Fe_2O_3	2.29	2.51	2.97
FeO	6.63	7.27	8.59
MnO	.15	.06	.17
MgO	4.13	2.35	4.24
CaO	8.64	4.36	7.70
Na_2O	3.60	5.50	2.88
K_2O	.08	1.91	.61
P_2O_5	.17	.38	.26
Total	100.0	100.00	100.00
qz	7.38	-	10.92
c	-	1.90	-
z	.02	.03	.02
or	.50	11.30	3.59
ab	30.50	46.55	24.39
an	33.24	19.36	28.31
di	7.19	-	7.03
hy	15.78	11.13	19.10
ol	-	3.16	-
mt	3.32	3.64	4.30
cr	.01	-	.01
il	1.76	2.15	1.83
ap	.40	.90	.61
ne	-	-	-

XRF PRECISION AND DETECTION LIMITS
(compiled from Weaver et al., 1990)

Oxide (wt%) Element (ppm)	Standard Deviation	XRF Detection Limit
SiO_2	0.210	0.20
TiO_2	0.004	0.01
Al_2O_3	0.078	0.20
Fe_2O_3	0.036	0.01
MnO	0.018	0.01
MgO	0.020	0.05
CaO	0.005	0.01
Na_2O	0.074	0.10
K_2O	0.033	0.01
P_2O_5	0.007	0.01
LOI	0.105	-
V	1.1	3
Cr	0.8	3
Ni	1.1	3
Zn	4.7	3
Ga	0.9	2
Rb	1.6	1
Sr	0.5	1
Y	2.7	1
Zr	10	1
Nb	1.0	2
Ba	20	20
La	2.5	5
Ce	4.0	5
Nd	4.0	10
Pb	1.7	1
Th	2.5	1

NORMALISATION VALUES

Primordial Mantle normalisation values (PRIM) (all ppm unless stated): from McDonough et al. (1992), a revision of the values of Sun and McDonough (1989).

Pb	0.071
Rb	0.635
Ba	6.990
Th	0.084
U	0.021
K	240.0
Nb	0.713
La	0.708
Ce	1.833
Sr	21.10
Nd	1.366
P_2O_5 (wt%)	0.019
Zr	11.20
Ti	1280
Y	4.550

CROSS SECTION A to A'
ANATOKI RIVER

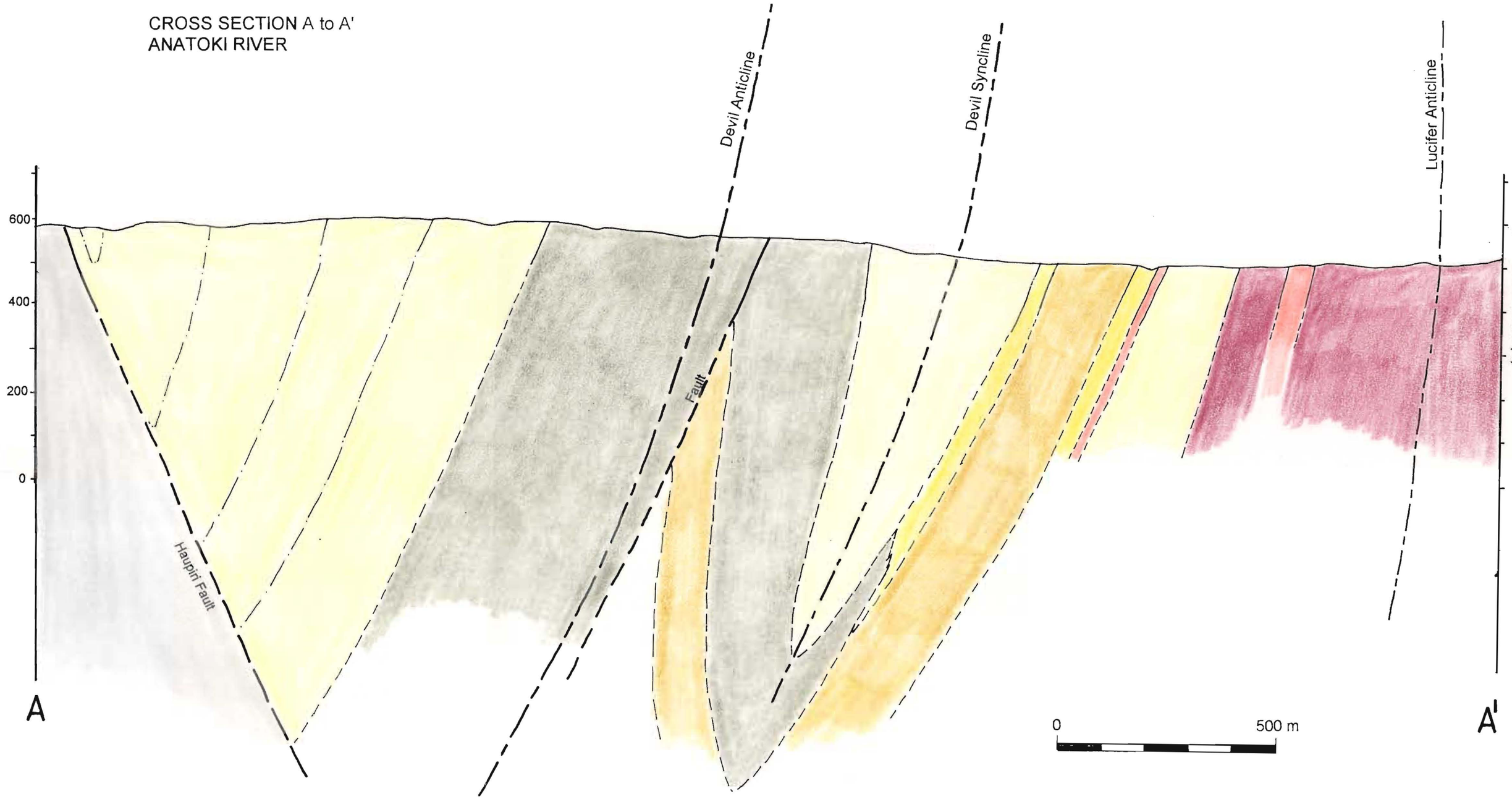

CROSS SECTION B to B'
ANATOKI RANGE

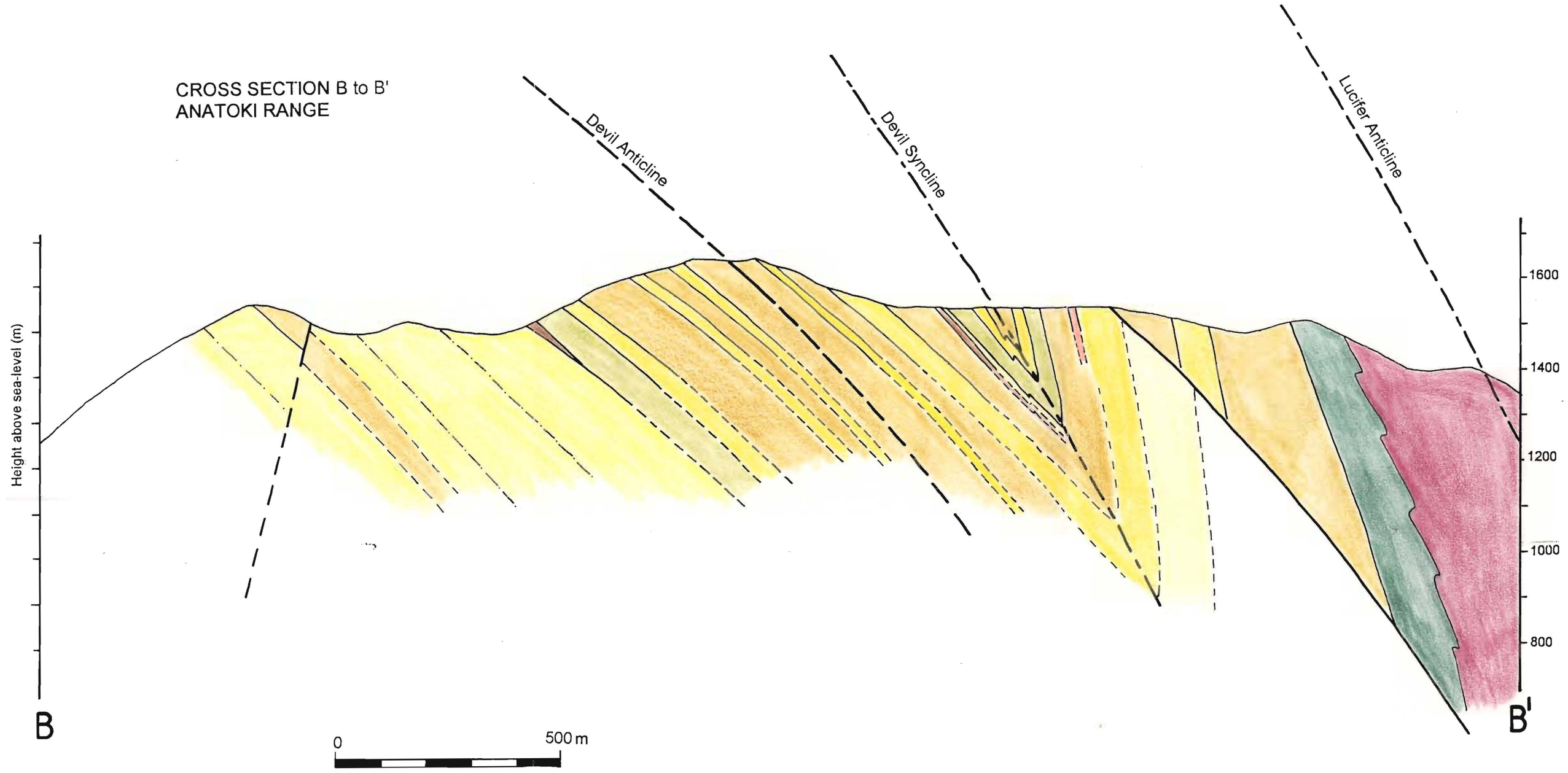

Diagramatic Isometric Block-Diagram of the Structure of the Anatoki Range - Anatoki River Area. View looking toward the southwest (scale 1:20 000).